

**DOTTORATO DI RICERCA IN
FISICA**
Ciclo XXXIII

Settore concorsuale : 02/A2

Settore Scientifico Disciplinare : FIS/02

**BOOTSTRAPPED NEWTONIAN
GRAVITY**

Presentata da:

Michele Lenzi

Coordinatore dottorato:

Prof. Michele Cicoli

Supervisore:

Prof. Roberto Casadio

Abstract

The aim of this thesis is to entertain the possibility of a quantum departure from the general relativistic description of compact sources in strong field regime and claim that a quantum understanding of the classical background could be necessary. We therefore develop an effective field theory providing a simplified framework to address the effects of non-linearities in strong gravitational backgrounds. Starting from a massless Fierz-Pauli-type lagrangian for the Newtonian potential and introducing the self-coupling terms, we arrive at a non-linear equation describing the effective gravitational potential of an arbitrarily compact homogeneous source. Unlike the general relativistic solutions no Buchdahl limit is found as the solutions display a regular behaviour in any compactness regime. Moreover, we provide a quantum interpretation of these results in terms of a quantum coherent state formalism. Such an approach proves to be widely capable of accounting for classical field configurations as well as providing some collective properties of the constituent soft quanta. The latter show a good agreement with some of the crucial relations of the corpuscular model. We do not interpret this approach as a model of phenomenological relevance but better as a simplified picture aimed at capturing novel quantum feature of black holes physics.

Contents

1	Introduction	1
1.1	Motivations and outline	1
1.2	Notation and conventions	4
2	Issues in classical and semiclassical gravity	5
2.1	Singularity problem	5
2.1.1	Stellar equilibrium and the Buchdahl limit	6
2.2	Quantum fields on classical curved background	9
2.2.1	Hawking radiation and related issues	10
3	Corpuscular black holes	15
3.1	Black hole's quantum N-portrait	16
3.1.1	Hawking evaporation as quantum depletion	17
3.1.2	Bekenstein entropy	18
3.2	Corpuscular picture of a gravitational collapse	19
4	Effective scalar theory for the gravitational potential	21
4.1	Effective scalar theory for post-Newtonian potential	22
4.2	Classical solutions	26
4.2.1	Homogeneous ball in vacuum	29
4.2.2	Gaussian matter distribution	31
5	Bootstrapped Newtonian gravity: classical picture	35
5.1	Bootstrapped gravitational potential	36
5.2	Homogeneous ball in vacuum	38
5.2.1	Outer vacuum solution	38
5.2.2	The inner pressure	39
5.2.3	The inner potential	40
5.3	Horizon and gravitational energy	51

6	Bootstrapped Newtonian gravity: quantum picture	57
6.1	Quantum coherent state	58
6.1.1	Static scalar potential	59
6.1.2	Newtonian potential for spherical sources	60
6.1.3	Newtonian potential of a uniform ball	61
6.2	Scaling relations from bootstrapped potential	63
6.2.1	Newtonian potential	66
6.2.2	Bootstrapped potential	67
6.2.3	Quantum source and GUP for the horizon	69
7	Conclusions and outlook	73
7.1	Conclusions	73
7.2	Remarks	75
7.3	Outlook	76
A	Post-Newtonian potential	77
B	Linearised Einstein-Hilbert action at NLO	81
C	Gravitational current	85
D	Comparison method	87
E	Energy balance	89
F	Effective wavenumber and graviton number for the Newtonian potential	91
G	Graviton number and mean wavelength for compact sources	93
G.1	Mean graviton wavenumber	94
G.2	Graviton number	95
	Bibliography	99

Chapter 1

Introduction

1.1 Motivations and outline

Black holes (BHs) can be safely considered one of the most important predictions of general relativity (GR) and represent a benchmark for any attempt at quantising gravity. According to GR, the gravitational collapse of any compact source will generate geodesically incomplete spacetimes if a trapping surface appears [1–3]. The less mathematical point of view [4–6] is that for any realistic matter density in GR, an infinite pressure is necessary to resist the collapse once a specific limit to the compactness is reached [7]. Matter will therefore inevitably shrink to the central singularity. However, within the general relativistic description, the BH interior is causally disconnected from the exterior and the singularity is therefore hidden by the *event horizon*. Such agnostic view may not be completely satisfactory as even if the singularity is irrelevant to a distant observer, it still contradicts one of the basic principles of quantum mechanics. Indeed, a concentration of a finite amount of energy in a point-like region clearly violates the Heisenberg uncertainty principle. One would therefore hope that the inclusion of quantum physics in the process could cure this problem in a similar fashion to the hydrogen atom, shown to have a regular structure irrespective of the singular behaviour as seen from the outside. With this heuristic comparison in mind, one should also expect that, in strong gravitational fields, the description of matter will likely require physics beyond the standard model as well [8, 9]. The first attempt to merge GR and quantum physics can be found in the pioneering work by Hawking [10] which paved the way to the theory of *quantum fields on curved spacetimes*. The main idea behind this approach is that in some regimes one can safely neglect quantum gravity effects and proceed to the quantization of elementary particle fields on classical backgrounds. The main prediction in this picture is the *Hawking radiation*, according to which BHs slowly evaporate by emitting thermal radiation rather than being inert objects. The lesson for us is two-fold. On one side, the possibility that BHs vanish as a consequence of the

evaporation process breaks the above classical argument that the central singularity is protected by the event horizon. Indeed, when the BH has radiated away completely one is left with the naked singularity at its center [11]. Nonetheless, this astonishing result shows that quantum effects due to strong gravitational fields could already arise at horizon scales. Therefore, while the purely general relativistic description begs for a quantum explanation only at Planck scales, the evaporation effect hints at a possible deviation from the classical description of macroscopic compact objects accounting for quantum effects outside the horizon.

The quantum corpuscular picture proposed by Dvali and Gomez [12] points in this direction. Their idea is to interpret BHs as purely quantum objects described as leaky states of gravitons, bound in their own gravitational trap, thus realizing a gravitational condensed state which shares similarities with a Bose-Einstein condensate (BEC) [13, 14]. The singularity would then naturally disappear as a consequence of the regular structure of the BEC and Hawking radiation emerges as a (semiclassical) quantum depletion effect of the marginal bound state of gravitons.

The above discussion is meant to highlight that the attempt to give a quantum mechanical description of the background itself could offer novel insights on some of the most mysterious issues of gravitational phenomena. Starting from this idea, the (more modest) task of this thesis is to provide a simplified framework to address the advocated quantum departure from GR and understand the effects of non linearities in the study of extremely compact sources. More explicitly, we construct an effective field theory for a scalar gravitational potential whose derivation is inspired by Deser's conjecture [15, 16] that GR should be recovered from the massless Fierz-Pauli action by adding gravitational self-interaction terms. For instance, he presented a compact reconstruction of the Einstein-Hilbert action by coupling the initial free massless spin two field in Minkowski spacetime, with its own energy-momentum tensor. On a closer inspection, however, this reconstruction does not appear free of ambiguities since, for instance, it is not unique [17]. Indeed, the energy-momentum tensor is obtained as the Noether current associated to diffeomorphism invariance but the current itself is defined up to identically conserved terms. Therefore only a specific choice of the coupling coefficients would lead to the Einstein-Hilbert action. However, no one really knows the microscopic dynamics realised in nature so that this feature turns out to be useful for the purpose of addressing modifications of GR. Such premises inspired a programme called bootstrapped Newtonian gravity [18, 19] which is the object of this thesis. Starting from a Fierz-Pauli-type action for the static Newtonian potential, non-linearities are introduced by coupling the potential to its own energy density. Furthermore, the coupling constants for the self-interaction terms are not restricted to their Einstein-Hilbert values in order to effectively accommodate for corrections arising from the underlying dynamics which, as mentioned above, we do not wish to restrict a priori. The direct

1.1 Motivations and outline

outcome of this programme is a non-linear equation, which is argued to determine the (regular) effective gravitational potential acting on test particles at rest, and which is generated by a static arbitrarily large source. When interpreted in terms of a suitable quantum coherent state, the bootstrapped potential eventually displays some of the key feature of the corpuscular model of BHs. We should anticipate that we will mostly name as gravitons the quanta in such configurations only in an evocative way since the true concept of quanta in a highly non-linear regime is either way not fully understood.

This thesis is organized as follows: In Chapter 2 we review some of the issues of the classical and semiclassical approach to BH physics. In particular, in Section 2.1 we will recall the Buchdahl theorem as a useful guideline in the description of regular compact object. We will then move to the semiclassical origin of the Hawking effect in Section 2.2, after providing minimal details of quantum field theory (QFT) on classical curved spacetime.

In Chapter 3 we will briefly introduce the main concepts behind the *classicalization* procedure in gravity with the purpose of showing the characteristic features of corpuscular BHs in Sec. 3.1. In Section 3.2 we also give a corpuscular picture of a gravitational collapse involving matter.

In Chapter 4 we show the construction of an effective field theory for the post-Newtonian potential up to second order in the Newton constant [20]. In Section 4.1 we derive the effective Lagrangian for the scalar potential starting from the massless Fierz-Pauli action. Then in Section 4.2 we explicitly solve the associated Euler-Lagrange equations of motion in presence of a homogeneous and gaussian matter density.

Chapter 5 is devoted to the explanation of the classical bootstrap programme following Refs. [18, 19]. In Section 5.1 we generalize the Lagrangian and equations of motion found in the previous Chapter which will in turn be solved in Section 5.2 for a homogeneous source, both in low and high compactness regime. In Section 5.3 we recover a Newtonian definition of the horizon and provide some energy considerations on the system.

In Chapter 6 we will finally provide a quantum picture of the bootstrapped potentials based on Ref. [21]. First, in Section 6.1 we review how to describe a static scalar potential in terms of a coherent state. Then in Section 6.2 we apply the above to the bootstrap solutions and make contact with the corpuscular features.

At last, in Chapter 7 we draw our conclusion of this approach and drop some clues for future directions.

1.2 Notation and conventions

In this work we use the mostly positive convention for the metric $(-, +, +, +)$. The flat Minkowski metric therefore reads

$$\eta_{\mu\nu} = \text{diag}(-1, +1, +1, +1) ,$$

in Cartesian coordinates. Four-vectors in Minkowski space are indicated as $x^\mu = (t, \mathbf{x})$ where we write in bold-face type the three-vectors in the three-dimensional space $\mathbb{R}^3 = \{\mathbf{x} = (x^1, x^2, x^3) : x^i \in \mathbb{R}\}$. We will usually omit the domain of integration when it is given by all of \mathbb{R}^3 . The four-derivative in Minkowski space is denoted as

$$\partial_\mu = \left(\frac{\partial}{\partial t}, \frac{\partial}{\partial x^1}, \frac{\partial}{\partial x^2}, \frac{\partial}{\partial x^3} \right) = (\partial_t, \partial_i) ,$$

and the d'Alambert operator consequently reads

$$\square = \partial_\mu \partial^\mu = -\partial_t^2 + \partial_{x^1}^2 + \partial_{x^2}^2 + \partial_{x^3}^2 = -\partial_t^2 + \Delta .$$

In spherically symmetric systems the coordinates are (r, θ, ϕ) and the prime “'” denotes partial derivation with respect to the radial coordinate $f' \equiv \partial f / \partial r$.

When considering a curved spacetime with metric $g_{\mu\nu}$ we write the Riemann tensor as

$$R^\lambda_{\mu\eta\nu} = \partial_\eta \Gamma^\lambda_{\mu\nu} - \partial_\nu \Gamma^\lambda_{\mu\eta} + \Gamma^\lambda_{\eta\rho} \Gamma^\rho_{\mu\nu} - \Gamma^\lambda_{\nu\rho} \Gamma^\rho_{\mu\eta} ,$$

in terms of the Christoffel symbols

$$\Gamma^\alpha_{\mu\nu} = \frac{1}{2} g^{\alpha\beta} (\partial_\mu g_{\nu\beta} + \partial_\nu g_{\mu\beta} - \partial_\beta g_{\mu\nu})$$

The Ricci tensor is $R_{\mu\nu} = R^\lambda_{\mu\lambda\nu}$ and the Ricci scalar $\mathcal{R} = g^{\mu\nu} R_{\mu\nu}$.

In this work we will use units in which the speed of light is taken to be unity ($c = 1$), while keeping both the Newton's constant G_N and the Planck's constant \hbar explicit, i.e.

$$G_N = \frac{\ell_p}{m_p} , \quad \hbar = \ell_p m_p .$$

Chapter 2

Issues in classical and semiclassical gravity

This chapter is just meant to draw the attention to some well established result and issues in GR and QFT on curved background. It is thus far from being exhaustive. Since the main topic of this thesis is providing novel insights on the physics of extremely compact objects where strong gravitational effects cannot be ignored, we will not focus on the problems of gravity as a field theory.

2.1 Singularity problem

Singularities represent the breakdown of our description of a physical system. Our formulation of the laws of physics ceases to work when a singularity appears. In GR a detailed mathematical formulation was provided by Penrose and Hawking in the sixties [1–3, 22] both for cosmology and gravitational collapse. However, since we will only deal with static compact sources it is convenient to approach the singularity issue from a different perspective. The Buchdahl theorem [7] provides a simple condition to be satisfied in order to avoid singularities in a gravitational collapse. The theorem states that under the following assumptions:

- GR is the correct theory of gravity;
- The system is spherically symmetric;
- The matter source is described as a perfect isotropic fluid;
- The energy is non-negative and non outward increasing, i.e. $\rho \geq 0$ and $\rho' \leq 0$;

the compactness of the source satisfies the Buchdahl bound

$$\frac{G_N M}{R} \leq \frac{4}{9}, \quad (2.1.1)$$

with

$$M = 4\pi \int_0^R dr r^2 \rho(r) , \quad (2.1.2)$$

the total mass of the finite size source $\rho(r)$ with $\rho(r) = 0$ for $r > R$. It is obvious that giving up any of the above assumptions provides a way to circumvent the singularity issue. Therefore, the Buchdahl theorem also proves to be useful to classify the different proposals of regular extremely compact objects [23]. In the following we will review the main steps leading to the result (2.1.1).

2.1.1 Stellar equilibrium and the Buchdahl limit

Since we are going to address the equilibrium of a static spherically symmetric compact object and we are assuming Einstein theory holds, the exterior metric will be given by the Schwarzschild solution [24]

$$ds_{ext}^2 = - \left(1 - \frac{R_H}{R}\right) dt^2 + \left(1 - \frac{R_H}{R}\right)^{-1} dr^2 + r^2 (d\theta^2 + \sin^2 \theta d\phi^2) , \quad (2.1.3)$$

where

$$R_H = \frac{2G_N M}{R} , \quad (2.1.4)$$

is the gravitational (or Schwarzschild) radius associated to a source of mass M . The Schwarzschild metric of course solves the Einstein equations

$$R_{\mu\nu} - \frac{1}{2}g_{\mu\nu} \mathcal{R} = 8\pi G_N T_{\mu\nu} , \quad (2.1.5)$$

with vanishing energy-momentum tensor. Since we want to question the stability of the system, we need to model the interior of the source. Let us then start by writing the general (regular) line element of a spherically symmetric static solution to the Einstein equations as

$$ds_{int}^2 = -e^\nu dt^2 + e^\lambda dr^2 + r^2 (d\theta^2 + \sin^2 \theta d\phi^2) , \quad (2.1.6)$$

with $\nu = \nu(r)$ and $\lambda = \lambda(r)$. In order to accomplish the requirements of the Buchdahl theorem, matter will be described in the useful perfect fluid approximation as

$$T_{\mu\nu} = p g_{\mu\nu} + (p + \rho) u_\mu u_\nu . \quad (2.1.7)$$

and it is at rest in this coordinate system $u^\mu = (e^{-\nu/2}, 0, 0, 0)$. The functions $p(r)$ and $\rho(r)$ respectively represent the isotropic pressure and energy density of the source. Among all Einstein equations (2.1.5) only the (00), (11) components together with the

2.1 Singularity problem

conservation equation $\nabla^\mu T_{\mu\nu} = 0$ will be useful to us (with ∇_μ the covariant derivative with respect to the metric). These equations read

$$8 \pi G_N r^2 p = e^{-\lambda} (\nu' r + 1) - 1 \quad (2.1.8)$$

$$8 \pi G_N r^2 \rho = e^{-\lambda} (\lambda' r - 1) + 1 \quad (2.1.9)$$

$$2p' = -\nu'(p + \rho) . \quad (2.1.10)$$

It is now quite easy to see that Eq. (2.1.9) can be integrated to give

$$e^{-\lambda} = 1 - \frac{2 G_N m(r)}{r} , \quad (2.1.11)$$

where $m(r)$ is the mass function defined by

$$m(r) = 4 \pi \int_0^r dx x^2 \rho(x) , \quad (2.1.12)$$

and obviously $m(R) = M$. The simple substitution of Eqs. (2.1.10) and (2.1.11) into Eq. (2.1.8) gives the differential equation

$$p' = (p + \rho) \frac{G_N m(r) + 4 \pi G_N r^3 p}{r [2 G_N m(r) - r]} , \quad (2.1.13)$$

known as the Tolman-Oppenheimer-Volkoff equation [5, 25] determining the pressure of a static ball of matter in GR. Upon providing any function $\rho(r)$ (or an equation of state $\rho(p)$), the condition that solutions to Eq. (2.1.13) must be finite should result in an upper bound for the compactness $G_N M/R$ of the source. Beyond this limit, an infinite pressure is needed to resist the collapse. Nevertheless, we can show a general result [7] which does not require an explicit density function but only assumes a non outward increasing behaviour, i.e. $\rho' < 0$. Indeed, if we make the substitution

$$e^\nu = \zeta^2 , \quad (2.1.14)$$

and eliminate the pressure between Eqs. (2.1.8) and (2.1.10), after rearranging a bit we end up with the following linear equation

$$\frac{d}{dr} \left[\frac{1}{r} \left(1 - \frac{2 G_N m(r)}{r} \right)^{1/2} \frac{d\zeta}{dr} \right] = \left(1 - \frac{2 G_N m(r)}{r} \right)^{-1/2} \left(\frac{G_N m(r)}{r^3} \right)' \zeta . \quad (2.1.15)$$

The initial conditions at $r = R$ are given by matching with the exterior Schwarzschild solution (2.1.3) and give

$$\zeta(R) = \left(1 - \frac{2 G_N M}{R} \right)^{1/2} \quad (2.1.16)$$

$$\zeta'(R) = \frac{G_N M}{R^2} \left(1 - \frac{2 G_N M}{R} \right)^{-1/2} . \quad (2.1.17)$$

Regularity of the metric functions further requires $\zeta(r) > 0$, and since the mean density $3m(r)/4\pi r^3$ decreases outward as the density ρ does, the right side of Eq. (2.1.15) is negative. The consequence is that upon integrating the left one from r to R , with the help of Eq. (2.1.17) we get

$$\frac{d\zeta}{dr} \geq \frac{G_N M r}{R^3} \left(1 - \frac{2G_N m(r)}{r}\right)^{-1/2}, \quad (2.1.18)$$

and further integrating from 0 to R with Eq. (2.1.16)

$$\zeta(0) \leq \left(1 - \frac{2G_N M}{R}\right)^{1/2} - \frac{G_N M}{R^3} \int_0^R \frac{dr r}{\left(1 - \frac{2G_N m(r)}{r}\right)^{1/2}}. \quad (2.1.19)$$

We can then find another upper bound for $\zeta(0)$ by recognizing that

$$\frac{m(r)}{r} = \frac{m(r)}{r^3} r^2 \geq \frac{M}{R^3} r^2, \quad (2.1.20)$$

where we again used the fact that the mean density is outward decreasing. In this way we can solve the integral in the above inequality and find that

$$\zeta(0) \leq \frac{3}{2} \left(1 - \frac{2G_N M}{R}\right)^{1/2} - \frac{1}{2}. \quad (2.1.21)$$

The condition that ζ needs to be positive then leads to the anticipated Buchdahl limit

$$\frac{G_N M}{R} \leq \frac{4}{9}. \quad (2.1.22)$$

Eq. (2.1.20) shows that this bound is saturated when the source has homogeneous density profile with

$$\rho(r) = \frac{3M}{4\pi R^3} \Theta(R - r), \quad (2.1.23)$$

and therefore $3m(r)/4\pi r^3 = 3M/4\pi R^3$. This can be seen even more explicitly as in this case Eq. (2.1.13) can be solved and gives

$$p = \rho \left(\frac{\sqrt{R^3 - 2G_N M r^2} - R \sqrt{R - 2G_N M}}{3R \sqrt{R - 2G_N M} - \sqrt{R^3 - 2G_N M r^2}} \right). \quad (2.1.24)$$

It is now easy to see that this pressure becomes infinite precisely when the equality holds in Eq. (2.1.1). In the Newtonian limit instead we have

$$p(r) = \frac{3(R^2 - r^2)G_N M^2}{8\pi R^6}, \quad (2.1.25)$$

which shows that Newtonian pressure is always finite and no upper limit occurs¹. The fact that with homogeneous density the bound (2.1.1) is saturated is not that surprising.

¹We should point that an upper bound exist for some specific density profiles in Newtonian physics as well. The important difference with GR is that Buchdahl limit is independent of the particular equation of state.

Indeed, if we imagine a maximum sustainable density exists, then the most massive object we can construct is the one having that density everywhere. This makes constant density stars an important, even if unrealistic, toy model in various contexts [23, 26, 27].

2.2 Quantum fields on classical curved background

QFT on classical backgrounds [28, 29] is conceived as an attempt to combine gravitational and quantum effects, in the absence of a viable quantum theory of gravity. The idea is to take Einstein's GR as the correct theory for gravitational phenomena and then generalize the quantization of fields in Minkowski space to a curved classical background. The Planck length $\ell_p \sim 10^{-35}$ m is usually considered as the fundamental length of quantum gravity. Therefore, if the distances involved are sufficiently larger than ℓ_p , it is possible to accurately describe the effect of classical curved backgrounds on quantum phenomena. We are here only interested in showing its most widely known and accepted physical consequence, i.e. the Hawking radiation [10]. Consequently, we will not enter the mathematical details of such approach (see Ref. [29] for a comprehensive description) and only provide minimum details to grasp the core physics.

We start by briefly reviewing the standard canonical quantization procedure on Minkowski space for the simplest case, i.e. a free massless scalar field $\Phi(t, \mathbf{x})$ satisfying the massless Klein-Gordon equation

$$\square \Phi(t, \mathbf{x}) = 0 . \quad (2.2.1)$$

The usual choice for elementary solutions to the above are the plane waves

$$u_{\mathbf{k}}(t, \mathbf{x}) = v_{\mathbf{k}}(\mathbf{x}) e^{-i k t} , \quad (2.2.2)$$

with $k = \sqrt{\mathbf{k} \cdot \mathbf{k}}$ and

$$v_{\mathbf{k}}(\mathbf{x}) \equiv \frac{e^{i \mathbf{k} \cdot \mathbf{x}}}{(2\pi)^{3/2}} , \quad (2.2.3)$$

satisfying the orthonormality relations

$$\int d\mathbf{x} v_{\mathbf{k}}^*(\mathbf{x}) v_{\mathbf{h}}(\mathbf{x}) = \delta(\mathbf{k} - \mathbf{h}) , \quad (2.2.4)$$

in the three-dimensional space² \mathbb{R}^3 . The $u_{\mathbf{k}}$ then form a complete orthonormal basis with respect to the Klein-Gordon scalar product

$$(u_{\mathbf{h}}, u_{\mathbf{k}}) \equiv i \int d\mathbf{x} [u_{\mathbf{k}}^*(t, \mathbf{x}) \partial_t u_{\mathbf{h}}(t, \mathbf{x}) - \partial_t u_{\mathbf{k}}^*(t, \mathbf{x}) u_{\mathbf{h}}(t, \mathbf{x})] = \delta(\mathbf{k} - \mathbf{h}) . \quad (2.2.5)$$

²We separate the plane waves in \mathbb{R}^3 from the time dependent part for later convenience.

The quantum field operator and its conjugate momentum can then be split into positive and negative frequencies

$$\hat{\Phi}(t, \mathbf{x}) = \int \frac{d\mathbf{k}}{(2\pi)^3} \sqrt{\frac{\ell_{\text{p}} m_{\text{p}}}{2k}} \left(\hat{a}_{\mathbf{k}} e^{-ikt+i\mathbf{k}\cdot\mathbf{x}} + \hat{a}_{\mathbf{k}}^{\dagger} e^{ikt-i\mathbf{k}\cdot\mathbf{x}} \right) \quad (2.2.6)$$

$$\hat{\Pi}(t, \mathbf{x}) = i \int \frac{d\mathbf{k}}{(2\pi)^3} \sqrt{\frac{\ell_{\text{p}} m_{\text{p}} k}{2}} \left(-\hat{a}_{\mathbf{k}} e^{-ikt+i\mathbf{k}\cdot\mathbf{x}} + \hat{a}_{\mathbf{k}}^{\dagger} e^{ikt-i\mathbf{k}\cdot\mathbf{x}} \right), \quad (2.2.7)$$

and must satisfy the equal time commutation relations

$$\left[\hat{\Phi}(t, \mathbf{x}), \hat{\Pi}(t, \mathbf{y}) \right] = i \hbar \delta(\mathbf{x} - \mathbf{y}). \quad (2.2.8)$$

The creation and annihilation operators therefore obey the standard commutation rules

$$[\hat{a}_{\mathbf{k}}, \hat{a}_{\mathbf{h}}^{\dagger}] = \delta(\mathbf{k} - \mathbf{h}), \quad [\hat{a}_{\mathbf{k}}, \hat{a}_{\mathbf{h}}] = [\hat{a}_{\mathbf{k}}^{\dagger}, \hat{a}_{\mathbf{h}}^{\dagger}] = 0 \quad (2.2.9)$$

and the Fock space of quantum states is built from the vacuum $\hat{a}_{\mathbf{k}} |0\rangle = 0$. A crucial property of this quantization procedure is its independence on the chosen inertial time t , since any other choice, related via Poincaré transformations, will not change the splitting (2.2.6). The immediate and key consequence is that the vacuum state will be invariant as well.

When considering a quantum field on a curved spacetime most of the above can be directly extended by introducing the generally covariant d'Alembertian operator so that Eq. (2.2.1) becomes

$$\square \Phi = g^{\mu\nu} \nabla_{\mu} \nabla_{\nu} \Phi = 0, \quad (2.2.10)$$

with ∇_{μ} the covariant derivative with respect to the background metric $g_{\mu\nu}$. One can therefore find an orthonormal basis f with respect to the extended Klein-Gordon product in the general spacetime

$$(f_1, f_2) = i \int d\Sigma^{\mu} [f_2^* \partial_{\mu} f_1 - f_1 \partial_{\mu} f_2^*], \quad (2.2.11)$$

where $d\Sigma^{\mu} = d\Sigma n^{\mu}$ with $d\Sigma$ the volume element of an initial data Cauchy surface Σ and n^{μ} its future directed unit normal vector. The main problem here is that different choices of the frequency modes f will in general lead to different definitions of the vacuum state and Fock space. There is no natural choice of the splitting of the modes unless the curved spacetime is stationary and one can identify a timelike Killing vector field (see Refs. [28, 30]).

2.2.1 Hawking radiation and related issues

As a natural consequence of the above picture, one should not be able to provide physical information about particles involved when a (dynamical) gravitational collapse takes

2.2 Quantum fields on classical curved background

place. Nevertheless, one can still recover a solid particle description when it is possible to identify stationary asymptotic regions [28, 30]. Indeed, the spacetime in presence of a collapsing source consists in an initial flat space, the dynamical region in which the collapse takes place and a Schwarzschild region when the BH has settled down. One can then construct a set of orthonormal modes ³ f_i^{in} which only contains positive frequencies with respect to the Minkowski time coordinate in the past and the analogous positive frequency orthonormal modes f_i^{out} in the future asymptotically flat region. However, the splitted positive and negative frequency modes in one region will in general be mixed in the other region, meaning that the corresponding vacuum states will not coincide.

Hawking [10] pushed this discrepancy to investigate the effects of the dynamical region on the hypothetical vacuum state $|in\rangle$ of the quantum field at past infinity. He found that the state $|in\rangle$ is not perceived as vacuum state by the observer at future infinity, meaning that the dynamical gravitational field triggered the particle creation. In fact, the f_i^{in}, f_i^{out} solutions to Eq. (2.2.10), satisfying the following orthonormality relations

$$(f_i, f_j) = \delta_{ij} = -(f_i^*, f_j^*) , \quad (f_i, f_j^*) = 0 , \quad (2.2.12)$$

where we omitted the *in, out* superscripts, let us write the field decompositions

$$\hat{\Phi} = \sqrt{\ell_p m_p} \sum_i \left[\hat{a}_i^{in} f_i^{in} + \hat{a}_i^{in\dagger} f_i^{in*} \right] \quad (2.2.13)$$

$$\hat{\Phi} = \sqrt{\ell_p m_p} \sum_i \left[\hat{a}_i^{out} f_i^{out} + \hat{a}_i^{out\dagger} f_i^{out*} \right] , \quad (2.2.14)$$

with the creation and annihilation operators satisfying the usual commutation relation

$$[\hat{a}_i, \hat{a}_j^\dagger] = \delta_{ij} , \quad [\hat{a}_i, \hat{a}_j] = [\hat{a}_i^\dagger, \hat{a}_j^\dagger] = 0 , \quad (2.2.15)$$

where again we omitted the *in, out* superscripts. The corresponding vacuum states at past and future infinity are then defined as $\hat{a}_i^{in} |in\rangle = 0$ and $\hat{a}_i^{out} |out\rangle = 0$. Since the two bases are complete one can expand one in terms of the other and because of the above discussion it is not guaranteed that positive and negative modes will remain separated. Therefore in general the two bases relate to each other through the so called *Bogoliubov transformations*, i.e.

$$f_i^{out} = \sum_j \left[\alpha_{ij} f_j^{in} + \beta_{ij} f_j^{in*} \right] , \quad (2.2.16)$$

which together with the orthonormality relations (2.2.12) lead to the condition

$$\sum_k \left[\alpha_{ik} \alpha_{jk}^* - \beta_{ik} \beta_{jk}^* \right] = \delta_{ij} . \quad (2.2.17)$$

³We will here switch to generic discrete indices i to avoid unnecessary notation complexity.

2. Issues in classical and semiclassical gravity

Moreover, by using the fact that $\hat{a}_i^{in} = (\hat{\Phi}, f_i^{in})$ and $\hat{a}_i^{out} = (\hat{\Phi}, f_i^{out})$ and the (2.2.12) again, one can expand the two sets of operators one into another as well

$$\hat{a}_i^{out} = \sum_j \left[\hat{a}_j^{in} \alpha_{ij}^* - \hat{a}_i^{in\dagger} \beta_{ij}^* \right] . \quad (2.2.18)$$

Already at this stage one can quantify the particle content of the initial vacuum state $|in\rangle$ as observed in the final stationary region. In fact, denoting the number of particles in the *out* “*i*” mode as

$$N_i^{out} = \hat{a}_i^{out\dagger} \hat{a}_i^{out} , \quad (2.2.19)$$

one can find

$$\langle in | N_i^{out} | in \rangle = \sum_j |\beta_{ij}|^2 , \quad (2.2.20)$$

where the result comes from substituting Eqs. (2.2.12) and (2.2.18). This means that the particle number in the $|in\rangle$ state as “measured” by an observer at future infinity will in general be non trivial, depending on the β_{ij} coefficients. If all the β_{ij} happen to vanish, then Eq. (2.2.17) reduces to

$$\sum_k \alpha_{ik} \alpha_{jk}^* = \delta_{ij} , \quad (2.2.21)$$

meaning that the two sets of basis are related by a unitary transformation and the $|in\rangle$ and $|out\rangle$ vacuum states are actually equivalent.

In Ref. [10] Hawking actually evaluated the β_{ij} coefficients for a generic collapse in which as already said we divide spacetime into a Minkowski initial region, the intermediate collapse region and the final Schwarzschild BH configuration. In particular, he found that BHs radiate at late times with a Planckian distribution of thermal radiation, i.e.

$$\langle in | N_i^{out} | in \rangle = \frac{\Gamma_i}{e^{8\pi\omega_i G_N M} - 1} , \quad (2.2.22)$$

where Γ_i is the *grey-body factor* measuring the fraction of each mode which enters the collapsing body as a consequence of the back-scattering with its potential barrier. The above spectrum actually coincides, apart from the grey-factor, with a black-body spectrum emitting at temperature

$$T_H = \frac{\hbar \kappa}{2\pi k_B} , \quad (2.2.23)$$

called *Hawking temperature*, with k_B being the *Boltzmann’s constant* and $\kappa = 1/4 G_N M$ the surface gravity of a Schwarzschild BH. One of the most problematic consequences

2.2 Quantum fields on classical curved background

of the above result appears when evaluating the corresponding energy emitted, which is given by the corresponding Stefan-Boltzmann law for a black-body, i.e.

$$\frac{dM}{dt} = -\gamma \frac{m_{\text{p}}^2}{G_{\text{N}} M^2} = -\gamma \frac{m_{\text{p}}^3}{\ell_{\text{p}} M^2}, \quad (2.2.24)$$

where γ is a numerical factor of order 10^{-5} .

Indeed the immediate aftermath is that the Hawking effect causes the BH to evaporate as the energy carried by the Hawking radiation is extracted from the BH itself. It is easy to evaluate the time of complete evaporation [31] as

$$\tau = \frac{\ell_{\text{p}}}{3\gamma} \left(\frac{M_{\text{initial}}}{m_{\text{p}}} \right)^3, \quad (2.2.25)$$

even if this reasoning only provides the correct order of magnitude as it can only be trusted, at most, up to the Planck scale. The quantum mechanical implication of the emission effect is quite dramatic. In fact, the quantum mechanical evolution of a physical system, in Minkowski space, is given by a unitary operator. One can expand the initial and final state on a basis in the Fock space and the operator will map the complex coefficients fixing the initial state into the corresponding one for the final state. Both of them can be written as pure states, i.e. $|\phi\rangle = \sum_i c_i |\psi_i\rangle$. However, when the gravitational collapse takes place and the causal structure thus differs from the Minkowski one, things change. Indeed, the Hawking prediction is that the initial $|in\rangle$ pure state is perceived at late times as a flux of thermal radiation, i.e. uncorrelated particles. Therefore, it will be described through a matrix density and quantum predictability based on unitary evolution of pure states is lost, together with all the information about the collapsed star. This goes under the name of *information loss paradox* [32–34].

The result (2.2.23) found by Hawking that BHs do possess a finite, even if very small, temperature is made even more appealing by the fact that it supports the formal analogy between the classical laws of BHs mechanics and the laws of thermodynamics [35–40]. Indeed, the *area law theorem* [37, 38], stating that the area of the event horizon never decreases in time, suggested that it formally behaves as the entropy of a closed thermodynamic system. This triggered the idea that one could extend the reasoning and find a connection with all the other laws of thermodynamic starting from the zeroth law which states the existence of a thermodynamic variable, the temperature, which is constant for systems in thermodynamic equilibrium. The fact that surface gravity κ of a stationary BH is constant on the event horizon then provided the analogous zeroth law for BHs. Nonetheless, the thermodynamic temperature of a classical BH, which is only expected to absorb particles, is necessarily the absolute zero, leading to an evident inconsistency with the laws of thermodynamic. This is why Eq. (2.2.23) justified the formal analogy as it showed an explicit connection between the (finite) temperature

of the BH and its surface gravity allowing as well to find the exact relation between entropy and area A of a BH

$$S_{\text{BH}} = \frac{k_{\text{B}}}{G_{\text{N}}} \frac{A}{4\hbar} . \quad (2.2.26)$$

Nevertheless, while Eq. (2.2.23) is justified by the quantum field on curved background approach, the full understanding of Eq.(2.2.26) would require a full quantum analysis of the system ideally permitting the count of the quantum degrees of freedom associated to the BH configuration.

At last, a connection with the singularity problem in the previous section can be made. In fact, one could argue that the BH singularity is not an issue at all as it is hidden behind the horizon and thus an external observer will never be able to see it. However, if one trusts the evaporation until the BH completely radiates away, then the singularity will inevitably turns into a naked singularity so that the above argument turns out to be a bit restricted. Therefore, the evaporation process strengthen the view that a departure from the general relativistic description of extremely compact objects is necessary at some point (see e.g. Ref. [41] for an alternative scenario).

Chapter 3

Corpuscular black holes

We already stressed that the focus of this work are gravitating compact objects as laboratories for testing strong gravitational effects. In particular, we address a possible deviation from the general relativistic description. In this context, a strong motivation is provided by the proposal by Dvali and Gomez [12] that BHs can be depicted as marginally bound states of soft (off-shell) gravitons. The origin of this innovative idea resides in an alternative UV-completion mechanism, the *classicalization*, introduced by the same authors and others [42–45]. From a quantum field theoretic perspective, Einstein’s gravity is a perfectly fine low-energy effective field theory [46, 47] but is non renormalizable from the Wilsonian viewpoint [48, 49]. Therefore at high-energy scales ¹ it ceases to be predictive. The Wilsonian approach is based on the idea that when we push a theory to the strong coupling regime, new degrees of freedom need to be introduced to recover a weakly coupled (and therefore perturbative) description. The electroweak theory is a great example of this procedure at work since the four-fermion interaction is completed in the UV with the introduction of three vector bosons (W^\pm, Z^0) as mediators of the weak interaction. The idea behind the classicalization scheme is that gravity *self-completes* by producing high-multiplicity states of its own low-energy degrees of freedom (the graviton massless spin 2 fields). The high-energy scattering should therefore produce states with a huge occupation number of quanta which will consequently be soft and weakly interacting. Such an approximately classical behaviour is the reason why the authors in Refs. [42–45] claimed that gravity self-completes via classicalization.

Let us now address, in light of the classicalization scheme, the task of describing BHs formation in a high energy scattering experiment [50] (see Refs. [51, 52] for some previous works on the topic). We shall then hypothetically consider the collision of two elementary particles with center of mass energy $\sqrt{s} \gg m_p$ and further assume that a BH will form when the system occupies a region whose size is smaller than

¹The natural scale for gravity being the Planck scale m_p (or ℓ_p).

the corresponding gravitational radius, i.e. $r \lesssim R_{\text{H}} \simeq \ell_{\text{p}} \sqrt{s}/m_{\text{p}}$. If we then trust classicalization, the system in the final state will be given by a large number N_{G} of soft gravitons. In other words, the process of BH formation is depicted as a $2 \rightarrow N$ scattering, where we trade the two initial “hard” quanta for N_{G} “soft” gravitons with typical Compton wavelength $\lambda_{\text{G}} = \hbar/\epsilon_{\text{G}} \simeq R_{\text{H}}$. Energy conservation $\sqrt{s} \simeq N_{\text{G}} \epsilon_{\text{G}}$ then implies that the number of such gravitons is very large, i.e. $N_{\text{G}} \simeq s/m_{\text{p}}^2 \gg 1$. This hypothetical result would thus signal that gravity prevents us from probing distances smaller than ℓ_{p} as such scales are screened by the production of semiclassical BHs with size $\lambda_{\text{G}} \gg \ell_{\text{p}}$. Finally, denoting the dimensionless coupling between the gravitons in the final state as

$$\alpha_{\text{G}} = \frac{\hbar G_{\text{N}}}{\lambda_{\text{G}}^2}, \quad (3.1)$$

it is easy to see that

$$\alpha_{\text{G}} N_{\text{G}} = 1. \quad (3.2)$$

This is the so called *maximal packing condition* and it shows that while the theory is still collectively in a strong coupling regime since the collective coupling $\alpha_{\text{G}} N_{\text{G}}$ is of order one, the single constituents are very weakly interacting between each other.

3.1 Black hole’s quantum N-portrait

The above picture gives BHs a central role and paves the way to an interesting non geometrical description of such objects in which the occupation number N_{G} is the key feature. Let us start by considering a purely gravitating ² spherical source of mass M and radius R well above its Schwarzschild radius, $R \gg R_{\text{H}}$. The gravitational field is then well described by the Newtonian potential

$$V_{\text{N}}(r) = -\frac{G_{\text{N}} M}{r}. \quad (3.1.1)$$

From a quantum point of view we interpret it as a superposition of non propagating gravitons which, as far as $R \gg R_{\text{H}}$, have very long wavelengths. In this regime, both the individual gravitons interactions and the interaction of one constituent with the collective potential produced by the other $N_{\text{G}} - 1$, can be safely neglected. Actually, there is no reason why a bound state should even form at this stage. On the other hand, it seems quite reasonable that when R approaches R_{H} , the gravitational energy grows and the gravitons start perceiving the self-sourcing due to the collective gravitational

²In this picture the role of matter is completely neglected and only originally serves to put gravitons together. We will come back later on this.

3.1 Black hole's quantum N-portrait

energy. The assumption made in Ref. [12] is that this interaction is strong enough to confine the gravitons inside a finite volume, i.e. the condensate is self-sustained at this point. The whole construction then follows from simple energy considerations. First, since the gravitons are now supposed to be localized, we can associate them an effective mass m via the Compton wavelength $\lambda_G = \hbar/m = \ell_p m_p/m$. The total energy will therefore be written as $M = N_G m$. The effective gravitational coupling of the interaction of one graviton with the rest of the others can then be written as

$$\alpha_G = \frac{|V_N(R = \lambda_G)|}{N_G} = \frac{\ell_p^2}{\lambda_G^2} = \frac{m^2}{m_p^2}, \quad (3.1.2)$$

allowing to write the collective binding potential per graviton as

$$U \simeq m V_{N_G}(\lambda_G) \simeq -N_G \alpha m. \quad (3.1.3)$$

The bound state will then simply form when the energy of the single graviton $E_K \simeq m$ is just below the amount needed to escape the potential well, this yields the condition

$$E_K + U = 0, \quad (3.1.4)$$

and translates into

$$\alpha_G N_G = 1, \quad (3.1.5)$$

which is the same *maximal packing* scaling (3.2) found before in the classicalization context. The most important consequence of this picture is that we can now relate everything to N_G . In fact, from Eq. (3.1.2) the mass of the gravitons can be written as $m = m_p/\sqrt{N_G}$, then the total mass and the gravitons wavelength

$$M = \sqrt{N_G} m_p, \quad (3.1.6)$$

$$\lambda_G = \sqrt{N_G} \ell_p \simeq R_H. \quad (3.1.7)$$

As we will show in the following sections, this picture allows to draw interesting considerations on the nature of Hawking radiation and Bekenstein-Hawking entropy.

3.1.1 Hawking evaporation as quantum depletion

The above framework describes BHs as leaky bound states of gravitons in which the escape energy is just above the ground state. Hence, the system is continuously losing gravitons through a quantum depletion effect, as one expects from homogeneous interacting Bose-Einstein condensates [53]. The microscopic dominant process leading to the leakage is the $2 \rightarrow 2$ graviton scattering which at first order gives the following depletion rate

$$\Gamma \simeq \frac{1}{N_G^2} N_G^2 \frac{\hbar}{\sqrt{N_G} \ell_p} + \mathcal{O}(N_G^{-1}), \quad (3.1.8)$$

where the first factor comes from the interaction strength ($N_G^{-2} = \alpha^2$), the second factor N_G^2 is combinatoric since we have N_G gravitons interacting with $N_G - 1 \simeq N_G$ gravitons and the third one comes from the characteristic energy of the process. This rate provides the time scale $\Delta t = \hbar \Gamma^{-1}$ of the emission process and allows us to find the depletion law

$$\frac{dN_G}{dt} \simeq -\hbar^{-1} \Gamma = -\frac{1}{\sqrt{N_G} \ell_p} + \mathcal{O}(N_G^{-1}) . \quad (3.1.9)$$

This emission process provides the link with the (purely gravitational part of) Hawking radiation as it accordingly leads to the standard decrease in the BH mass

$$\frac{dM}{dt} \simeq \frac{m_p}{\sqrt{N_G}} \frac{dN_G}{dt} \simeq -\frac{m_p}{N_G \ell_p} = -\frac{m_p^3}{\ell_p M^2} . \quad (3.1.10)$$

Upon defining the temperature

$$T = \frac{\hbar}{\sqrt{N_G} \ell_p} = \frac{m_p}{\sqrt{N_G}} , \quad (3.1.11)$$

which shows the same qualitative behaviour as the Hawking temperature (2.2.23), we see that BHs emit at a rate

$$\frac{dM}{dt} \simeq -\frac{T^2}{\hbar} , \quad (3.1.12)$$

with evaporation time given by

$$\tau \simeq N_G^{3/2} \ell_p = \ell_p \left(\frac{M}{m_p} \right)^3 . \quad (3.1.13)$$

Therefore, the Hawking temperature in this picture is not a thermodynamic quantity³. It emerges as a direct consequence of the phenomenon of quantum depletion of the Bose-Einstein condensate, in the semiclassical limit

$$N_G \rightarrow \infty, \quad \ell_p \rightarrow 0 , \quad (3.1.14)$$

while keeping $\lambda_G = \sqrt{N_G} \ell_p$ and \hbar finite. The classical limit of course reproduces the classical result that BHs have zero temperature.

3.1.2 Bekenstein entropy

Having a simple description of the quantum degrees of freedom of the BH, one would hope to give a straightforward interpretation the Bekenstein entropy. Indeed, on simply accounting the exponential scaling of the degeneracy of the N_G graviton states we find

$$S \simeq \log n_{\text{states}} \simeq N_G \simeq \frac{R_H^2}{\ell_p^2} . \quad (3.1.15)$$

in qualitative agreement with the Bekenstein-Hawking formula (2.2.26) where entropy scales with the horizon area.

³The thermodynamic temperature of a cold Bose-Einstein condensate is actually zero.

3.2 Corpuscular picture of a gravitational collapse

To summarize, the above proposal describes BHs by a large number of gravitons in the same (macroscopically large) state, thus realising a Bose-Einstein condensate at the critical point [54–60]. In particular, the constituents of such a self-gravitating object are assumed to be marginally bound in their gravitational potential well ⁴, whose size is given by the characteristic Compton-de Broglie wavelength $\lambda_G \sim R_H$ and whose depth is proportional to the very large number $N_G \sim M^2/m_p^2$ of soft quanta in this condensate [64–68]. In this picture, the role of matter is argued to be essentially negligible by considering the number of its degrees of freedom is subdominant with respect to the gravitational ones, especially when representing BHs of astrophysical size (see also Ref. [69–71]).

We shall here argue instead that matter actually plays an important role in the gravitational collapse ⁵. We will thus provide a qualitative description (based on Ref. [72]) showing that when the contribution of gravitons is properly related to the presence of ordinary baryonic matter, not only the picture enriches, but it also becomes clearly connected to the post-Newtonian approximation. The basic idea is very easy to explain: suppose we consider N baryons of rest mass μ very far apart, so that their total ADM energy [73] is simply given by $M = N \mu \equiv M_0$, where M_0 is the rest mass of the source. As these baryons fall towards each other, while staying inside a sphere of radius R , their (negative) gravitational energy is given by

$$U_{BG} \sim N \mu V_N \sim -\frac{\ell_p M^2}{m_p R}, \quad (3.2.1)$$

where $V_N \sim -\ell_p M/m_p R$ is the (negative) Newtonian potential. In terms of quantum physics, this gravitational potential can be represented by the expectation value of a scalar field $\hat{\Phi}$ over a coherent state $|g\rangle$,

$$\langle g | \hat{\Phi} | g \rangle \sim V_N. \quad (3.2.2)$$

A detailed coherent state description of classical scalar fields will be presented in Chapter 6. Let us only anticipate that the graviton number N_G generated by matter inside the sphere of radius R is determined by the normalisation of the coherent state and reproduces Bekenstein’s area law (3.1.15), that is

$$N_G \sim \frac{M^2}{m_p^2} \sim \frac{R_H^2}{\ell_p^2}, \quad (3.2.3)$$

⁴For improvements on this approximation, see Refs. [61–63].

⁵Of course, one could also envisage the creation of BHs by focusing gravitational waves, but highly energetic processes involving matter would presumably be needed in order to produce those waves in the first place.

where R_{H} is now the gravitational radius (2.1.4) of the sphere of baryons. In addition to that, assuming most gravitons have the same wave-length λ_{G} , the (negative) energy of each single graviton is correspondingly given by

$$\epsilon_{\text{G}} \sim \frac{U_{\text{BG}}}{N_{\text{G}}} \sim -\frac{m_{\text{p}} \ell_{\text{p}}}{R}, \quad (3.2.4)$$

which yields the typical Compton-de Broglie length $\lambda_{\text{G}} \sim R$. The graviton self-interaction energy is a crucial ingredient of the corpuscular picture as it is assumed to be responsible for the existence of the bound state of gravitons. In this context, it is easily shown to reproduce the (positive) post-Newtonian energy,

$$U_{\text{GG}}(R) \sim N_{\text{G}} \epsilon_{\text{G}} \langle g | \hat{\Phi} | g \rangle \sim \frac{\ell_{\text{p}}^2 M^3}{m_{\text{p}}^2 R^2}. \quad (3.2.5)$$

This view is consistent with the standard lore, since the $U_{\text{GG}} \ll |U_{\text{BG}}|$ for a star with size $R \gg R_{\text{H}}$. Furthermore, for $R \simeq R_{\text{H}}$, one has

$$U(R_{\text{H}}) \equiv U_{\text{BG}}(R_{\text{H}}) + U_{\text{GG}}(R_{\text{H}}) \simeq 0, \quad (3.2.6)$$

which is precisely the *maximal packing* condition (3.2). Unfortunately, this is only a speculation at this stage as the post-Newtonian approach fails to provide consistent results for $R \simeq R_{\text{H}}$. One could however entertain the idea that this condition justifies the *maximal packing* as an exclusive feature of BH configurations. We also remark once more the quantum picture is based on identifying the quantum state of the gravitational potential as a coherent state of (virtual) soft gravitons, which provides a link between the microscopic dynamics of gravity, understood in terms of interacting quanta, and the macroscopic description of a curved background. These issues will be addressed in the following Chapters.

Chapter 4

Effective scalar theory for the gravitational potential

In this Chapter we shall refine the post-Newtonian construction of Section 3.2 which is mainly based on simple energy considerations. Indeed, in the Newtonian theory, energy is a well-defined quantity and is conserved along physical trajectories (barring friction), which ensures the existence of a scalar potential for the gravitational force. In GR [74], the very concept of energy becomes much more problematic (see, e.g. [75] and References therein) and there is no invariant notion of a scalar potential. Even if one just considers the motion of test particles, the existence of conserved quantities along geodesics requires the presence of Killing vector fields. In sufficiently symmetric space-times, one may therefore end up with equations of motion containing potential terms, whose explicit form will still depend on the choice of observer (time and spatial coordinates). Overall, such premises allow for a “Newtonian-like” description of gravitating systems with strong space-time symmetries, like time-independence and isotropy, which can in turn be quantised by standard methods [47, 76].

We are aware that such a reduction of the degrees of freedom will not lead to any realistic conclusion on the microscopic nature of the gravitational interaction. However, it represents a useful simplification which will let us investigate spherically symmetric systems in analogy with what is usually done in GR when studying equilibrium configurations of the TOV equation (2.1.13). Actually, we are here particularly interested in static and isotropic compact sources, for which one can indeed determine an effective theory for the gravitational potential, up to a certain degree of confidence. When the local curvature of space-time is weak and test particles propagate at non-relativistic speed, non-linearities are suppressed. The geodesic equation of motion thereby takes the form of the standard Newtonian law with a potential determined by the Poisson equation, and Post-Newtonian corrections can be further obtained by including non-linear interaction terms. The inclusion of these non-linear terms in the quantum effective

description of the gravitational potential are precisely what we are going to address in this Chapter, inspired by the results of Section 3.2.

In the following, we will derive the effective action for a static and spherically symmetric potential from the Einstein-Hilbert action in the weak field and non-relativistic approximations. We shall then show that including higher order terms yields classical results in agreement with the standard post-Newtonian expansion of the Schwarzschild metric. Few explicit solutions to the corresponding classical field equations are studied.

4.1 Effective scalar theory for post-Newtonian potential

It is well known that a scalar field can be used as the potential for the velocity of a classical fluid [77, 78]. We will show here that it can also be used in order to describe the usual post-Newtonian correction that appears in the weak field expansion of the Schwarzschild metric. It is important to recall that this picture implicitly assumes the choice of a specific reference frame for static observers (for more details, see Appendix A)

Let us start from the Einstein-Hilbert action with matter [74]

$$S = S_{\text{EH}} + S_{\text{M}} = \int d^4x \sqrt{-g} \left(-\frac{1}{16\pi G_{\text{N}}} \mathcal{R} + \mathcal{L}_{\text{M}} \right), \quad (4.1.1)$$

where \mathcal{R} is the Ricci scalar and \mathcal{L}_{M} is the Lagrangian density for the baryonic matter that sources the gravitational field. In order to recover the post-Newtonian approximation in this framework, we must assume the local curvature is small, so that the metric can be written as $g_{\mu\nu} = \eta_{\mu\nu} + h_{\mu\nu}$, where $\eta_{\mu\nu}$ is the flat Minkowski metric and $|h_{\mu\nu}| \ll 1$. The Ricci scalar then takes the simple form

$$\mathcal{R} = \square h - \partial^\mu \partial^\nu h_{\mu\nu} + \mathcal{O}(h^2), \quad (4.1.2)$$

where \square is the d'Alembertian in flat space, the trace $h = \eta_{\mu\nu} h^{\mu\nu}$, and the linearised Einstein field equation is given by

$$-\square h_{\mu\nu} + \eta_{\mu\nu} \square h + \partial_\mu \partial^\lambda h_{\lambda\nu} + \partial_\nu \partial^\lambda h_{\lambda\mu} - \eta_{\mu\nu} \partial^\lambda \partial^\rho h_{\lambda\rho} - \partial_\mu \partial_\nu h = 16\pi G_{\text{N}} T_{\mu\nu}. \quad (4.1.3)$$

In the de Donder gauge,

$$2\partial^\mu h_{\mu\nu} = \partial_\nu h, \quad (4.1.4)$$

the trace of the field equation yields

$$\square h = 16\pi G_{\text{N}} T, \quad (4.1.5)$$

4.1 Effective scalar theory for post-Newtonian potential

where $T = \eta^{\mu\nu} T_{\mu\nu}$, and Eq. (4.1.3) reduces to

$$-\square h_{\mu\nu} = 16 \pi G_N \left(T_{\mu\nu} - \frac{1}{2} \eta_{\mu\nu} T \right) . \quad (4.1.6)$$

In addition to the weak field limit, we assume that all matter in the system moves with a characteristic velocity much slower than the speed of light in the (implicitly) chosen reference frame $x^\mu = (t, \mathbf{x})$. The only relevant component of the metric is therefore $h_{00}(\mathbf{x})$, and its time derivatives are also neglected¹. The Ricci scalar reduces to

$$\mathcal{R} \simeq \Delta h_{00}(\mathbf{x}) , \quad (4.1.7)$$

and the stress-energy tensor is accordingly determined solely by the energy density in this non-relativistic regime,

$$T_{\mu\nu} = \frac{2}{\sqrt{-g}} \frac{\delta S_M}{\delta g^{\mu\nu}} = 2 \frac{\delta \mathcal{L}_M}{\delta g^{\mu\nu}} - g_{\mu\nu} \mathcal{L}_M \simeq u_\mu u_\nu \rho(\mathbf{x}) , \quad (4.1.8)$$

where $u^\mu = \delta_0^\mu$ is the four-velocity of the static source fluid. Note further that the above stress-energy tensor follows from the simple matter Lagrangian

$$\mathcal{L}_M \simeq -\rho(\mathbf{x}) , \quad (4.1.9)$$

as one can see from the variation of the baryonic matter density [79]

$$\delta \rho = \frac{1}{2} \rho (g_{\mu\nu} + u_\mu u_\nu) \delta g^{\mu\nu} , \quad (4.1.10)$$

and the well-known formula

$$\delta (\sqrt{-g}) = -\frac{1}{2} \sqrt{-g} g_{\mu\nu} \delta g^{\mu\nu} . \quad (4.1.11)$$

This is indeed the case of interest to us here, since we do not consider explicitly the matter dynamics but only how (static) matter generates the gravitational field in the non-relativistic limit, in which the matter pressure is negligible [77, 78]². In this approximation, Eq. (4.1.6) takes the very simple form

$$\Delta h_{00}(\mathbf{x}) = -8 \pi G_N T_{00}(\mathbf{x}) = -8 \pi G_N \rho(\mathbf{x}) , \quad (4.1.12)$$

since $T_{00} = \rho$ to leading order. Finally, we know the Newtonian potential $V = V_N$ is generated by the density ρ according to the Poisson equation

$$\Delta V = 4 \pi G_N \rho , \quad (4.1.13)$$

¹For static configurations, the gauge condition (4.1.4) becomes Eq. (B.13), and is always satisfied.

²A non-negligible matter pressure complicates the system significantly and it will be considered later in Chapter 5.

4. Effective scalar theory for the gravitational potential

which lets us identify $h_{00} = -2V$.

It is now straightforward to introduce an effective scalar field theory for the gravitational potential. First of all, we shall just consider (static) spherically symmetric systems, so that $\rho = \rho(r)$ and $V = V(r)$, correspondingly. We replace the Einstein-Hilbert action S_{EH} in Eq. (4.1.1) with the massless Fierz-Pauli action so that, in the approximation (4.1.8) and (4.1.9), we obtain the total Lagrangian (see Appendix B)

$$\begin{aligned} L_{\text{N}}[V] &\simeq 4\pi \int_0^\infty r^2 dr \left(\frac{1}{32\pi G_{\text{N}}} h_{00} \Delta h_{00} + \frac{h_{00}}{2} \rho \right) \\ &= 4\pi \int_0^\infty r^2 dr \left(\frac{V \Delta V}{8\pi G_{\text{N}}} - \rho V \right) \\ &= -4\pi \int_0^\infty r^2 dr \left[\frac{(V')^2}{8\pi G_{\text{N}}} + \rho V \right], \end{aligned} \quad (4.1.14)$$

where we integrated by parts³ and

$$\Delta f \equiv r^{-2} (r^2 f')'. \quad (4.1.15)$$

Varying this Lagrangian with respect to V , we obtain Eq. (4.1.13) straightforwardly⁴.

In order to go beyond the Newtonian approximation, we need to modify the latter functional by adding non-linearities. We start by computing the Hamiltonian,

$$H_{\text{N}}[V] = -L_{\text{N}}[V] = 4\pi \int_0^\infty r^2 dr \left(-\frac{V \Delta V}{8\pi G_{\text{N}}} + \rho V \right), \quad (4.1.16)$$

as follows from the static approximation. If we evaluate this expression on-shell by means of Eq. (4.1.13), we get the Newtonian potential energy

$$\begin{aligned} U_{\text{N}}[V] &= 2\pi \int_0^\infty r^2 dr \rho V \\ &= \frac{1}{2G_{\text{N}}} \int_0^\infty r^2 dr V \Delta V \\ &= -4\pi \int_0^\infty r^2 dr \frac{(V')^2}{8\pi G_{\text{N}}}, \end{aligned} \quad (4.1.17)$$

where we also assumed that boundary terms vanish at $r = 0$ and $r = \infty$ as usual in the last line (for an alternative but equivalent derivation, see Appendix C). One can therefore view the above U_{N} as given by the interaction of the matter distribution with the gravitational field or, following Ref. [72] (see also Ref. [80]), as the volume integral

³The boundary conditions that ensure vanishing of boundary terms will be explicitly shown when necessary.

⁴Were one to identify the Lagrangian density in Eq. (4.1.14) with the pressure p_{N} of the gravitational field, it would appear the Newtonian potential has the equation of state $p_{\text{N}} = -\rho_{\text{N}}/3$ [77, 78].

4.1 Effective scalar theory for post-Newtonian potential

of the gravitational current proportional to the gravitational energy U_N per unit volume $\delta\mathcal{V} = 4\pi r^2 \delta r$, that is ⁵

$$J_V \simeq 4 \frac{\delta U_N}{\delta\mathcal{V}} = -\frac{[V']^2}{2\pi G_N} . \quad (4.1.18)$$

The appearance of the above contribution can in fact be found at the next-to-leading order (NLO) in the expansion of the theory (4.1.1). As is shown in Appendix B, the current J_V is in particular proportional to the NLO term (B.10) coming from the geometric part of the action. Upon including this new source term, together with its matter counterpart (B.11) from the expansion of the matter Lagrangian, we obtain the total Lagrangian in Eq. (B.12) for a self-interacting scalar field V , namely

$$\begin{aligned} L[V] &= 4\pi \int_0^\infty r^2 dr \left[\frac{V \Delta V}{8\pi G_N} - \rho V + q_\Phi (2V\rho - J_V)V \right] \\ &= 4\pi \int_0^\infty r^2 dr \left[\frac{V \Delta V}{8\pi G_N} - V\rho(1 - 2q_\Phi V) + \frac{q_\Phi}{2\pi G_N} V (V')^2 \right] \\ &= -4\pi \int_0^\infty r^2 dr \left[\frac{(V')^2}{8\pi G_N} (1 - 4q_\Phi V) + V\rho(1 - 2q_\Phi V) \right] , \end{aligned} \quad (4.1.19)$$

where the parameter q_Φ keeps track of NLO terms in the expansion (see again Appendix B for the details). It is important to remark that, beyond the linear order, the construction of an effective theory from the Einstein-Hilbert action (4.1.1) is plagued by inconsistencies when coupled to matter. In order to overcome these issues, the NLO has therefore been constructed from the Pauli-Fierz action so as not to spoil the Newtonian approximation [15–17, 81–84]. We will show in the following that the post-Newtonian correction (A.21) is indeed properly recovered for $q_\Phi = 1$.

The Euler-Lagrange equation for V is given by

$$\begin{aligned} 0 &= \frac{\delta\mathcal{L}}{\delta V} - \frac{d}{dr} \left(\frac{\delta\mathcal{L}}{\delta V'} \right) \\ &= 4\pi r^2 \left[-\rho + 4q_\Phi \rho V + \frac{q_\Phi}{2\pi G_N} (V')^2 \right] + \frac{1}{G_N} [r^2 V' (1 - 4q_\Phi V)]' , \end{aligned} \quad (4.1.20)$$

and we obtain the field equation

$$(1 - 4q_\Phi V) \Delta V = 4\pi G_N \rho (1 - 4q_\Phi V) + 2q_\Phi (V')^2 . \quad (4.1.21)$$

This differential equation is obviously hard to solve analytically for a general source. We will therefore expand the field V up to first order in the coupling q_Φ ⁶,

$$V(r) = V_{(0)}(r) + q_\Phi V_{(1)}(r) , \quad (4.1.22)$$

⁵The factor of 4 in the expression (4.1.18) of J_V is chosen in order to recover the expected first post-Newtonian correction in the vacuum potential for the coupling constant $q_\Phi = 1$ (see Appendix B and Section 4.2.1 for details).

⁶Since Eq. (4.1.21) is obtained from a Lagrangian defined up to first order in q_Φ , higher-order terms in the solution would not be meaningful.

4. Effective scalar theory for the gravitational potential

and solve Eq. (4.1.21) order by order. In particular, we have

$$\Delta V_{(0)} = 4 \pi G_N \rho , \quad (4.1.23)$$

which, when $q_B = 1$, is just the Poisson Eq. (4.1.13) for the Newtonian potential and

$$\Delta V_{(1)} = 2 (V'_{(0)})^2 , \quad (4.1.24)$$

which gives the correction at first order in q_Φ .

To linear order in q_Φ , the on-shell Hamiltonian (4.1.16) is also replaced by

$$\begin{aligned} H[V] &= -L[V] \\ &\simeq 4 \pi \int_0^\infty r^2 dr \left\{ -\frac{V}{2} \left[\rho + \frac{q_\Phi}{2 \pi G_N} (V')^2 \right] + \rho V - \frac{q_\Phi}{2 \pi G_N} V (V')^2 \right\} \\ &\simeq 2 \pi \int_0^\infty dr r^2 \left[\rho V (1 - 4 q_\Phi V) - q_\Phi \frac{3}{2 \pi G_N} V (V'^2) \right] , \end{aligned} \quad (4.1.25)$$

where we used Eq. (4.1.21). In the following, we will still denote the on-shell contribution containing the matter density ρ with

$$U_{\text{BG}} = 2 \pi \int_0^\infty r^2 dr \rho [V_{(0)} + q_\Phi (V_{(1)} - 4 V_{(0)}^2)] + \mathcal{O}(q_\Phi^2) , \quad (4.1.26)$$

which reduces to the Newtonian U_N in Eq. (4.1.17) for $q_\Phi = 0$, and the rest as

$$U_{\text{GG}} = -3 q_\Phi G_N \int_0^\infty r^2 dr V_{(0)} (V'_{(0)})^2 + \mathcal{O}(q_\Phi^2) . \quad (4.1.27)$$

4.2 Classical solutions

We will now study the general classical solutions to Eqs. (4.1.23) and (4.1.24). Since we are interested in static and spherically symmetric sources, it is convenient to consider eigenfunctions of the Laplace operator,

$$\Delta j_0(k r) = -k^2 j_0(k r) , \quad (4.2.1)$$

that is, the spherical Bessel function of the first kind

$$j_0(k r) = \frac{\sin(k r)}{k r} , \quad (4.2.2)$$

which enjoys the normalisation

$$4 \pi \int_0^\infty r^2 dr j_0(p r) j_0(k r) = \frac{2 \pi^2}{k^2} \delta(p - k) . \quad (4.2.3)$$

Assuming the matter density is a smooth function of the radial coordinate, we can project it on the above modes,

$$\tilde{\rho}(k) = 4 \pi \int_0^\infty r^2 dr j_0(k r) \rho(r) , \quad (4.2.4)$$

4.2 Classical solutions

and likewise

$$\tilde{V}_{(n)}(k) = 4\pi \int_0^\infty r^2 dr j_0(kr) V_{(n)}(r) . \quad (4.2.5)$$

Inverting these expressions, one obtains the expansions in Laplacian eigenfunctions,

$$f(r) = \int_0^\infty \frac{k^2 dk}{2\pi^2} j_0(kr) \tilde{f}(k) , \quad (4.2.6)$$

in which we used

$$\int \frac{d^3k}{(2\pi)^3} = \int_0^\infty \frac{k^2 dk}{2\pi^2} , \quad (4.2.7)$$

since all our functions only depend on the radial momentum $k \geq 0$.

The zero-order Eq. (4.1.23) in momentum space reads

$$\tilde{V}_{(0)}(k) = -4\pi \frac{G_N \tilde{\rho}(k)}{k^2} , \quad (4.2.8)$$

which can be inverted to yield the solution

$$V_{(0)}(r) = -2G_N \int_0^\infty \frac{dk}{\pi} j_0(kr) \tilde{\rho}(k) . \quad (4.2.9)$$

The r.h.s. of Eq. (4.1.24) can then be written as

$$2(V'_{(0)}(r))^2 = 8G_N^2 \left(\int_0^\infty \frac{k dk}{\pi} j_1(kr) \tilde{\rho}(k) \right)^2 , \quad (4.2.10)$$

where we used Eq. (4.2.8) and

$$[j_0(kr)]' = -k j_1(kr) . \quad (4.2.11)$$

The first-order Eq. (4.1.24) is however easier to solve directly in coordinate space usually.

For example, for a point-like source of mass M_0 , whose density is given by

$$\rho = M_0 \delta^{(3)}(\mathbf{x}) = \frac{M_0}{4\pi r^2} \delta(r) , \quad (4.2.12)$$

one finds

$$\tilde{\rho}(k) = M_0 \int_0^\infty dr j_0(kr) \delta(r) = M_0 , \quad (4.2.13)$$

and Eq. (4.2.8) yields the Newtonian potential outside a spherical source of mass M_0 , that is

$$V_{(0)}(r) = -2 \frac{G_N M_0}{r} \int_0^\infty \frac{dz}{\pi} j_0(z) = -\frac{G_N M_0}{r} . \quad (4.2.14)$$

4. Effective scalar theory for the gravitational potential

Note that this solution automatically satisfies the regularity condition

$$\lim_{r \rightarrow \infty} V_{(0)}(r) = 0 . \quad (4.2.15)$$

Next, for $r > 0$, one has

$$\begin{aligned} 2 (V'_{(0)}(r))^2 &= \frac{8 G_{\text{N}}^2 M_0^2}{r^4} \left(\int_0^\infty \frac{z \, dz}{\pi} j_1(z) \right)^2 \\ &= \frac{2 G_{\text{N}}^2 M_0^2}{r^4} , \end{aligned} \quad (4.2.16)$$

and Eq. (4.1.24) admits the general solution

$$V_{(1)} = A_1 - \frac{G_{\text{N}} M_1}{r} + \frac{G_{\text{N}}^2 M_0^2}{r^2} . \quad (4.2.17)$$

On imposing the same boundary condition (4.2.15) to $V_{(1)}$, one obtains $A_1 = 0$. The arbitrary constant M_1 results in a (arbitrary) shift of the ADM mass,

$$M = M_0 + q_{\Phi} M_1 , \quad (4.2.18)$$

and one is therefore left with the potential

$$V = -\frac{G_{\text{N}} M}{r} + q_{\Phi} \frac{G_{\text{N}}^2 M^2}{r^2} + \mathcal{O}(q_{\Phi}^2) . \quad (4.2.19)$$

This expression matches the expected post-Newtonian form (A.21) at large r for $q_{\Phi} = 1$. It also clearly shows the limitation of the present approach: at small r , the post-Newtonian correction $V_{(1)}$ grows faster than $V_{(0)} = V_{\text{N}}$ and our perturbative approach will necessarily break down.

We can also evaluate the potential energy (4.1.25) generated by the point-like source. The baryon-graviton energy (4.1.26) of course diverges, but we can regularise the matter density (4.2.12) by replacing $\delta(r) \rightarrow \delta(r - r_0)$, where $0 < r_0 \ll G_{\text{N}} M_0$. We then find

$$U_{\text{BG}} \simeq -\frac{G_{\text{N}} M_0 M}{2 r_0} - q_{\Phi} \frac{3 G_{\text{N}}^2 M^3}{2 r_0^2} . \quad (4.2.20)$$

With the same regularisation, we obtain the graviton-graviton energy

$$U_{\text{GG}} \simeq -3 q_{\Phi} G_{\text{N}} \int_{r_0}^{\infty} r^2 \, dr V_{(0)} (V'_{(0)})^2 = q_{\Phi} \frac{3 G_{\text{N}}^2 M^3}{2 r_0^2} , \quad (4.2.21)$$

which precisely cancels against the first order correction to U_{BG} in Eq. (4.2.20), and

$$U = U_{\text{BG}} + U_{\text{GG}} = -\frac{G_{\text{N}} M_0 M}{2 r_0} . \quad (4.2.22)$$

Of course, for $r \simeq r_0 \ll G_{\text{N}} M_0$, the post-Newtonian term in Eq. (4.2.19) becomes much larger than the Newtonian contribution, which pushes the above U_{BG} and U_{GG} beyond

4.2 Classical solutions

the regime of validity of our approximations. Nonetheless, it is important to notice that, given the effective Lagrangian (4.1.19), the total gravitational energy (4.2.22) for a point-like source will never vanish and the maximal packing condition (3.2) cannot be realised. This is consistent with the concept of corpuscular BHs as quantum objects with a (very) large spatial extensions $R \sim R_{\text{H}}$.

For the reasons above, we shall next study extended distributions of matter, which will indeed lead to different, more sensible results within the scope of our approach.

4.2.1 Homogeneous ball in vacuum

For an arbitrary matter density, it is hopeless to solve the equation (4.1.24) for $V_{(1)}$ analytically. Let us then consider the very simple case in which ρ is uniform inside a sphere of radius R ,

$$\rho(r) = \frac{3 M_0}{4 \pi R^3} \Theta(R - r) , \quad (4.2.23)$$

where Θ is the Heaviside step function and

$$M_0 = 4 \pi \int_0^\infty r^2 dr \rho(r) \quad (4.2.24)$$

is the rest mass of the spherical source. For this matter density, we shall now solve Eqs. (4.1.23) and (4.1.24) with boundary conditions that ensure V is regular both at the origin $r = 0$ and infinity, that is

$$V'_{(n)}(0) = \lim_{r \rightarrow \infty} V_{(n)}(r) = 0 , \quad (4.2.25)$$

and smooth across the border $r = R$,

$$\lim_{r \rightarrow R^-} V_{(n)}(r) = \lim_{r \rightarrow R^+} V_{(n)}(r) , \quad \lim_{r \rightarrow R^-} V'_{(n)}(r) = \lim_{r \rightarrow R^+} V'_{(n)}(r) . \quad (4.2.26)$$

The solution to Eq. (4.1.23) inside the sphere is then given by

$$V_{(0)\text{in}}(r) = \frac{G_{\text{N}} M_0}{2 R^3} (r^2 - 3 R^2) \quad (4.2.27)$$

while outside

$$V_{(0)\text{out}}(r) = -\frac{G_{\text{N}} M_0}{r} , \quad (4.2.28)$$

which of course equal the Newtonian potential.

At first order in q_{Φ} we instead have

$$V_{(1)\text{in}}(r) = \frac{G_{\text{N}}^2 M_0^2}{10 R^6} (r^4 - 15 R^4) \quad (4.2.29)$$

4. Effective scalar theory for the gravitational potential

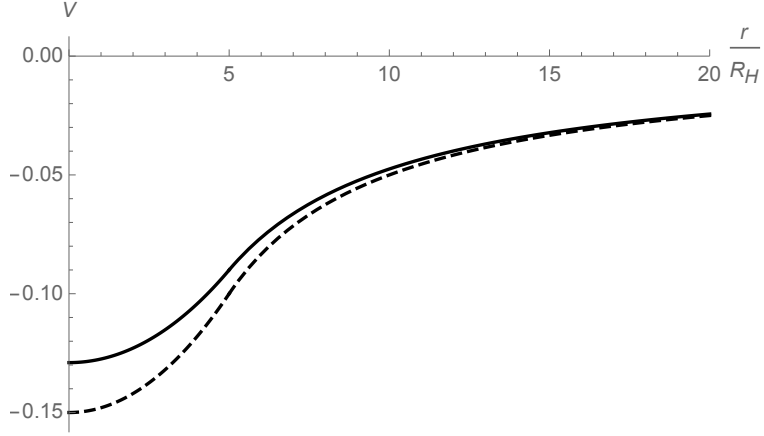


Figure 4.1: Potential to first order in q_Φ (solid line) vs Newtonian potential (dashed line) for $R = 10 G_N M \equiv 5 R_H$ and $q_\Phi = 1$.

and

$$V_{(1)\text{out}}(r) = \frac{G_N^2 M_0^2}{5 R} \frac{5 R - 12 r}{r^2} . \quad (4.2.30)$$

The complete outer solution to first order in q_Φ is thus given by

$$V_{\text{out}}(r) = -\frac{G_N M_0}{r} \left(1 + q_\Phi \frac{12 G_N M_0}{5 R} \right) + q_\Phi \frac{G_N^2 M_0^2}{r^2} + \mathcal{O}(q_\Phi^2) . \quad (4.2.31)$$

From this outer potential, we see that, unlike for the point-like source, we are left with no arbitrary constant and the ADM mass is determined as

$$M = M_0 \left(1 + q_\Phi \frac{12 G_N M_0}{5 R} \right) + \mathcal{O}(q_\Phi^2) , \quad (4.2.32)$$

and, replacing this expression into the solutions, we finally obtain

$$V_{\text{in}}(r) = \frac{G_N M}{2 R^3} (r^2 - 3 R^2) + q_\Phi \frac{G_N^2 M^2}{10 R^6} (r^4 - 12 R^2 r^2 + 21 R^4) + \mathcal{O}(q_\Phi^2) \quad (4.2.33)$$

$$V_{\text{out}}(r) = -\frac{G_N M}{r} + q_\Phi \frac{G_N^2 M^2}{r^2} + \mathcal{O}(q_\Phi^2) . \quad (4.2.34)$$

We can now see that the outer field again reproduces the first post-Newtonian result (A.21) of Appendix A when $q_\Phi = 1$ (see Figs. 4.1 and 4.2 for two examples).

Since the density (4.2.23) is sufficiently regular, we can evaluate the corresponding gravitational energy (4.1.25) without the need of a regulator. The baryon-graviton energy (4.1.26) is found to be

$$\begin{aligned} U_{\text{BG}}(R) &= 2 \pi \int_0^R r^2 dr \rho [V_{(0)\text{in}} + q_\Phi (V_{(1)\text{in}} - 4 V_{(0)\text{in}}^2)] + \mathcal{O}(q_\Phi^2) \\ &= -\frac{3 G_N M^2}{5 R} - q_\Phi \frac{267 G_N^2 M^3}{350 R^2} + \mathcal{O}(q_\Phi^2) \\ &\equiv U_{(0)\text{BG}}(R) + q_\Phi U_{(1)\text{BG}}(R) + \mathcal{O}(q_\Phi^2) , \end{aligned} \quad (4.2.35)$$

4.2 Classical solutions

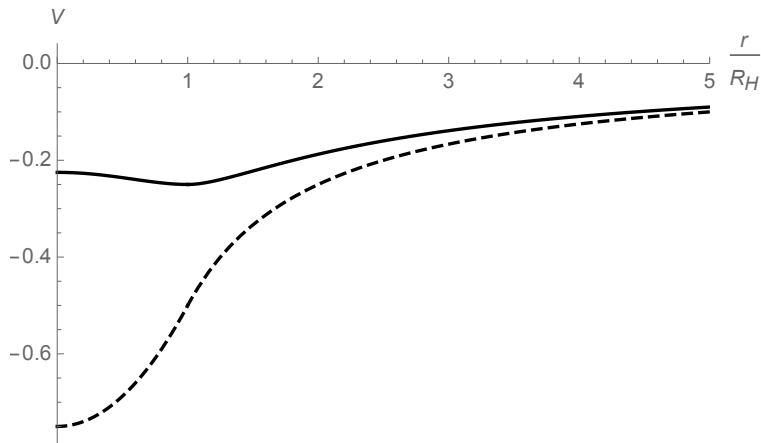


Figure 4.2: Potential to first order in q_Φ (solid line) vs Newtonian potential (dashed line) for $R = 2 G_N M \equiv R_H$ and $q_\Phi = 1$.

where $U_{(0)\text{BG}}$ is just the Newtonian contribution and $U_{(1)\text{BG}}$ the post-Newtonian correction. Analogously, the self-sourcing contribution (4.1.27) gives

$$\begin{aligned} U_{\text{GG}}(R) &= -3 q_\Phi \frac{1}{G_N} \left[\int_0^R r^2 dr V_{(0)\text{in}} (V'_{(0)\text{in}})^2 + \int_R^\infty r^2 dr V_{(0)\text{out}} (V'_{(0)\text{out}})^2 \right] + \mathcal{O}(q_\Phi^2) \\ &= q_\Phi \frac{153 G_N^2 M_0^3}{70 R^2} + \mathcal{O}(q_\Phi^2). \end{aligned} \quad (4.2.36)$$

Since now $U_{\text{GG}} > q_\Phi |U_{(1)\text{BG}}|$, adding the two terms together yields the total gravitational energy

$$U(R) = -\frac{3 G_N M^2}{5 R} + q_\Phi \frac{249 G_N^2 M^3}{175 R^2} + \mathcal{O}(q_\Phi^2), \quad (4.2.37)$$

which appears in line with what was estimated in Ref. [72]: the (order q_Φ) post-Newtonian energy is positive, and would equal the Newtonian contribution for a source of radius

$$R \simeq \frac{83 G_N M}{35} \simeq 1.2 R_H, \quad (4.2.38)$$

where we set $q_\Phi = 1$. One has therefore recovered the “maximal packing” condition (3.2) of Refs. [12–14, 85–88] in the limit $R \sim R_H$ from a regular matter distribution. However, note that, strictly speaking, the above value of R falls outside the regime of validity of our approximations.

4.2.2 Gaussian matter distribution

As an example of even more regular matter density, we can consider a Gaussian distribution of width σ ,

$$\rho(r) = \frac{M_0 e^{-\frac{r^2}{\sigma^2}}}{\pi^{3/2} \sigma^3}, \quad (4.2.39)$$

4. Effective scalar theory for the gravitational potential

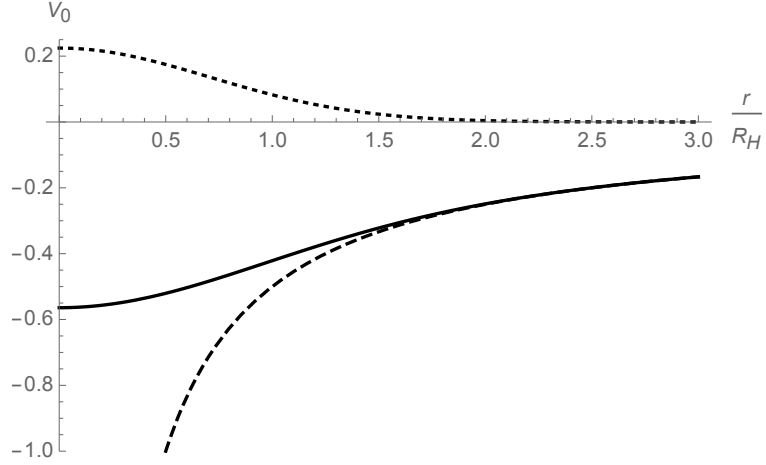


Figure 4.3: Newtonian potential (solid line) for Gaussian matter density with $\sigma = 2 G_N M_0$ (dotted line) vs Newtonian potential (dashed line) for point-like source of mass M_0 .

where again

$$M_0 = 4 \pi \int_0^\infty r^2 dr \rho(r) . \quad (4.2.40)$$

Let us remark that the above density is essentially zero for $r \gtrsim R \equiv 3 \sigma$, which will allow us to make contact with the previous case.

For this matter density, we shall now solve Eqs. (4.1.23) and (4.1.24) with the boundary conditions (4.2.25) that ensure V is regular both at the origin $r = 0$ and at infinity. We first note that Eq. (4.2.4) yields

$$\tilde{\rho}(k) = M_0 e^{-\frac{\sigma^2 k^2}{4}} , \quad (4.2.41)$$

from which

$$\begin{aligned} V_{(0)}(r) &= -2 G_N M_0 \int_0^\infty \frac{dk}{\pi} j_0(k r) e^{-\frac{\sigma^2 k^2}{4}} \\ &= -\frac{G_N M_0}{r} \text{Erf}(r/\sigma) . \end{aligned} \quad (4.2.42)$$

For a comparison with the analogous potential generated by a point-like source with the same mass M_0 , see Fig. 4.3. For $r \gtrsim R = 3 \sigma = 3 R_H/2$, the two potentials are clearly indistinguishable, whereas $V_{(0)}$ looks very similar to the case of homogeneous matter for $0 \leq r < R$ (see Fig. 4.1).

The first-order equation (4.1.24) now reads

$$\Delta V_{(1)} = 2 \frac{G_N^2 M_0^2}{r^4} \left[\text{Erf}(r/\sigma) - \frac{2r}{\sqrt{\pi} \sigma} e^{-\frac{r^2}{\sigma^2}} \right]^2 \equiv 2 G_N^2 M_0^2 G(r) , \quad (4.2.43)$$

4.2 Classical solutions

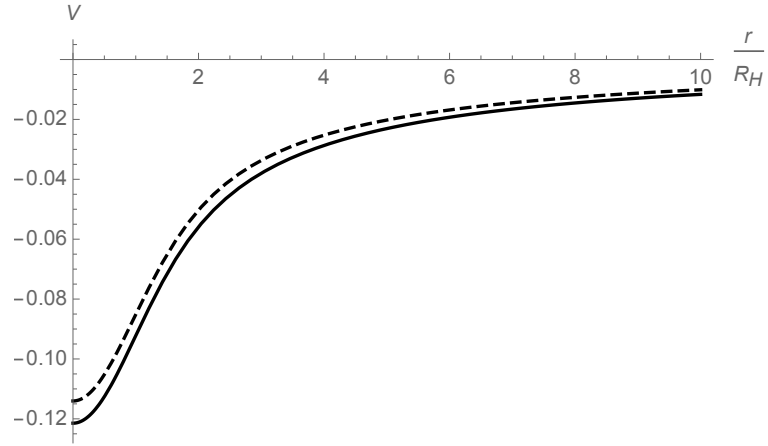


Figure 4.4: Potential up to first order in q_Φ (solid line) vs Newtonian potential (dashed line) for Gaussian matter density with $\sigma = 2 G_N M \equiv R_H$ (with $q_\Phi = 1$).

and we note that

$$G(r) \simeq \begin{cases} \frac{16 r^2}{9 \pi \sigma^6} & \text{for } r \rightarrow 0 \\ \frac{1}{r^4} & \text{for } r \rightarrow \infty, \end{cases} \quad (4.2.44)$$

which are the same asymptotic behaviours one finds for a homogeneous source of size $R \sim \sigma$. We can therefore expect the proper solution to Eq. (4.2.43) behaves like Eq. (4.2.29) for $r \rightarrow 0$ and (4.2.30) for $r \rightarrow \infty$. In fact, one finds

$$V_{(1)} = 2 G_N^2 M_0^2 \left\{ \frac{[\text{erf}(\frac{r}{\sigma})]^2 - 1}{\sigma^2} - \frac{\sqrt{2} \text{erf}(\sqrt{2} \frac{r}{\sigma})}{\sqrt{\pi} \sigma r} + \frac{[\text{erf}(\frac{r}{\sigma})]^2}{2 r^2} + \frac{2 e^{-\frac{r^2}{\sigma^2}} \text{erf}(\frac{r}{\sigma})}{\sqrt{\pi} \sigma r} \right\} \quad (4.2.45)$$

in which we see the second term in curly brackets again leads to a shift in the ADM mass,

$$M = M_0 \left(1 + q_\Phi \frac{2 \sqrt{2} G_N M_0}{\sqrt{\pi} \sigma} \right), \quad (4.2.46)$$

while the third term reproduces the usual post-Newtonian potential (A.21) for $r \gg \sigma$. For an example of the complete potential up to first order in q_Φ , see Fig. 4.4. Note that for the relatively small value of σ used in that plot, the main effect of $V_{(1)}$ in Eq. (4.2.45) is to increase the ADM mass according to Eq. (4.2.46), which lowers the total potential significantly with respect to the Newtonian curve for $M = M_0$ shown in Fig. 4.3.

Chapter 5

Bootstrapped Newtonian gravity: classical picture

In Chapter 4 we studied an effective equation for the gravitational potential of a static source which contains a gravitational self-interaction term besides the usual Newtonian coupling with the matter density. This equation was derived in details from a Fierz-Pauli Lagrangian, and it can therefore be viewed as stemming from the truncation of the relativistic theory at some “post-Newtonian” order (for the standard post-Newtonian formalism, see Ref. [89]). However, since the “post-Newtonian” correction $V_{\text{PN}} \sim M^2/r^2$ is positive and grows faster than the Newtonian potential $V_{\text{N}} \sim M/r$ near the surface of the source, one is allowed to consider only matter sources with radius $R \gg R_{\text{H}}$ in this approximation. This consistency condition clearly excludes the possibility to study very compact matter sources and, in particular, those with $R \simeq R_{\text{H}}$ which are on the verge of forming a BH. Moreover, since we are mainly interested in investigating the possibility that matter collapsed inside a BH ends up in a static configuration, a pressure term which prevents the gravitational collapse needs to be included from the onset. For this reason, we here modify the effective theory used in Chapter 4 in order to consistently supplement the matter density with the pressure as sources of the gravitational potential, as it naturally happens in GR. In addition, for the ultimate purpose of describing very compact sources, we shall here study the non-linear equation of the resulting effective theory at face value, without requiring that the corrections it introduces with respect to the Newtonian potential remain small.

This procedure, which essentially consists in including a gravitational self-interaction in the Poisson equation and treat it non-perturbatively, is what we call *bootstrapping Newtonian gravity*. We then use this assumption to study systems with generic compactness $G_{\text{N}} M/R \sim R_{\text{H}}/R$, from the regime $R \gg R_{\text{H}}$, in which we recover the standard post-Newtonian picture, to $R \ll R_{\text{H}}$ where we find the source is enclosed within a horizon. The latter is defined according to the Newtonian view as the location at which

the escape velocity of test particles equals the speed of light. Of course, it should be possible to treat the single microscopic constituents of the source in this test particle approximation and the presence of an horizon therefore refers to their inability to escape the gravitational pull.

Like in Chapter 4, we shall just consider (static) spherically symmetric systems, so that all quantities depend only on the radial coordinate r , and the matter density $\rho = \rho(r)$ will also be assumed homogeneous inside the source ($r \leq R$) for the sake of simplicity. The pressure will instead be determined consistently from the condition of staticity.

5.1 Bootstrapped gravitational potential

We already showed in Chapter 4 that a non-linear equation for the potential $V = V(r)$ describing the gravitational pull on test particles generated by a matter density $\rho = \rho(r)$ can be obtained starting from the Newtonian Lagrangian $L_N[V]$ (4.1.14) after including the effects of self-interaction by coupling the field with its own energy density. In other words, we coupled the field V with the gravitational current J_V in Eq. (4.1.18). As mentioned at the beginning of this Chapter, we now need to add a pressure term accounting for the pressure p which prevents the system from collapsing. From a purely Newtonian point of view, pressure only represents an external contribution required by hydrostatic equilibrium. Such a Newtonian approach has been pursued in Ref. [19] and, as one would expect, it was found that the pressure energy becomes very large when describing static compact sources with a size $R \lesssim R_H$. We must therefore add a corresponding potential energy U_B as a source of the gravitational potential, as it naturally happens in GR, where the gravitational field is coupled to the energy-momentum tensor [74]. The most straightforward way to do so in this context, is to define U_B as the potential energy associated with the work done by the force responsible for the pressure p , such that

$$p \simeq -\frac{\delta U_B}{\delta \mathcal{V}} = J_B . \quad (5.1.1)$$

We will accordingly have to couple the potential field with the energy densities J_V and J_B . In a similar fashion, we can then interpret the analogous higher order term coming from the matter Lagrangian (see Appendix B) as the coupling of a matter current

$$J_\rho = -2V^2 \quad (5.1.2)$$

5.1 Bootstrapped gravitational potential

with the matter sector, *i.e.* with the total matter energy density $\rho + 3 q_B p$. Upon including these new source terms, we obtain the total Lagrangian

$$\begin{aligned} L[V] &= L_N[V] - 4\pi \int_0^\infty r^2 dr [q_V J_V V + 3 q_B J_B V + q_\rho J_\rho (\rho + 3 q_B p)] \\ &= -4\pi \int_0^\infty r^2 dr \left[\frac{(V')^2}{8\pi G_N} (1 - 4 q_V V) + V (\rho + 3 q_B p) \right. \\ &\quad \left. - 2 q_\rho V^2 (\rho + 3 q_B p) \right]. \end{aligned} \quad (5.1.3)$$

The parameters q_V , q_B and q_ρ play the role of coupling constants¹ for the three different currents J_V , J_B and J_ρ respectively. They also allow us to control the origin of nonlinearities, as we recover the Newtonian Lagrangian (4.1.14) by setting all of them equal to zero.

The associated effective Hamiltonian is simply given by

$$H[V] = -L[V], \quad (5.1.4)$$

and the Euler-Lagrange equation for V reads

$$(1 - 4 q_V V) \Delta V = 4\pi G_N (\rho + 3 q_B p) - 16\pi G_N q_\rho V (\rho + 3 q_B p) + 2 q_V (V')^2. \quad (5.1.5)$$

The latter must be supplemented with the conservation equation that determines the pressure,

$$p' = -V' (\rho + p), \quad (5.1.6)$$

which can be seen as a correction to the usual Newtonian formula that accounts for the contribution of the pressure to the energy density, or as an approximation for the Tolman-Oppenheimer-Volkoff equation (2.1.13) of GR.

Although we showed the three parameters q_V , q_B and q_ρ explicitly, we shall only consider $q_V = 3 q_B = q_\rho = 1$ in the following for the sake of simplicity. In this case, Eq. (5.1.5) reduces to

$$\Delta V = 4\pi G_N (\rho + p) + \frac{2 (V')^2}{1 - 4V}, \quad (5.1.7)$$

from which we see that the differences with respect to the Poisson Eq. (4.1.13) are given by the inclusion of the pressure p and the derivative self-interaction term in the right hand side. In the next sections, we shall analyse Eq. (5.1.7) as an effective

¹Different values of q_V , q_B and q_ρ can be implemented in order to obtain the approximate potentials for different motions of test particles in GR and describe different interiors. This is the difference with the parameter q_Φ in Chapter 4 which was just an expansion parameter to keep track of NLO terms.

description of the static gravitational field V generated by a static source of density ρ in flat space-time. In other words, we abandon, or disregard, its geometric origin given by the Einstein-Hilbert action and proceed by assuming there exists a reference frame in which the motion of test particles are described by Newton's law with a potential that solves Eq. (5.1.7).

5.2 Homogeneous ball in vacuum

Since we are interested in compact sources, we will consider the simplest case in which the matter density is homogeneous and vanishes outside the sphere of radius $r = R$ (4.2.23), as in Section 4.2.1. Of course, the uniform density (4.2.23) is not expected to be compatible with an equation of state, since the pressure $p = p(r)$ must depend on the radial position so as to maintain equilibrium [19]. We remark once more that uniform density is not very realistic and is here used just for mathematical convenience and because of its extremal role in the Buchdahl limit (2.1.1) in GR ². Moreover, the uniform density profile can also be viewed as a crude approximation of the density in the corpuscular model of BHs, in which the energy is distributed throughout the entire inner volume [12–14, 55, 56, 58, 59, 62, 69, 71, 85–88, 91–93].

The potential must satisfy the regularity condition in the centre

$$V'_{\text{in}}(0) = 0 \tag{5.2.1}$$

and be smooth across the surface $r = R$, that is

$$V_{\text{in}}(R) = V_{\text{out}}(R) \equiv V_R \tag{5.2.2}$$

$$V'_{\text{in}}(R) = V'_{\text{out}}(R) \equiv V'_R, \tag{5.2.3}$$

where we defined $V_{\text{in}} = V(0 \leq r \leq R)$ and $V_{\text{out}} = V(R \leq r)$.

5.2.1 Outer vacuum solution

In the vacuum, where $\rho = p = 0$, Eq. (5.1.6) is trivially satisfied and Eq. (5.1.7) reads

$$\Delta V = \frac{2(V')^2}{1 - 4V}, \tag{5.2.4}$$

which is exactly solved by

$$V_{\text{out}} = \frac{1}{4} \left[1 - \left(1 + \frac{6 G_{\text{N}} M}{r} \right)^{2/3} \right]. \tag{5.2.5}$$

²More realistic energy densities with physically motivated equations of state are considered in Ref. [90].

5.2 Homogeneous ball in vacuum

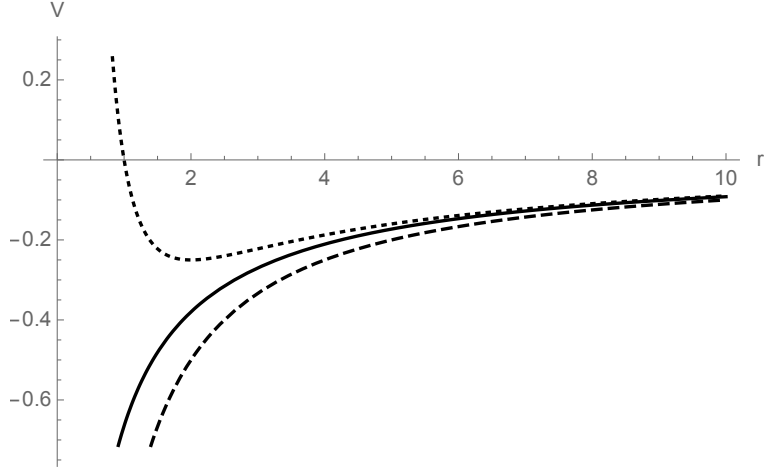


Figure 5.1: Potential V_{out} (solid line) vs Newtonian potential (dashed line) vs order G_N^2 expansion of V_{out} (dotted line) for $r > 0$ (all quantities are in units of $G_N M$).

where two integration constants were fixed by requiring the expected Newtonian behaviour in terms of the ADM-like mass M for large r . In fact, the large r expansion now reads

$$V_{\text{out}} \underset{r \rightarrow \infty}{\simeq} -\frac{G_N M}{r} + \frac{G_N^2 M^2}{r^2} - \frac{8 G_N^3 M^3}{3 r^3}, \quad (5.2.6)$$

and contains the expected post-Newtonian term V_{PN} of order G_N^2 without any further assumptions [20].

From Eq. (5.2.5), we also obtain

$$V_R = V_{\text{out}}(R) = \frac{1}{4} \left[1 - \left(1 + \frac{6 G_N M}{R} \right)^{2/3} \right], \quad (5.2.7)$$

and

$$V'_R = V'_{\text{out}}(R) = \frac{G_N M}{R^2 (1 + 6 G_N M/R)^{1/3}}, \quad (5.2.8)$$

which we will often use since they appear in the boundary conditions (5.2.2) and (5.2.3).

5.2.2 The inner pressure

We first consider the conservation Eq. (5.1.6) and notice that, for $0 \leq r \leq R$, we can write it as

$$\frac{(\rho_0 + p)'}{\rho_0 + p} = -V', \quad (5.2.9)$$

5. Bootstrapped Newtonian gravity: classical picture

which allows us to express the total effective energy density as

$$\rho_0 + p = \alpha e^{-V} . \quad (5.2.10)$$

The integration constant can be determined by imposing the usual boundary condition

$$p(R) = 0 , \quad (5.2.11)$$

which finally yields

$$p = \rho_0 [e^{V_R - V} - 1] , \quad (5.2.12)$$

where V_R is given in Eq. (5.2.7).

5.2.3 The inner potential

The field equation (5.1.7) for $0 \leq r \leq R$ becomes

$$\begin{aligned} \Delta V &= 4\pi G_N \rho_0 e^{V_R - V} + \frac{2(V')^2}{1 - 4V} \\ &= \frac{3G_N M_0}{R^3} e^{V_R - V} + \frac{2(V')^2}{1 - 4V} , \end{aligned} \quad (5.2.13)$$

and we notice that $\rho_0 e^{V_R} < \rho_0$ since $V_R < 0$. The relevant solutions V_{in} to Eq. (5.2.13) must also satisfy the regularity condition (5.2.1) and the matching conditions (5.2.2) and (5.2.3), with V_R and V'_R respectively given in Eq. (5.2.7) and (5.2.8). Since Eq. (5.2.13) is a second order (ordinary) differential equation, the three boundary conditions (5.2.1), (5.2.2) and (5.2.3) will not only fix the potential V_{in} uniquely, but also the ratio of the proper mass parameter $G_N M_0/R$ for any given value of the compactness $G_N M/R$.

It is hard to find the complete solution of the above problem for general compactness. An approximate analytic solution to Eq. (5.2.13) can be found quite straightforwardly only in the regimes of low and intermediate compactness (*i.e.* for $G_N M/R \ll 1$ and $G_N M/R \simeq 1$). On the other hand, for $G_N M \gg R$, the non-linearity of Eq. (5.2.13) and the interplay between M_0 and the boundary conditions (5.2.1), (5.2.2) and (5.2.3) make it very difficult to find any (approximate or numerical) solutions. In fact, even a slight error in the estimate of $M_0 = M_0(M, R)$ can spoil the solution completely. For this reason, we will take advantage of the comparison method [94–97] which essentially consists in finding two bounding functions V_{\pm} (upper and lower approximate solutions) such that $E_+(r) < 0$ and $E_-(r) > 0$ for $0 \leq r \leq R$, where

$$E_{\pm} \equiv \Delta V_{\pm} - \frac{3G_N M_0^{\pm}(M)}{R^3} e^{V_R - V_{\pm}} - \frac{2(V'_{\pm})^2}{1 - 4V_{\pm}} . \quad (5.2.14)$$

5.2 Homogeneous ball in vacuum

Comparison theorems then guarantee that the proper solution will lie in between the two bounding functions (see Appendix D for more details ³), that is

$$V_- < V_{\text{in}} < V_+ . \quad (5.2.15)$$

The advantage of this method is twofold. It will serve as a tool for finding approximate solutions in the regime of large compactness and will also allow us to check the accuracy of the approximate analytic solution for low and intermediate compactness.

Small and intermediate compactness

For the radius R of the source much larger or of the order of $G_{\text{N}} M$, an analytic approximation V_{s} for the solution V_{in} can be found by simply expanding around $r = 0$, and turns out to be

$$V_{\text{s}} = V_0 + \frac{G_{\text{N}} M_0}{2 R^3} e^{V_R - V_0} r^2 . \quad (5.2.16)$$

where $V_0 \equiv V_{\text{in}}(0) < 0$ and V_R is given in Eq. (5.2.7). We remark that the regularity condition (5.2.1) requires that all terms of odd order in r in the Taylor expansion about $r = 0$ must vanish.

We can immediately notice that the above form is qualitatively similar to the Newtonian solution shown in Section 4.2.1. Like the latter, the present case does not show any singularity in the potential for $r = 0$ and the pressure,

$$p \simeq \rho_0 \left[e^{V_R - V_0 - B r^2} - 1 \right] , \quad (5.2.17)$$

is also regular in $r = 0$,

$$p(0) = \rho_0 \left[e^{-(V_0 - V_R)} - 1 \right] > 0 , \quad (5.2.18)$$

since $V_0 < V_R < 0$.

The two matching conditions at $r = R$ can now be written as

$$\begin{cases} 2 R (V_R - V_0) \simeq G_{\text{N}} M_0 e^{V_R - V_0} \\ R^2 V'_R \simeq G_{\text{N}} M_0 e^{V_R - V_0} , \end{cases} \quad (5.2.19)$$

One can solve the second equation of the system above for V_0 to obtain

$$V_0 = \frac{1}{4} \left[1 - (1 + 6 G_{\text{N}} M/R)^{2/3} \right] + \ln \left[\frac{M_0}{M} (1 + 6 G_{\text{N}} M/R)^{1/3} \right] , \quad (5.2.20)$$

³We just remark here that the comparison theorems do not require that the approximate solutions V_{\pm} have the same functional forms of the exact solution V_{in} .

5. Bootstrapped Newtonian gravity: classical picture

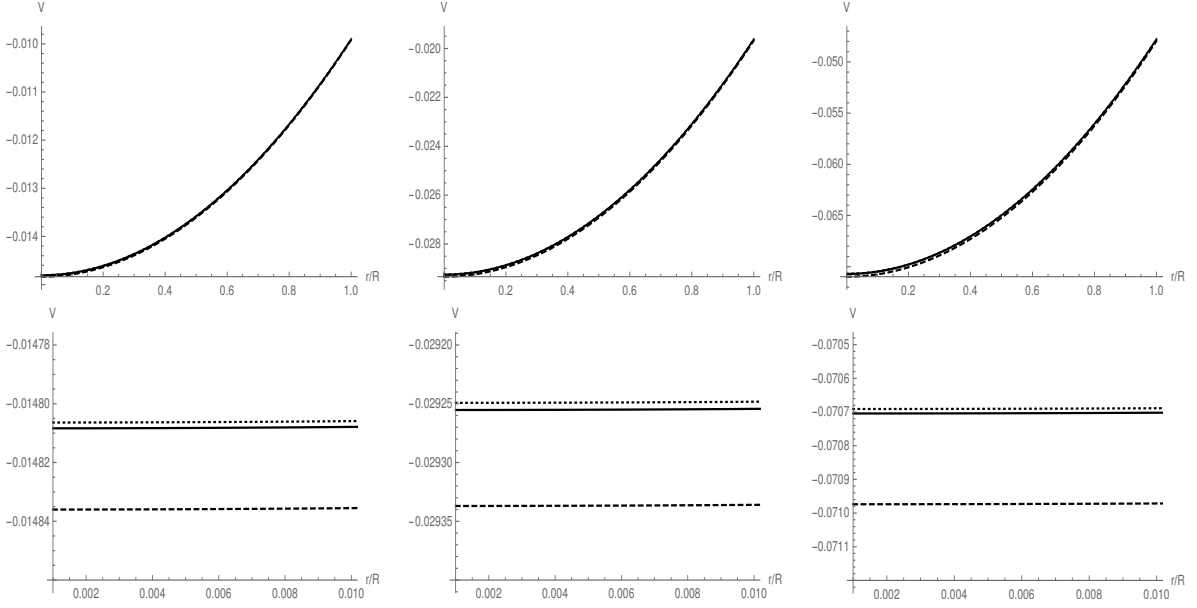


Figure 5.2: Numerical solution to Eq. (5.2.13) (solid line) *vs* approximate solution $V_s = V_+$ in Eq. (5.2.22) (dotted line) *vs* lower bounding function $V_- = C V_s$ (dashed line), for $G_N M/R = 1/100$ (top left panel, with $C = 1.002$), $G_N M/R = 1/50$ (top central panel, with $C = 1.003$) and $G_N M/R = 1/20$ (top right panel, with $C = 1.004$). The bottom panels show the region $0 \leq r \leq R/100$ where the difference between the three potentials is the largest.

which is written in terms of M_0 and M . Using the first equation in (5.2.19), one then finds

$$M_0 = \frac{M e^{-\frac{G_N M}{2R(1+6G_N M/R)^{1/3}}}}{(1+6G_N M/R)^{1/3}}. \quad (5.2.21)$$

This last expression, along with the one for V_0 , can be used to write the approximate solution (5.2.16) in terms of M only as

$$V_s = \frac{R^3 \left[(1+6G_N M/R)^{1/3} - 1 \right] + 2G_N M (r^2 - 4R^2)}{4R^3 (1+6G_N M/R)^{1/3}}, \quad (5.2.22)$$

where we remark that this expression contains only the terms of the first two orders in the series expansion about $r = 0$.

We can now estimate the accuracy of the approximation (5.2.16) by means of the comparison method. The plots in Fig. 5.2 and 5.3 show that V_s is already in good agreement with the numerical solution for both small and intermediate compactness and the smaller the ratio $G_N M/R$, the less V_s differs from the numerical solution. Indeed, the approximate solution V_s fails in the large compactness regime, which will be studied in the next subsection. The same plots also tell us that V_s is actually an upper bounding

5.2 Homogeneous ball in vacuum

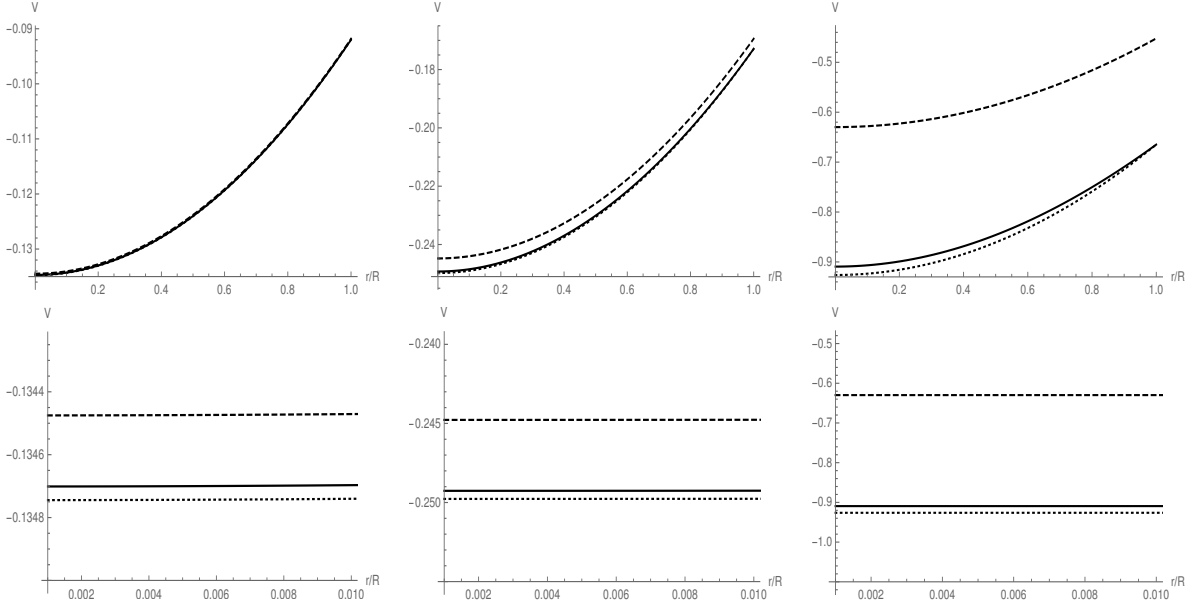


Figure 5.3: Numerical solution to Eq. (5.2.13) (solid line) *vs* approximate solution $V_s = V_-$ in Eq. (5.2.22) (dotted line) *vs* upper bounding function $V_+ = C V_s$ (dashed line), for $G_N M/R = 1/10$ (top left panel, with $C = 0.998$), $G_N M/R = 1/5$ (top central panel, with $C = 0.980$) and $G_N M/R = 1$ (top right panel, with $C = 0.680$). The bottom panels show the region $0 < r < R/100$ where the difference between the three expressions is the largest.

function V_+ up to $G_N M/R \simeq 1/20$, but becomes a lower bounding function V_- for higher compactness (this can be verified by showing that it satisfies the required conditions described in Appendix D). The other bounding function (V_- or V_+) can be found by simply multiplying V_s by a suitable constant factor C determined according to the theorem in Appendix D (with $C > 1$ for small compactness and $C < 1$ for intermediate compactness). This means that the approximate solution (5.2.16) overestimates the expected true potential V_{in} for low compactness, whereas it underestimates V_{in} when the compactness grows beyond $G_N M/R \simeq 1/20$. We also note that the gap between the above V_- and V_+ increases for increasing compactness, which signals the need for a better estimate of $M_0 = M_0(M)$ in order to narrow this gap and gain more precision for describing the intermediate compactness. The latter regime is particularly useful for understanding objects that have collapsed to a size of the order of their gravitational radius. We should remark that, in this analysis, we actually employed the comparison method in the whole range $0 \leq r < \infty$ by defining $V_{\pm} = C_{\pm} V_{\text{out}}$, for $r > R$, where V_{out} is the exact solution in Eq. (5.2.5) (see Figs. 5.4 and 5.5). This means that we did not require that the lower function V_- (for $G_N M/R \lesssim 1/20$) and the upper function V_+ (for $G_N M/R \gtrsim 1/20$) satisfy the boundary conditions (5.2.2) and (5.2.3) at $r = R$. However, since we have the analytical form for V_{out} in its entire range of applicability,

5. Bootstrapped Newtonian gravity: classical picture

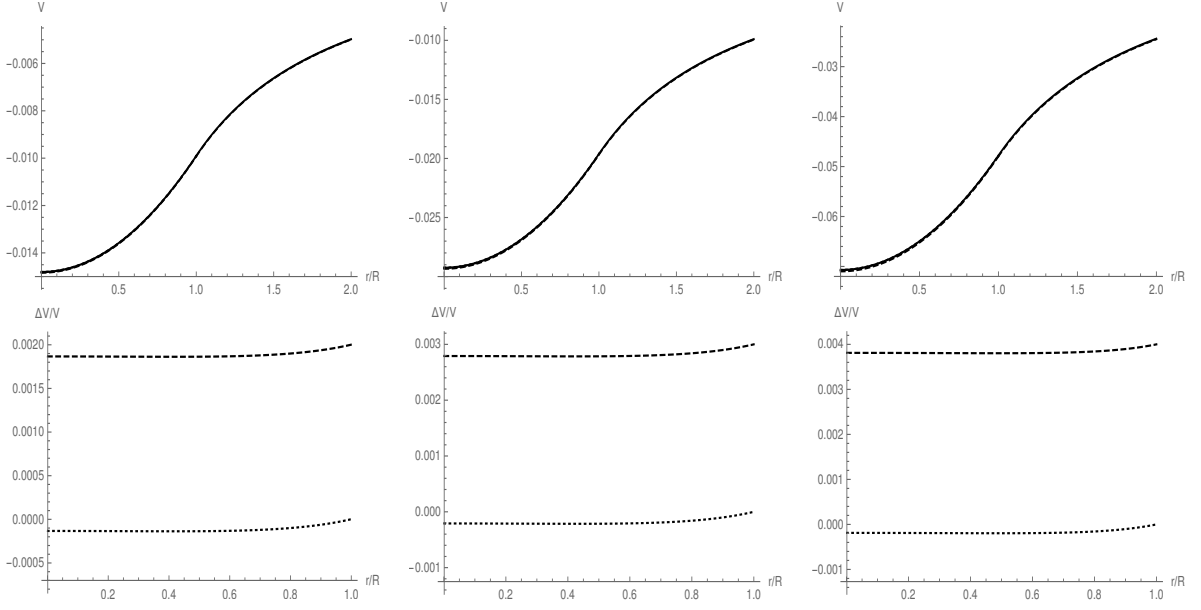


Figure 5.4: Upper panels: numerical solution V_n to Eq. (5.2.13) matched to the exact outer solution (5.2.5) (solid line) *vs* approximate solution $V_s = V_+$ in Eq. (5.2.22) (dotted line) *vs* lower bounding function V_- (dashed line) for $G_N M/R = 1/100$ (top left), $G_N M/R = 1/50$ (top middle) and $G_N M/R = 1/20$ (top right). Bottom panels: relative difference $(V_s - V_n)/V_n$ (dotted line) *vs* $(V_- - V_n)/V_n$ (dashed line) in the interior region for $G_N M/R = 1/100$ (bottom left), $G_N M/R = 1/50$ (bottom middle) and $G_N M/R = 1/20$ (bottom right). The negative sign of $(V_s - V_n)/V_n$ shows that the approximate solution is an upper bounding function $V_s = V_+$ in this range of compactness.

all that is needed to ensure that V_{\pm} are the upper and lower bounding functions is for the constants C_{\pm} which multiply the expression for V_{out} to be smaller, respectively larger than one.

As stated earlier, the analytic approximation (5.2.22) works best in the regime of small compactness, in which we can further Taylor expand all quantities to second order in $G_N M/R \ll 1$ to obtain

$$V_0 \simeq -\frac{3 G_N M}{2 R} \left(1 - \frac{4 G_N M}{3 R} \right), \quad (5.2.23)$$

and finally use Eq. (5.2.21) to obtain

$$M_0 \simeq M \left(1 - \frac{5 G_N M}{2 R} \right), \quad (5.2.24)$$

in qualitative agreement with the result of Ref. [19], where however the effect of the pressure on the potential was neglected.

The above expressions for M_0 and V_0 can be used to write the inner potential (5.2.16)

5.2 Homogeneous ball in vacuum

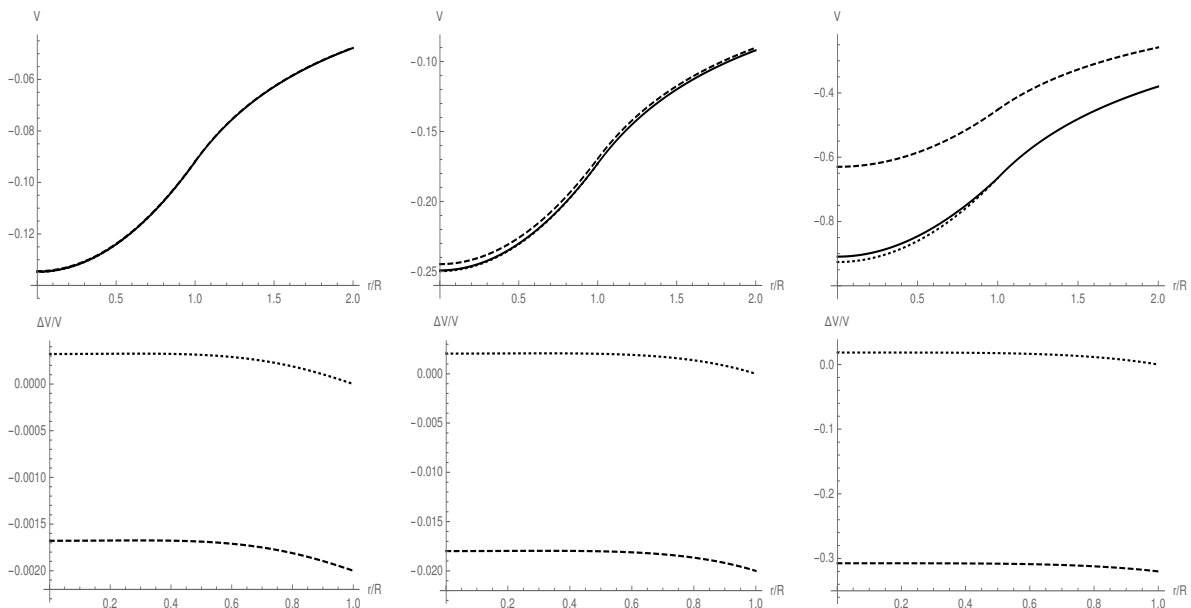


Figure 5.5: Upper panels: numerical solution V_n to Eq. (5.2.13) matched to the exact outer solution (5.2.5) (solid line) *vs* approximate solution $V_s = V_-$ in Eq. (5.2.22) (dotted line) *vs* upper bounding function V_+ (dashed line) for $G_N M/R = 1/10$ (top left), $G_N M/R = 1/5$ (top middle) and $G_N M/R = 1$ (top right). Bottom panels: relative difference $(V_s - V_n)/V_n$ (dotted line) *vs* $(V_+ - V_n)/V_n$ (dashed line) in the interior region for $G_N M/R = 1/10$ (bottom left), $G_N M/R = 1/5$ (bottom middle) and $G_N M/R = 1$ (bottom right). The negative sign of $(V_s - V_n)/V_n$ shows that the approximate solution is a lower bounding function $V_s = V_-$ in this range of compactness. The rapid growth in modulus of $(V_+ - V_n)/V_n$ with the compactness signals the need of a better estimate of $M = M(M_0)$ for a more accurate description.

in a much simpler form in terms of M as

$$V_{\text{in}} \simeq \frac{G_N M}{2R} \left(1 - \frac{2G_N M}{R} \right) \frac{r^2 - 3R^2}{R^2}. \quad (5.2.25)$$

As expected, the solution for small compactness, which can be useful for describing stars with a radius orders of magnitude larger in size than their gravitational radius, qualitatively tracks the Newtonian case. This can also be seen from Fig. 5.6. The limitations of the small compactness approximation can be inferred from Eq. (5.2.25). For $2G_N M \equiv R_H \sim R$ the last term vanishes and V_{in} becomes a constant.

Finally, it is important to remark that, as opposed to what was done in Ref. [19], the pressure now acts as a source and can be consistently evaluated with the help of Eqs. (5.2.12) and (5.2.16). The plots in Fig. 5.7 clearly show that the pressure can be well approximated by the Newtonian formula in the regime of low compactness, to wit

$$p \simeq \frac{3G_N M^2 (R^2 - r^2)}{8\pi R^6}, \quad (5.2.26)$$

5. Bootstrapped Newtonian gravity: classical picture

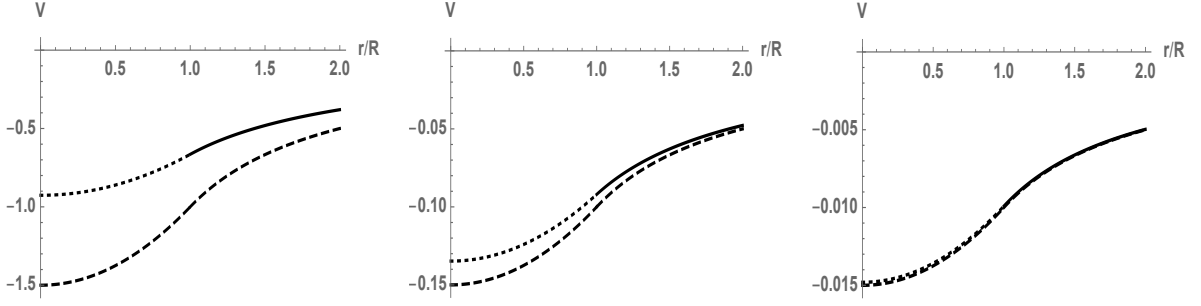


Figure 5.6: Potential V_{out} (solid line) *vs* approximate solution (5.2.22) (dotted line) *vs* Newtonian potential (dashed line), for $G_N M/R = 1$ (left panel), $G_N M/R = 1/10$ (center panel) and $G_N M/R = 1/100$ (right panel).

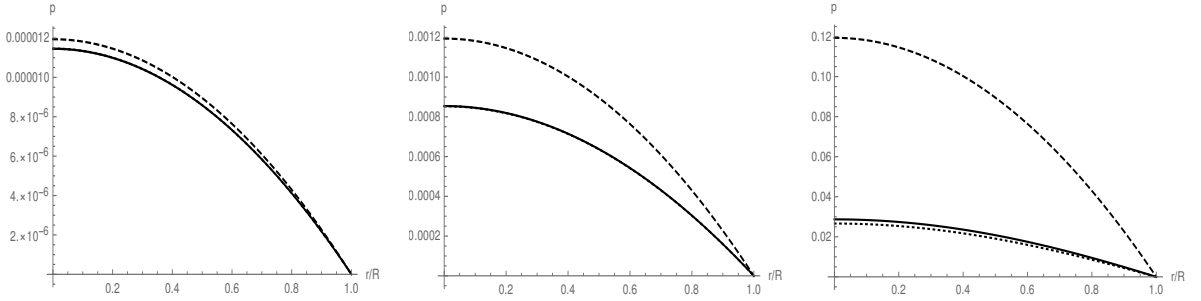


Figure 5.7: Pressure obtained from the expansion (5.2.16) (solid line) *vs* numerical pressure (dotted line) *vs* Newtonian pressure (5.2.26) (dashed line), for $G_N M/R = 1/100$ (left panel), $G_N M/R = 1/10$ (center panel) and $G_N M/R = 1$ (right panel).

again in qualitative agreement with Ref. [19]. Nevertheless, the same plots indicate that it rapidly departs from the Newtonian expression when we approach the regime of intermediate compactness, while remaining almost identical to the numerical approximation.

Large compactness

For $G_N M/R \gg 1$, rather than employing a Taylor expansion like we did for small compactness, it is more convenient to fully rely on comparison methods [94–97] and start from the exact solution of the simpler equation

$$\psi'' = \frac{3 G_N M_0}{R^3} e^{V_R - \psi}, \quad (5.2.27)$$

which is given by

$$\psi(r; A, B) = -A \left(B + \frac{r}{R} \right) + 2 \ln \left[1 + \frac{3 G_N M_0}{2 A^2 R} e^{A(B+r/R)+V_R} \right], \quad (5.2.28)$$

5.2 Homogeneous ball in vacuum

where the constants A , B and M_0 can be fixed (for any value of R) by imposing the boundary conditions (5.2.1), (5.2.2) and (5.2.3). Regularity at $r = 0$ in particular yields

$$M_0 = \frac{2 A^2 R}{3 G_N} e^{-AB - V_R} . \quad (5.2.29)$$

Eq. (5.2.3) for the continuity of the derivative across $r = R$ then reads

$$A \tanh(A/2) = R V'_R . \quad (5.2.30)$$

For large compactness, $R V'_R \sim (G_N M/R)^{2/3} \gg 1$, and we can approximate the above equation as

$$A \simeq R V'_R . \quad (5.2.31)$$

The continuity Eq. (5.2.2) for the potential finally reads

$$2 \ln \left(1 + e^{R V'_R} \right) - R V'_R (1 + B) = V_R , \quad (5.2.32)$$

and can be used to express B in terms of M and R . Putting everything together, we obtain

$$\begin{aligned} \psi(r; M, R) &\simeq \frac{1}{4} \left\{ 1 - \frac{1 + (2 G_N M/R) (1 + 2 r/R)}{(1 + 6 G_N M/R)^{1/3}} + 8 \ln \left[\frac{1 + e^{\frac{G_N M r/R^2}{(1+6 G_N M/R)^{1/3}}}}{1 + e^{\frac{G_N M/R}{(1+6 G_N M/R)^{1/3}}}} \right] \right\} \\ &\simeq \frac{1}{2} \left(\frac{G_N M}{\sqrt{6} R} \right)^{2/3} \left(\frac{2r}{R} - 5 \right) , \end{aligned} \quad (5.2.33)$$

and

$$\begin{aligned} \frac{M_0}{M} &\simeq \frac{G_N M/R}{3 (1 + 6 G_N M/R)^{2/3} \left\{ 1 + \cosh \left[\frac{G_N M/R}{(1+6 G_N M/R)^{1/3}} \right] \right\}} \\ &\simeq \frac{1}{3} \left(\frac{2 G_N M}{9 R} \right)^{1/3} e^{-\left(\frac{G_N M}{\sqrt{6} R} \right)^{2/3}} , \end{aligned} \quad (5.2.34)$$

in which we showed the leading behaviours for $G_N M \gg R$. It is important to remark that the condition (5.2.1) is not apparently satisfied by the above approximate expressions, although it was imposed from the very beginning, which shows once more how complex is to obtain analytical approximations for the problem at hand.

The solutions to the complete equation (5.2.13) could then be written as

$$V_{\text{in}} = f(r; A, B) \psi(r; A, B) , \quad (5.2.35)$$

where A , B and M_0 should again be computed from the three boundary conditions, so that V_{in} eventually depends only on the parameters M and R . Since solving for

5. Bootstrapped Newtonian gravity: classical picture

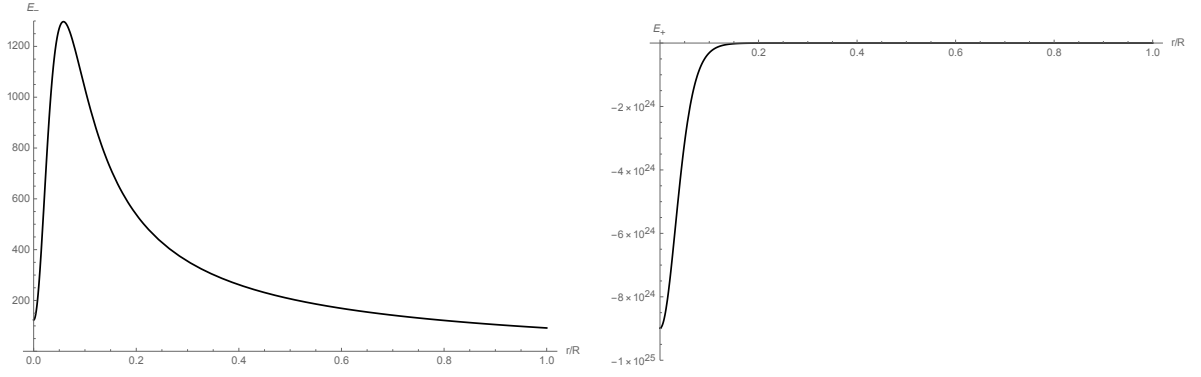


Figure 5.8: Left panel: E_- for $C_- = 1$. Right panel: E_+ for $C_+ = 1.6$. Both plots are for $G_N M/R = 10^3$.

$f = f(r)$ is not any simpler than the original task, we shall instead just find lower and upper bounds, that is constants C_{\pm} such that

$$C_- < f(r) < C_+ , \quad (5.2.36)$$

in the whole range $0 \leq r \leq R$. In particular, we consider the bounding functions

$$V_{\pm} = C_{\pm} \psi(r; A_{\pm}, B_{\pm}) , \quad (5.2.37)$$

where A_{\pm} , B_{\pm} and C_{\pm} are constants computed by imposing the boundary conditions (5.2.1), (5.2.2) and (5.2.3) and such that $E_+(r) < 0$ and $E_-(r) > 0$ for $0 \leq r \leq R$.

In details, we first determine a function $V_C = C \psi(r; A, B)$ which satisfies the three boundary conditions for any constant C . Eq. (5.2.1) yields the same expression (5.2.29), whereas the l.h.s. of Eq. (5.2.30) is just rescaled by the factor C and continuity of the derivative therefore gives the approximate solution

$$C A \simeq R V'_R . \quad (5.2.38)$$

Eq. (5.2.2) for the continuity of the potential likewise reads

$$2 C \ln \left(1 + e^{R V'_R / C} \right) - R V'_R (1 + B) = V_R , \quad (5.2.39)$$

Upon solving the above equations one then obtains $V_C = C \psi(r; A(M, R, C), B(M, R, C))$ and $M_0 = M_0(M, R, C)$. For fixed values of R and M , one can then numerically determine a constant C_+ such that $E_+ < 0$ and a constant $C_- < C_+$ such that $E_- > 0$.

For example, for the compactness $G_N M/R = 10^3$, we can use $C_- \simeq 1$ and $C_+ \simeq 1.6$, and the plots of E_- and E_+ are shown in Fig. 5.8. In particular, the minimum value of $|E_+| \simeq 14$. The corresponding potentials V_{\pm} along with $\tilde{V} = \tilde{C} \psi$, where $\tilde{C} = (C_+ + C_-)/2$, are displayed in Fig. 5.9. It is easy to see that the three approximate

5.2 Homogeneous ball in vacuum

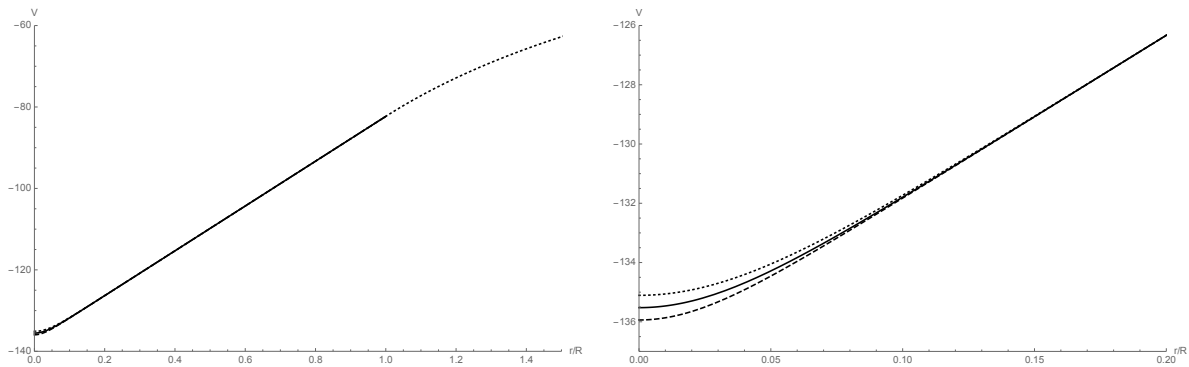


Figure 5.9: Left panel: approximate inner potentials V_- (dashed line), \tilde{V} (solid line) and V_+ (dotted line) for $0 \leq r \leq R$ and exact outer potential V_{out} (dotted line) for $r > R$. Right panel: approximate inner potentials V_- (dashed line), \tilde{V} (solid line) and V_+ (dotted line) for $0 \leq r \leq R/5$. Both plots are for $G_{\text{N}} M/R = 10^3$.

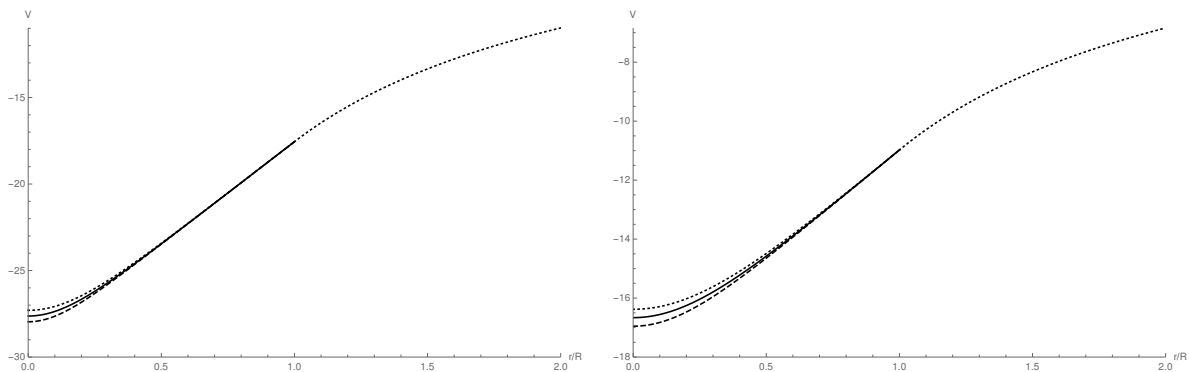


Figure 5.10: Approximate inner potentials V_- (dashed line), \tilde{V} (solid line) and V_+ (dotted line) for $0 \leq r \leq R$ and exact outer potential V_{out} (dotted line) for $r > R$ and for $G_{\text{N}} M/R = 10^2$ (left panel, with $C_- = 1.042$ and $C_+ = 1.52$) and $G_{\text{N}} M/R = 50$ (right panel, with $C_- = 1.073$ and $C_+ = 1.5$)

solutions essentially coincide almost everywhere, except near $r = 0$ where they start to fan out, albeit still very slightly (the right panel of Fig. 5.9 shows a close-up of this effect). A similar behaviour is obtained for larger values of $G_{\text{N}} M/R$. For smaller values of the compactness up to $G_{\text{N}} M/R \simeq 50$, the approximation (5.2.38) is still quite accurate (see Fig. 5.10), even if the smaller the compactness the bigger the difference between V_{\pm} . Actually, the error in the derivative of the potential at $r = R$ is of the order of 0.01% and 0.6% for $G_{\text{N}} M/R = 10^2$ and $G_{\text{N}} M/R = 50$, respectively. In order to obtain a comparable precision for lower compactness, the approximate expression (5.2.38) should be improved, but we do not need to do that given how accurate is the perturbative expansion employed in Section 5.2.3.

From the left panel of Fig. 5.9, it is clear that for $G_{\text{N}} M/R = 10^3$ the potential V_{in} is practically linear, except near $r = 0$ where it turns into a quadratic shape, in

5. Bootstrapped Newtonian gravity: classical picture

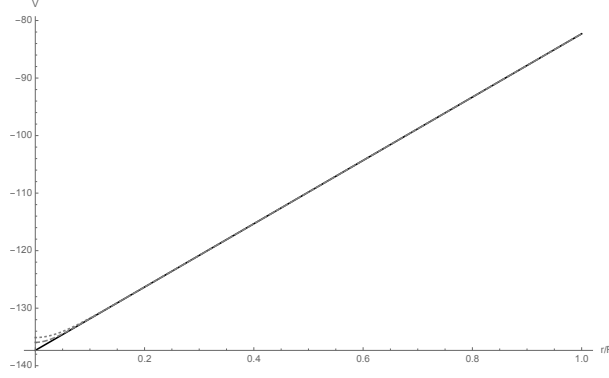


Figure 5.11: Approximate inner potentials V_- (dashed line), V_{lin} (solid line) and V_+ (dotted line) for $0 \leq r \leq R$. Both plots are for $G_{\text{N}} M/R = 10^3$.

order to ensure the regularity condition (5.2.1). An approximate expression for the source proper mass M_0 in terms of M can then be obtained from the simple linear approximation

$$V_{\text{lin}} \simeq V_R + V'_R (r - R) , \quad (5.2.40)$$

where V_R and V'_R are given by the usual expressions (5.2.7) and (5.2.8), and which is shown in Fig. 5.11 for $G_{\text{N}} M/R = 10^3$. Upon replacing the approximation (5.2.40) into the equation (5.2.13) for $r = R$, we obtain

$$\frac{M_0}{M} \simeq \frac{2(1 + 5 G_{\text{N}} M/R)}{3(1 + 6 G_{\text{N}} M/R)^{4/3}} , \quad (5.2.41)$$

and further approximating for $G_{\text{N}} M/R \gg 1$

$$\frac{G_{\text{N}} M_0}{R} \sim \left(\frac{G_{\text{N}} M}{R} \right)^{2/3} . \quad (5.2.42)$$

The linear approximation is not very useful when it comes to evaluate the maximum value of the pressure, which we expect to occur in the origin at $r = 0$, precisely where this approximation must fail. We therefore consider again the approximation $\tilde{V} = \tilde{C} \psi$, which replaced into Eq. (5.2.12) gives rise to the pressure shown in Fig. 5.12. Since the full expression is very cumbersome, we just show the leading order contribution for large compactness

$$p \simeq \frac{G_{\text{N}} M^2 e^{\frac{1}{2} \left(\frac{G_{\text{N}} M}{\sqrt{6} R} \right)^{2/3} \left(3 - \frac{5}{\tilde{C}} \right)}}{2 \pi \tilde{C}^2 R^4 (6 G_{\text{N}} M/R)^{2/3}} \left[e^{\left(\frac{G_{\text{N}} M}{\sqrt{6} R} \right)^{2/3} \left(1 - \frac{r}{R} \right)} - 1 \right] , \quad (5.2.43)$$

which yields

$$p(0) \simeq \frac{G_{\text{N}} M^2 e^{\frac{5}{2} \left(\frac{\tilde{C}-1}{\tilde{C}} \right) \left(\frac{G_{\text{N}} M}{\sqrt{6} R} \right)^{2/3}}}{2 \pi \tilde{C}^2 R^4 (6 G_{\text{N}} M/R)^{2/3}} , \quad (5.2.44)$$

5.3 Horizon and gravitational energy

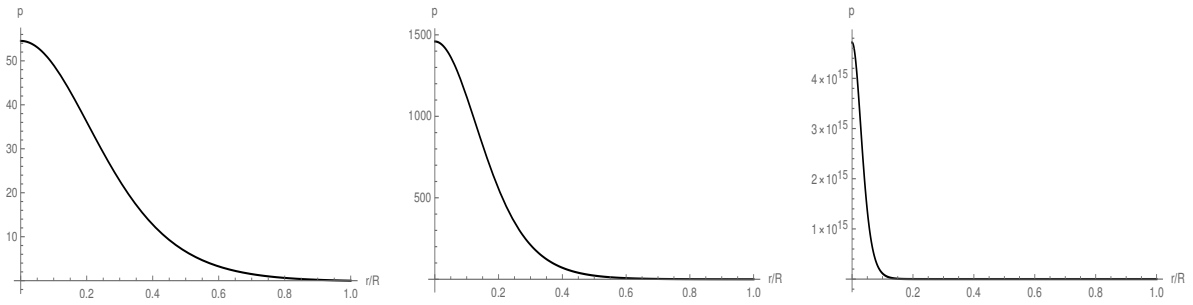


Figure 5.12: Pressure evaluated using the approximation $\tilde{V} = \tilde{C} \psi$ for $G_{\text{N}} M/R = 50$ (left panel), $G_{\text{N}} M/R = 100$ (center panel) and $G_{\text{N}} M/R = 1000$ (right panel). The constant $\tilde{C} = (C_+ + C_-)/2$, where C_+ and C_- are the same as in Figs. 5.9 and 5.10 for the corresponding cases.

where we find that $\tilde{C} > 1$ for $G_{\text{N}} M/R \gg 1$. It is clear from this expression and Fig. 5.12 how rapidly the pressure grows near the origin when the compactness increases, but still remaining finite and regular everywhere even for very large compactness. In Fig. 5.13 we can see the comparison of the above approximate expression with the graphs shown in Fig. 5.12. Of course the biggest the compactness the more rapidly the approximation (5.2.43) approaches the results of Fig. 5.12. In Figs. 5.14 and 5.15 we instead plot the comparison between the approximation (5.2.43) with $\tilde{C} = (C_+ + C_-)/2$ and the pressure evaluated from Eq. (5.2.12) and $V_{\pm} = C_{\pm} \psi$. The values of C_- and C_+ are the same as in Figs. 5.9 and 5.10 for the corresponding compactness.

5.3 Horizon and gravitational energy

The approach we used so far completely neglects any geometrical aspect of gravity. In particular, it is well known that collapsing matter is responsible for the emergence of BH geometries, providing us with the associated Schwarzschild radius (2.1.4). In GR, this marks the boundary between sources which we consider as stars ($R \gg R_{\text{H}}$) and BHs ($R \lesssim R_{\text{H}}$). Moreover, if the pressure is isotropic, stars must have a radius $R > (9/8) R_{\text{H}}$, otherwise the necessary pressure diverges (see Chapter 2 for details on the Buchdahl limit).

We found that the pressure is always finite in our bootstrapped picture, hence there is no analogue of the Buchdahl limit. This means that the source can have arbitrarily large compactness, including $R < R_{\text{H}}$. Lacking precise geometrical quantities, we will follow a Newtonian argument and define the horizon as the value r_{H} of the radius at which the escape velocity of test particles equals the speed of light, namely

$$2V(r_{\text{H}}) = -1, \quad (5.3.1)$$

5. Bootstrapped Newtonian gravity: classical picture

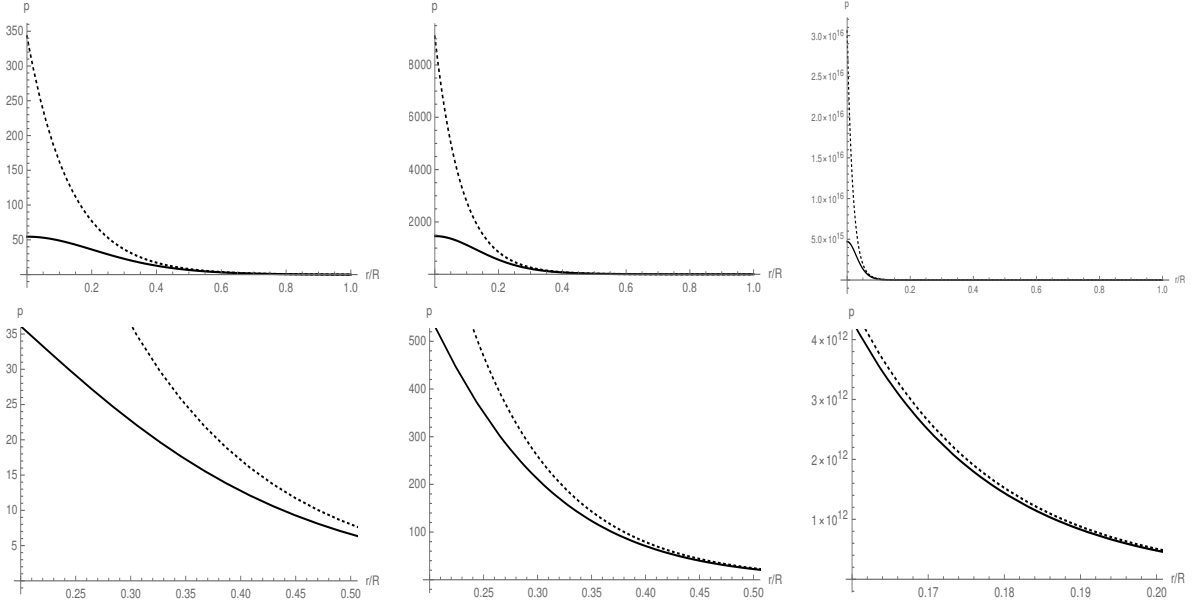


Figure 5.13: Comparison between the approximate pressure (5.12) (dotted line) *vs* solution of Eq. (5.2.43) with $\tilde{V} = \tilde{C} \psi$ and $\tilde{C} = (C_+ + C_-)/2$ (solid line) for $G_N M/R = 50$ (top left panel), $G_N M/R = 100$ (top central panel), $G_N M/R = 1000$ (top right panel), and the corresponding close-ups in the bottom panels.

as in Ref. [19]⁴. Of course, when the source is diluted no horizon should exist and the above definition correctly reproduces this expectation, since that condition is never fulfilled for small compactness (see Figs. 5.2 and 5.3). In fact, we can find a limiting lower value for the compactness at which Eq. (5.3.1) has a solution, by requiring

$$2V_{\text{in}}(r_{\text{H}} = 0) = -1, \quad (5.3.2)$$

which gives $G_N M/R \simeq 0.46$ if we use $V(0) = V_0$ from Eq. (5.2.20). Upon increasing the compactness, the horizon radius r_{H} will increase and eventually approach the radius R of the matter source, which occurs when

$$2V_{\text{in}}(r_{\text{H}} = R) = 2V_{\text{out}}(R) = -1, \quad (5.3.3)$$

where $V_{\text{out}}(R) = V_R$ is given by the exact expression in Eq. (5.2.7). This yields the compactness $G_N M/R \simeq 0.69$ and $r_{\text{H}} \simeq R \simeq 1.43 G_N M$. For even larger values of the compactness, the horizon radius will always appear in the outer potential (5.2.5) and therefore remain fixed at this value in terms of M . We can summarise the situation as

⁴An effective metric outside the bootstrapped source has been found in Ref. [98]. In that context the usual notion of horizon can be recovered.

5.3 Horizon and gravitational energy

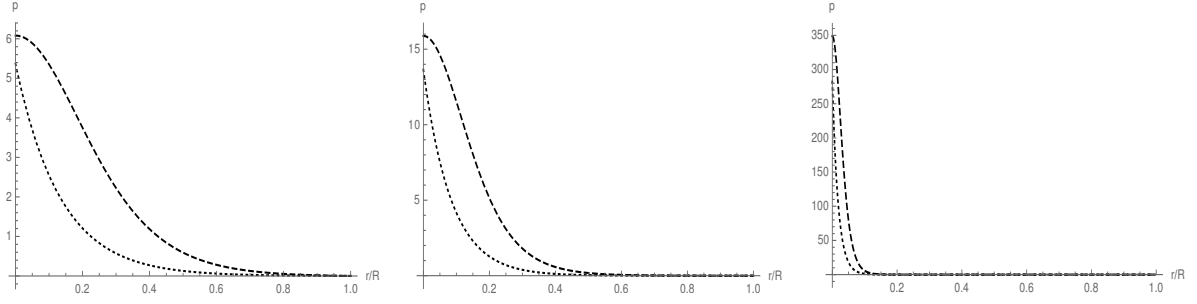


Figure 5.14: Pressure evaluated from $V_- = C_- \psi$ (dashed line) *vs* pressure evaluated from $\tilde{V} = \tilde{C} \psi$ (dotted line) for $G_N M/R = 50$ (left panel), $G_N M/R = 100$ (center panel) and $G_N M/R = 1000$ (right panel).

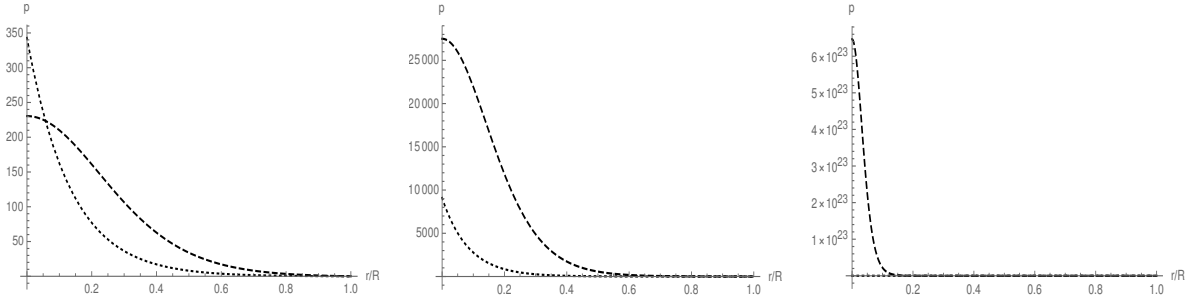


Figure 5.15: Pressure evaluated from $V_+ = C_+ \psi$ (dashed line) *vs* pressure evaluated from $\tilde{V} = \tilde{C} \psi$ with $\tilde{C} = (C_+ + C_-)/2$ (dotted line) for $G_N M/R = 50$ (left panel), $G_N M/R = 100$ (center panel) and $G_N M/R = 1000$ (right panel).

follows

$$\left\{ \begin{array}{ll} \text{no horizon} & \text{for } G_N M/R \lesssim 0.46 \\ 0 < r_H \leq R \simeq 1.4 G_N M & \text{for } 0.46 \lesssim G_N M/R \leq 0.69 \\ r_H \simeq 1.4 G_N M & \text{for } G_N M/R \gtrsim 0.69 . \end{array} \right. \quad (5.3.4)$$

The above values of the compactness further correspond to proper masses

$$\frac{M_0}{M} \simeq \begin{cases} 0.56 & \text{for } G_N M/R \simeq 0.46 \\ 0.47 & \text{for } G_N M/R \simeq 0.69 , \end{cases} \quad (5.3.5)$$

so that, when the horizon is precisely at the surface of the source, we have

$$r_H \simeq 1.4 G_N M \simeq 3 G_N M_0 . \quad (5.3.6)$$

It is also important to remark that the horizon r_H lies inside the source for a relatively narrow range of the compactness (see Fig. 5.16 for the corresponding potentials).

5. Bootstrapped Newtonian gravity: classical picture

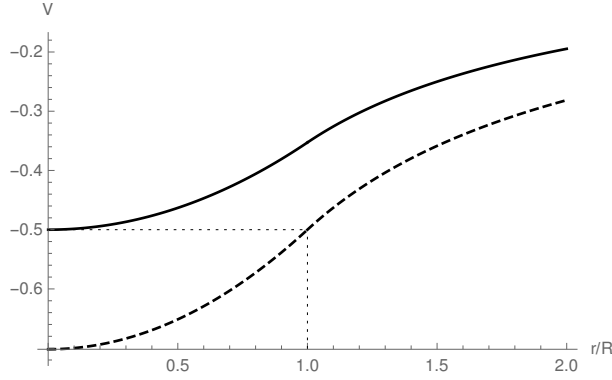


Figure 5.16: Potentials corresponding to $r_H = 0$ (solid line) and $r_H = R$ (dashed line).

We can next estimate the gravitational potential energy U_G from the effective Hamiltonian (5.1.4) (with $q_V = 3q_B = q_\rho = 1$). For calculation and conceptual purposes, it is convenient to separate U_G into three different parts: the “baryon-graviton” contribution, for which the radial integral has only support inside the matter source, given by

$$U_{\text{BG}} = 4\pi \int_0^\infty r^2 dr (\rho + p) V (1 - 2V) = \frac{3M_0}{R^3} \int_0^R r^2 dr e^{V_R - V_{\text{in}}} V_{\text{in}} (1 - 2V_{\text{in}}) \quad (5.3.7)$$

where we employed Eq. (5.2.12); the “graviton-graviton” contribution due to the potential self-interaction inside the source

$$U_{\text{GG}}^{\text{in}} = \frac{1}{2G_N} \int_0^R r^2 dr (V'_{\text{in}})^2 (1 - 4V_{\text{in}}) \quad (5.3.8)$$

and outside the source

$$U_{\text{GG}}^{\text{out}} = \frac{1}{2G_N} \int_R^\infty r^2 dr (V'_{\text{out}})^2 (1 - 4V_{\text{out}}) , \quad (5.3.9)$$

While the contribution from the outside is exactly given by

$$U_{\text{GG}}^{\text{out}} = \frac{G_N M^2}{2R} . \quad (5.3.10)$$

the inner contributions U_{BG} and $U_{\text{GG}}^{\text{in}}$ can only be evaluated within the approximations for the potential employed in the previous sections.

The energy contributions for objects of low compactness $G_N M/R \ll 1$ can be evaluated straightforwardly. Starting from the approximate expression in (5.2.24) and (5.2.25) the total energy is calculated to be

$$U_G = U_{\text{BG}} + U_{\text{GG}}^{\text{in}} + U_{\text{GG}}^{\text{out}} \simeq -\frac{3G_N M^2}{5R} + \frac{9G_N^2 M^3}{7R^2} , \quad (5.3.11)$$

where we immediately notice the usual newtonian term at the lowest order.

5.3 Horizon and gravitational energy

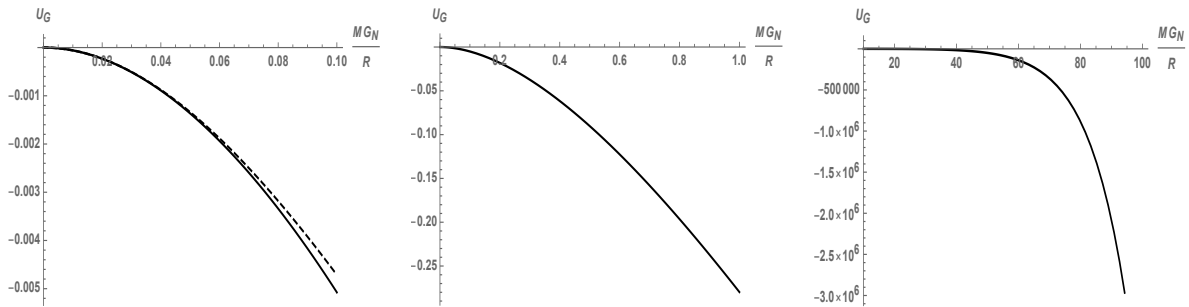


Figure 5.17: Total gravitational potential energy U_G . Left panel: U_G in the low compactness regime from the analytic approximations valid in the low and intermediate regime (continuous line) *vs* U_G from Eq. (5.3.11) (dashed line). Center panel: U_G in the low and intermediate compactness regime. Right panel: U_G in the high compactness regime.

One can also calculate the three components of the gravitational potential energy in the regime of intermediate compactness $G_N M/R \sim 1$, but the explicit expressions would be too cumbersome to display. Instead, the left panel of Fig. 5.17 shows a comparison in the regime of low compactness between the above expression for U_G and the one obtained starting from the analytic approximations from Eqs. (5.2.21) and (5.2.22), which are valid both for sources of low and intermediate compactness. It can be seen that the two approximations lead to similar results for objects that have low compactness. The center panel also shows the behaviour of U_G for objects of intermediate compactness. As expected, the gravitational potential energy becomes more and more negative as the density of the source increases.

We conclude with the high compactness regime, in which the increase in modulus of the negative gravitational potential energy is even more dramatic, as shown in the right panel of Fig. 5.17. To make things easier, we are going to evaluate the contributions (5.3.7) and (5.3.8) in the limit $G_N M/R \gg 1$, with the help of the linear approximation (5.2.40) and (5.2.41). The leading order in $G_N M/R \gg 1$ then reads

$$U_{\text{BG}} \simeq -\frac{125 R}{3 G_N} e^{\left(\frac{G_N M}{\sqrt{6} R}\right)^{2/3}} \quad (5.3.12)$$

and

$$U_{\text{GG}}^{\text{in}} \simeq \frac{5 G_N M^2}{36 R}. \quad (5.3.13)$$

One expects that this negative and large potential energy U_G is counterbalanced by the positive energy (E.11) associated with the pressure (5.2.43) inside the matter source.

Of course, the total energy of the system should still be given by the ADM-like mass M , which must therefore equal the sum of the matter proper mass M_0 and the energy associated with the pressure (see Appendix E for more details about the energy balance).

Chapter 6

Bootstrapped Newtonian gravity: quantum picture

Like the Newtonian analogue, the bootstrapped potential determines the gravitational pull acting on test particles at rest ¹. It can therefore be used in order to describe the mean field force acting on the constituents of the system, namely the baryons in the static matter source as well as the gravitons in the potential itself. In order to gain some insight into the quantum structure of such self-gravitating systems, the solutions for the bootstrapped potential will be here described in terms of the quantum coherent state of a free massless scalar field, analogously to what was done for the Newtonian potential in Ref. [20] (see also Ref. [62, 99] for a model of BHs, Ref. [100] for general solitons and Refs. [91] for photons in a static electric or magnetic field). This analysis will be carried out in details both in the Newtonian approximation, which corresponds to sources of small compactness, and for the large compactness case. The analysis of the coherent state will allow us to recover the scaling (3.1.6) for the ADM mass M in terms of the number of gravitons N_G in all cases, whereas the scaling (3.1.7) for the mean wavelength will appear to require the fine-tuned maximal packing $R \sim R_H$. However, by considering the quantum nature of the source in rather general terms, we will also find that the classical bootstrapped relation between the BH mass M and the proper mass M_0 of the source implies a Generalised Uncertainty Principle (GUP) [52, 101–112] for the horizon size. Moreover, consistency of this GUP with the properties of the coherent state indeed suggests that the compactness of the source should be at most of order one and the scaling relation (3.1.7) can therefore be recovered in a fully quantum description of BHs. Such a bound on the maximum compactness of self-gravitating objects is at the heart of the so called *classicalization* of gravity [42–44, 113], according

¹In a quantum field theory description, this dynamics would be obtained from transition amplitudes yielding the propagator of the test particle. We here assume that all the required approximations leading to the effective appearance of a potential hold.

to which quantum fluctuations involved in processes above the Planck scale should be suppressed precisely by the formation of BHs viewed as quasi-classical configurations.

6.1 Quantum coherent state

We will first review how to describe a generic static potential V by means of the coherent state of a free massless scalar field. This will allow us to introduce a formal way of counting the number of quanta N_G for any such potential. We remark that a clear understanding of the physical meaning of the number of quanta so defined, in a field configuration that is not in general perturbatively related with the vacuum, could possibly be obtained only by studying the dynamical process leading to the formation of such a configuration. Of course, there is little hope of solving this problem analytically in a non-linear theory. Like in Refs. [20, 72], we shall instead take a similar approach to that for general solitons in quantum field theory found in Ref. [100] (see also Ref. [62, 99] for a model of BHs and Refs. [91] for photons in QED). We remark, in fact, that for our purposes, the number N_G is mostly an auxiliary quantity which allows us to tackle the issue of classicalization by means of the corresponding scaling relations (3.1.6) and (3.1.7) for BHs, discussed in Chapter 3.

We start by setting the stage for the quantum interpretation of the dimensionless $V = V(\mathbf{x})$ based on simple Fourier transforms. In order to fix the notation, we expand the potential in the normalised plane waves (2.2.3) as

$$V(\mathbf{x}) = \int_{\mathbb{R}^3} \frac{d\mathbf{k}}{(2\pi)^3} \tilde{V}(\mathbf{k}) v_{\mathbf{k}}(\mathbf{x}) , \quad (6.1.1)$$

where, in turn, one has

$$\tilde{V}(\mathbf{k}) = \int_{\mathbb{R}^3} d\mathbf{x} V(\mathbf{x}) v_{\mathbf{k}}^*(\mathbf{x}) , \quad (6.1.2)$$

with $\tilde{V}(\mathbf{k}) = \tilde{V}^*(-\mathbf{k})$.

Next, we will specialise to spherically symmetric cases and apply the construction to the Newtonian potential generated by a uniform ball of matter, for which the Fourier transform can be computed explicitly ². This exercise will allow us to introduce in the next Section a different way of analysing cases, like the bootstrapped Newtonian potential, for which this cannot be done analytically.

²The even simpler cases of the Newtonian potential for a point-like source and for a Gaussian source can be found in Chapter 4.

6.1.1 Static scalar potential

As it was done in Ref. [20], the first step consists in rescaling the dimensionless potential V so as to obtain a canonically normalised real scalar field ³

$$\Phi = \frac{V}{\sqrt{G_N}} = \sqrt{\frac{m_p}{\ell_p}} V . \quad (6.1.3)$$

This let us then quantise Φ as a free massless field as in Section 2.2. Classical configurations of the scalar field must be given by suitable states in the Fock space, and we note that a natural choice for $V = V(\mathbf{x})$ is given by a coherent state,

$$\hat{a}_{\mathbf{k}} |g\rangle = g_{\mathbf{k}} e^{i\gamma_{\mathbf{k}}(t)} |g\rangle , \quad (6.1.4)$$

such that the expectation value of the quantum field $\hat{\Phi}$ reproduces the classical potential, namely

$$\sqrt{\frac{\ell_p}{m_p}} \langle g | \hat{\Phi}(t, \mathbf{x}) |g\rangle = V(\mathbf{x}) . \quad (6.1.5)$$

From the expansion (2.2.6), one can easily compute the left hand side of Eq. (6.1.5) by making use of Eq. (6.1.4). Comparing with Eq. (6.1.1) then yields

$$g_{\mathbf{k}} = \frac{1}{\ell_p} \sqrt{\frac{k}{2}} \tilde{V}(\mathbf{k}) \quad (6.1.6)$$

and $\gamma_{\mathbf{k}}(t) = k t$, with the latter condition turning (propagating) plane waves into standing waves.

We are particularly interested in the total number of quanta in this coherent state, whose general expression is given by

$$\begin{aligned} N &= \int \frac{d\mathbf{k}}{(2\pi)^3} \langle g | \hat{a}_{\mathbf{k}}^\dagger \hat{a}_{\mathbf{k}} |g\rangle \\ &= \int \frac{d\mathbf{k}}{(2\pi)^3} g_{\mathbf{k}}^2 \\ &= \frac{1}{2\ell_p^2} \int \frac{d\mathbf{k}}{(2\pi)^3} k \tilde{V}^2(\mathbf{k}) , \end{aligned} \quad (6.1.7)$$

and in their mean wavelength $\lambda \simeq 1/\bar{k} \equiv N/\langle k \rangle$, where the mean wavenumber is given by

$$\begin{aligned} \langle k \rangle &= \int \frac{d\mathbf{k}}{(2\pi)^3} \langle g | k \hat{a}_{\mathbf{k}}^\dagger \hat{a}_{\mathbf{k}} |g\rangle \\ &= \int \frac{d\mathbf{k}}{(2\pi)^3} k g_{\mathbf{k}}^2 \\ &= \frac{1}{2\ell_p^2} \int \frac{d\mathbf{k}}{(2\pi)^3} k^2 \tilde{V}^2(\mathbf{k}) . \end{aligned} \quad (6.1.8)$$

³We recall that a canonically normalised scalar field has dimensions of $\sqrt{\text{mass}/\text{length}}$.

The above general expressions will next be specified for the Newtonian potential generated by spherically symmetric sources.

6.1.2 Newtonian potential for spherical sources

The Newtonian potential $V(\mathbf{x}) = V_N(r)$ for a spherically symmetric source of static energy density $\rho = \rho(r)$, can be described by means of the Lagrangian (4.1.14) whose corresponding Euler-Lagrange equation of motion is the Poisson equation in spherical coordinates (4.1.13). Since the system is static, the (on-shell) Hamiltonian is simply given by $H_N[V_N] = -L_N[V_N]$ as in Section 4.1. After introducing the rescaled field Φ of Eq. (6.1.3), we also need to rescale the Hamiltonian by a factor of 4π in order to canonically normalise the kinetic term⁴, to wit

$$H_N[\Phi] = 4\pi H_N[V_N] . \quad (6.1.9)$$

If we then promote $\Phi = \Phi(t, r)$ and rescale the matter density

$$\tilde{\rho} = 4\pi\sqrt{G_N}\rho = 4\pi\sqrt{\frac{\ell_p}{m_p}}\rho \quad (6.1.10)$$

we obtain

$$H_N[\Phi] = 4\pi \int_0^\infty r^2 dr \left[\frac{1}{2} \partial_\mu \Phi \partial^\mu \Phi + \tilde{\rho} \Phi \right] . \quad (6.1.11)$$

The previous general analysis for the coherent state can now be adapted to the spherically symmetric case by just replacing the plane waves (2.2.3) with the spherical Bessel functions (4.2.2),

$$v_{\mathbf{k}}(\mathbf{x}) \rightarrow j_0(kR) \equiv \frac{\sin(kR)}{kR} . \quad (6.1.12)$$

By substituting Eq. (6.1.1) into Eq. (4.1.13), we obtain the general result

$$\tilde{V}_N(k) = -\frac{4\pi\ell_p\tilde{\rho}(k)}{m_pk^2} , \quad (6.1.13)$$

which, together with Eq. (6.1.6), leads to

$$g_k = -\frac{4\pi\tilde{\rho}(k)}{m_p\sqrt{2}k^3} . \quad (6.1.14)$$

The spherically symmetric versions of Eqs. (6.1.7) and (6.1.8) then read

$$N_G = \int_0^\infty \frac{dk}{2\pi^2} k^2 g_k^2 , \quad (6.1.15)$$

⁴See Ref. [20] for more details.

6.1 Quantum coherent state

and

$$\langle k \rangle = \int_0^\infty \frac{dk}{2\pi^2} k^3 g_k^2, \quad (6.1.16)$$

where the suffix G emphasises that the quantity is evaluated in the coherent state representing the gravitational potential.

6.1.3 Newtonian potential of a uniform ball

Note that all expressions above can be explicitly computed if we know the coefficients g_k . As a workable example, we will again consider the homogeneous source (4.2.23) and recall from Section 4.2.1 the corresponding Newtonian solution

$$V_N = \begin{cases} \frac{G_N M}{2 R^3} (r^2 - 3 R^2) & \text{for } 0 \leq r < R \\ -\frac{G_N M}{r} & \text{for } r > R, \end{cases} \quad (6.1.17)$$

where $M = M_0$ is the ADM mass equal to the rest mass in this Newtonian case.

The Fourier transform of the density (4.2.23) is given by

$$\tilde{\rho}(k) = 4\pi \int_0^\infty dr r^2 \rho(r) j_0(kr) = \frac{3M}{k^2 R^2} \left[\frac{\sin(kR)}{kR} - \cos(kR) \right], \quad (6.1.18)$$

and the coherent state eigenvalues then read

$$g_k = \frac{12\pi M}{\sqrt{2} m_p k^{7/2} R^2} \left[\cos(kR) - \frac{\sin(kR)}{kR} \right]. \quad (6.1.19)$$

The mean wavenumber (6.1.16) can be easily evaluated from this expression,

$$\begin{aligned} \langle k \rangle &= \frac{36 M^2}{m_p^2 R^4} \int_0^\infty \frac{dk}{k^4} \left[\cos(kR) - \frac{\sin(kR)}{kR} \right]^2 \\ &= \frac{36 M^2}{m_p^2 R} \int_0^\infty \frac{dz}{z^4} \left[\cos z - \frac{\sin z}{z} \right]^2 \\ &= \frac{12\pi M^2}{5 m_p^2 R} = -4\pi \frac{U_N}{\ell_p m_p}, \end{aligned} \quad (6.1.20)$$

where

$$U_N = -\frac{3 G_N M^2}{5 R} \quad (6.1.21)$$

is precisely the gravitational potential energy of the spherically symmetric homogeneous source (4.2.23), a result consistent with the linearity of the Newtonian interaction ⁵.

⁵We note that the factor of 4π in the right hand side of Eq. (6.1.20) is just a consequence of the canonical rescaling (6.1.9).

6. Bootstrapped Newtonian gravity: quantum picture

While the mean wave number $\langle k \rangle$ above is finite, the number of gravitons (6.1.15) diverges in the infrared (IR), *i.e.* $k^2 g_k^2 \rightarrow \infty$ for $k \rightarrow 0$. This is also expected as the potential (6.1.17) has infinite spatial support and we could simply introduce a cut-off $k_0 = 1/R_\infty$ to account for the necessarily finite life-time of a realistic source [20]. In this case,

$$\begin{aligned} N_G &= \frac{36 M^2}{m_p^2 R^4} \int_{k_0}^{\infty} \frac{dk}{k^5} \left[\cos(k R) - \frac{\sin(k R)}{k R} \right]^2 \\ &= \frac{36 M^2}{m_p^2} \int_{R/R_\infty}^{\infty} \frac{dz}{z^5} \left[\cos z - \frac{\sin z}{z} \right]^2 \end{aligned} \quad (6.1.22)$$

$$\simeq 4 \frac{M^2}{m_p^2} \log \left(\frac{R_\infty}{2 R} \right). \quad (6.1.23)$$

The corpuscular scaling (3.1.6) with the square of the energy M of the system already appears at this stage, but we can still understand better the logarithmic divergence for $R_\infty \rightarrow \infty$ in order to make full sense of it.

As pointed out in Ref. [100], the fact that the energy (or the mean wavenumber) is finite despite the diverging number of constituents is a direct consequence of a decreasing energy contribution coming from gravitons with lower and lower momenta. We can in fact separate two contributions by introducing a scale Λ which splits the phase space of gravitons into *effective* (hard) and IR (soft) modes,

$$\begin{aligned} \langle k \rangle &= \int_0^\Lambda \frac{dk}{2\pi^2} k^3 g_k^2 + \int_\Lambda^\infty \frac{dk}{2\pi^2} k^3 g_k^2 \\ &\equiv k_{\text{IR}} + k_{\text{eff}}, \end{aligned} \quad (6.1.24)$$

where we require $k_{\text{eff}}(\Lambda) \gg k_{\text{IR}}(\Lambda)$. Indeed the scale Λ remains somewhat arbitrary, since it is just defined by requiring that $k_{\text{eff}}(\Lambda) \simeq \langle k \rangle$ to a good approximation. The accuracy of the approximation is clearly measured by the ratio $k_{\text{IR}}/k_{\text{eff}}$ which we plot in Fig. 6.1 (see Appendix F for the details). The interesting fact is that we can identify a threshold value $\Lambda_R \simeq 1/R$ which only depends on the size R of the source and not on M . Values of $\Lambda_\alpha = \Lambda_R/\alpha = 1/\alpha R$ with $\alpha > 1$ correspond to $k_{\text{IR}}/k_{\text{eff}} < 1$ and are acceptable approximations, with the level of precision set by α (*e.g.* $k_{\text{IR}}/k_{\text{eff}} \simeq 0.1$ for $\alpha = 5$). In particular, we find

$$k_{\text{eff}} = \frac{M^2}{m_p^2 R} f(\alpha), \quad (6.1.25)$$

with $f(\alpha)$ given explicitly in Eq. (F.1).

We can now use the scale Λ_α in order to identify the number N_G^{eff} of effective (hard) gravitons and the number N_G^{IR} of IR gravitons, namely

$$\begin{aligned} N_G &= \int_0^{\Lambda_\alpha} \frac{dk}{2\pi^2} k^2 g_k^2 + \int_{\Lambda_\alpha}^\infty \frac{dk}{2\pi^2} k^2 g_k^2 \\ &= N_G^{\text{IR}} + N_G^{\text{eff}}. \end{aligned} \quad (6.1.26)$$

6.2 Scaling relations from bootstrapped potential

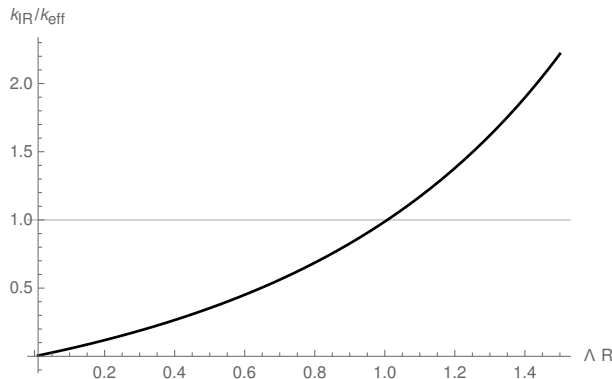


Figure 6.1: Ratio between k_{IR} and k_{eff} for varying Λ . The threshold is $\Lambda_R \simeq 1/R$.

The finite number of gravitons contributing to $k_{\text{eff}} \simeq \langle k \rangle$ is given by

$$N_{\text{G}}^{\text{eff}} = \frac{M^2}{m_{\text{p}}^2} g(\alpha) , \quad (6.1.27)$$

where $g(\alpha)$ is a numerical factor displayed in Eq. (F.4). The infinity (for $R_{\infty} \rightarrow \infty$) in the total amount (6.1.23) comes from N_{G}^{IR} , which counts the very soft gravitons contributing the small k_{IR} . It is now quite straightforward to evaluate the mean graviton wavelength as

$$\begin{aligned} \lambda_{\text{G}} &\simeq \frac{N_{\text{G}}^{\text{eff}}}{k_{\text{eff}}} = R \frac{f(\alpha)}{g(\alpha)} \\ &\equiv R h(\alpha) . \end{aligned} \quad (6.1.28)$$

Since $h(\alpha) < 1$ for $\alpha > 1$ (see Fig. 6.2), we have

$$\lambda_{\text{G}}(\alpha) \simeq h(\alpha) R \leq \alpha R , \quad (6.1.29)$$

and the average wavelength consistently belongs to the effective part of the spectrum (that is, $1/\lambda_{\text{G}}(\alpha) > \Lambda_{\alpha}$).

We conclude this section by remarking once more that the important results are that $N_{\text{G}}^{\text{eff}}$ only depends on the ADM energy M precisely like in Eq. (3.1.6), whereas λ_{G} is only proportional to R , and none of this quantities associated with the coherent state for the Newtonian potential therefore depend on the compactness of the source. The corpuscular scaling (3.1.7) for BHs, namely $\lambda_{\text{G}} \simeq R_{\text{H}} \sim M$, could therefore be obtained only by assuming $R \sim R_{\text{H}}$. This all should not be surprising since the Newtonian theory is linear, hence nothing special happens in it when $R \sim R_{\text{H}}$ and a BH is formed.

6.2 Scaling relations from bootstrapped potential

The bootstrapped potential solutions described in Chapter 5 were shown to satisfy the same regularity conditions (5.2.1), (5.2.2) and (5.2.3) of the Newtonian potential

6. Bootstrapped Newtonian gravity: quantum picture

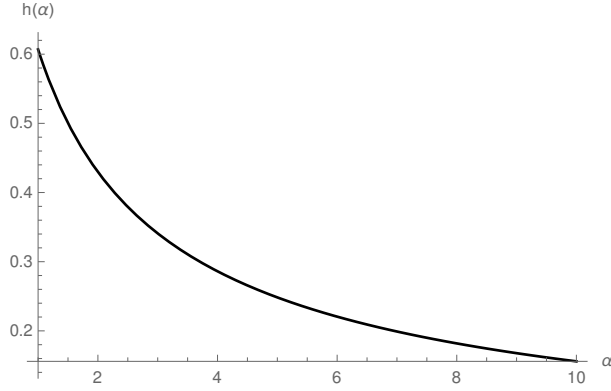


Figure 6.2: Plot of the function $h = h(\alpha)$.

and approach the Newtonian behaviour far from the source

$$V_{\text{out}}(r) \simeq V_{\text{N}} = -\frac{G_{\text{N}} M}{r} \quad \text{for } r \gg R^* , \quad (6.2.1)$$

where M is the total ADM energy which is equal to the rest mass M_0 only in the Newtonian case. The scale R^* conveniently introduced above represents a distance (well) beyond which the potential can be safely approximated by the Newtonian expression in the outer vacuum. It is therefore natural to identify R^* as the larger between the gravitational radius of the matter source with energy M and the actual size R of the matter source,

$$R^* = \max\{G_{\text{N}} M, R\} . \quad (6.2.2)$$

The quantum construction in this case is analogous to what was done in Sections 6.1.2 and 6.1.3 but we first need to clarify a subtle aspect. After following the prescription (6.1.3), the Lagrangian (5.1.3) reads (with $q_V = 3q_B = q_\rho = 1$)

$$L[\Phi] = 4\pi \int_0^\infty r^2 dr \left[-\frac{1}{2} \partial_\mu \Phi \partial^\mu \Phi - \mu \Phi \left(1 - 2\sqrt{G_{\text{N}}} \Phi \right) + 2\sqrt{G_{\text{N}}} \Phi \partial_\mu \Phi \partial^\mu \Phi \right] \quad (6.2.3)$$

where $\mu = \rho + p$. As in Section 6.1.2 we rescaled the Lagrangian by a total factor 4π . While for the Newtonian case this was sufficient to guarantee a canonically normalized kinetic term, here the derivative interaction spoils this property and in general $H[\Phi] = -L[\Phi]$ does not hold anymore. Nevertheless, we will only use the whole approach for the purpose of studying the quantum properties of the static bootstrapped potential $V(r)$ so that the derivative term does not ruin the whole picture ⁶. Everything is now set for a quantum interpretation of the bootstrapped potential in terms of a coherent state following the approach of Section 6.1. Unfortunately, the calculations of the number

⁶If one were to study the quantum dynamics described by the above Lagrangian then a further rescaling of the field Φ would be necessary to diagonalize the kinetic term [114].

6.2 Scaling relations from bootstrapped potential

of gravitons and their mean wavelength are now made more difficult by the fact that we cannot compute the Fourier transform of the scalar potential $V = V(r)$ and the integrals in k in Eqs. (6.1.7) and (6.1.8) cannot be done exactly. For this reason, we shall employ a different procedure, detailed in Appendix G, which amounts to rewriting Eq. (6.1.8) as the spatial integral (G.8)⁷, that is

$$\begin{aligned} \langle k \rangle &= \frac{2\pi}{\ell_p^2} \int_0^\infty dr r^2 [V'(r)]^2 \\ &= \frac{2\pi}{\ell_p^2} \int_0^R dr r^2 [V'_{\text{in}}(r)]^2 + \frac{2\pi}{\ell_p^2} \int_R^\infty dr r^2 [V'_{\text{out}}(r)]^2, \end{aligned} \quad (6.2.4)$$

and then use a similar argument to that of Section 6.1.3. The main difference is that, since we integrate along the radial coordinate, we must determine a length scale R_γ such that the integral from 0 to R_γ provides the main contribution to $\langle k \rangle$ in Eq. (6.2.4).

We separate the two possible cases with $R_\gamma < R$ and $R_\gamma > R$, respectively, and define

$$k_{\text{eff}} = \begin{cases} \frac{2\pi}{\ell_p^2} \int_0^{R_\gamma} dr r^2 [V'_{\text{in}}(r)]^2 & \text{for } 0 \leq R_\gamma < R \\ \frac{2\pi}{\ell_p^2} \int_0^R dr r^2 [V'_{\text{in}}(r)]^2 + \frac{2\pi}{\ell_p^2} \int_R^{R_\gamma} dr r^2 [V'_{\text{out}}(r)]^2 & \text{for } R_\gamma > R \end{cases} \quad (6.2.5)$$

and

$$k_\infty = \begin{cases} \frac{2\pi}{\ell_p^2} \int_{R_\gamma}^R dr r^2 [V'_{\text{in}}(r)]^2 + \frac{2\pi}{\ell_p^2} \int_R^\infty dr r^2 [V'_{\text{out}}(r)]^2 & \text{for } 0 \leq R_\gamma < R \\ \frac{2\pi}{\ell_p^2} \int_{R_\gamma}^\infty dr r^2 [V'_{\text{out}}(r)]^2 & \text{for } R_\gamma > R. \end{cases} \quad (6.2.6)$$

The ratio

$$\frac{k_\infty}{k_{\text{eff}}} = \gamma, \quad (6.2.7)$$

with $\gamma < 1$, defines the scale R_γ for which k_{eff} approximates $\langle k \rangle$ within the required precision (similarly to the parameter α used in Section 6.1.3). The analysis in Appendix G.2 shows that the number of gravitons scales as M^2/m_p^2 , under quite general assumptions, and contains the same logarithmic divergence as in the Newtonian case, with R^* replacing R , that is

$$N_G \simeq 4 \frac{M^2}{m_p^2} \log \left(\frac{R_\infty}{R^*} \right). \quad (6.2.8)$$

⁷It is crucial that the N_G is still IR divergent while $\langle k \rangle$ is finite, as shown explicitly in Appendix G.

6. Bootstrapped Newtonian gravity: quantum picture

We shall therefore rely on the argument of Section 6.1.3 and assume that the number of gravitons effectively contributing up to the scale R_γ is finite and proportional to M^2/m_p^2 ,

$$N_G^{\text{eff}} \sim \frac{M^2}{m_p^2}. \quad (6.2.9)$$

In the following, we will estimate the scale R_γ for the Newtonian potential as a test of the method and then apply it to the bootstrapped potential.

6.2.1 Newtonian potential

We start with the Newtonian potential in order to test the validity of the above Eqs. (6.2.4), (6.2.5) and (6.2.6). The first important check is that Eq. (6.2.4) indeed reproduces the result (6.1.20),

$$\begin{aligned} \langle k \rangle &= \frac{2\pi}{\ell_p^2} \int_0^R dr r^4 \frac{G_N^2 M^2}{R^6} + \frac{2\pi}{\ell_p^2} \int_R^{R_\infty} dr \frac{G_N^2 M^2}{r^2} \\ &= \frac{2\pi M^2}{5 m_p^2 R} + \frac{2\pi M^2}{m_p^2 R} \\ &= \frac{12\pi M^2}{5 m_p^2 R}. \end{aligned} \quad (6.2.10)$$

It is then easy to verify that Eqs. (6.2.5) and (6.2.6) give

$$k_{\text{eff}} = \begin{cases} \frac{2\pi M^2 R_\gamma^5}{5 m_p^2 R^6} & \text{for } 0 \leq R_\gamma < R \\ \frac{12\pi M^2}{5 m_p^2 R} - \frac{2\pi M^2}{m_p^2 R_\gamma} & \text{for } R_\gamma > R \end{cases} \quad (6.2.11)$$

and

$$k_\infty = \begin{cases} \frac{12\pi M^2}{5 m_p^2 R} - \frac{2\pi M^2 R_\gamma^5}{5 m_p^2 R^6} & \text{for } 0 \leq R_\gamma < R \\ -\frac{2\pi M^2}{m_p^2 R_\gamma} & \text{for } R_\gamma > R. \end{cases} \quad (6.2.12)$$

After replacing these expression into Eq. (6.2.7), it turns out that $\gamma < 1$ implies $R_\gamma \gtrsim R$, as shown in Fig. 6.3. One can in fact solve Eq. (6.2.7) for R_γ and find

$$R_\gamma = \frac{5}{6} \left(\frac{\gamma + 1}{\gamma} \right) R. \quad (6.2.13)$$

It would be tempting to set a direct connection with the momentum scale Λ_α introduced in Section 6.1.3 and state that $\Lambda_{\alpha=\gamma} = 1/R_\gamma$, but we could not find a strict proof of this

6.2 Scaling relations from bootstrapped potential

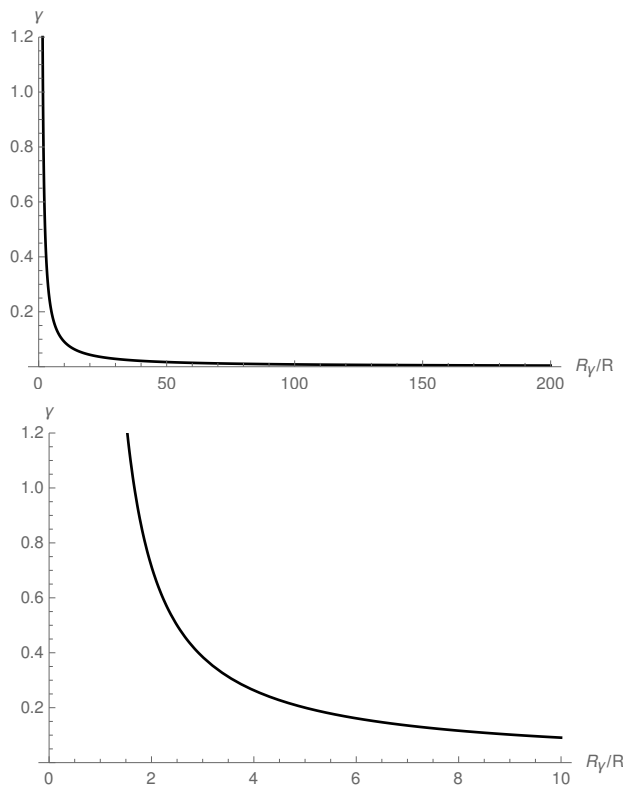


Figure 6.3: Ratio $k_\infty/k_{\text{eff}} = \gamma$ for the Newtonian potential (left panel) and a close-up view for small R_γ (right panel).

relation. It is nonetheless reassuring that Eq. (6.2.13) further supports the conclusion that in the Newtonian regime the only relevant scale for $\langle k \rangle$ is the radius R of the source. In any case it is sufficient for our purposes to assume that $\Lambda_\alpha = 1/R_\gamma$ for precisions $\gamma \sim \alpha$ and show that the mean wavelength computed with the effective gravitons alone is qualitatively the same as in Eq. (6.1.28).

6.2.2 Bootstrapped potential

We can finally consider the bootstrap solutions of Chapter 5. When the compactness is small, the solutions in Eq. (5.2.5) and (5.2.25) follow rather closely the Newtonian behaviour and the results of Section 6.2.1 become a very good approximation.

When the compactness is instead large, things change significantly. The outer potential is always given by the exact solution (5.2.5) while for the inner potential we will

6. Bootstrapped Newtonian gravity: quantum picture

consider the linear approximation (5.2.40). In so doing, Eq. (6.2.4) gives

$$\begin{aligned}
\langle k \rangle &\simeq \frac{2\pi}{\ell_p^2} \int_0^R dr r^2 (V'_R)^2 + \frac{2\pi}{\ell_p^2} \int_R^\infty dr r^2 \left[\frac{G_N M}{(1 + 6 G_N M/r)^{1/3} r^2} \right]^2 \\
&= \frac{2\pi R^3 (V'_R)^2}{3\ell_p^2} + \frac{2\pi G_N^2 M^2}{\ell_p^2} \int_R^\infty \frac{dr}{(1 + 6 G_N M/r)^{2/3} r^2} \\
&= \frac{\pi G_N M}{\ell_p^2} \left[\frac{2 G_N M}{(1 + 6 G_N M/R)^{2/3} R} + \left(1 + \frac{6 G_N M}{R} \right)^{1/3} - 1 \right] \\
&\simeq \frac{M}{\ell_p m_p} \left(\frac{G_N M}{R} \right)^{1/3}, \tag{6.2.14}
\end{aligned}$$

where V'_R is given in Eq. (5.2.8) and the last expression contains just the leading order in the compactness $G_N M/R \gg 1$. Like in the Newtonian case, the mean wave number $\langle k \rangle$ is finite, despite the number of gravitons diverges again and with the same behaviour and functional dependence (see Appendix G.2 for the details). Given these similarities with the Newtonian regime, we exploit the same method described in Section 6.2.1 in order to find the scale R_γ for the bootstrapped potentials. We only consider the case $R_\gamma > R$ as it is the only one in which one can have $\gamma < 1$. Hence, Eqs. (6.2.5) and (6.2.6) yield

$$k_{\text{eff}} = \frac{2\pi R (G_N M/R)^2}{3\ell_p^2 (1 + 6 G_N M/R)^{2/3}} + \frac{\pi M}{\ell_p m_p} \left[\left(1 + \frac{6 G_N M}{R} \right)^{1/3} - \left(1 + \frac{6 G_N M}{R_\gamma} \right)^{1/3} \right] \tag{6.2.15}$$

and

$$k_\infty = \frac{\pi M}{\ell_p m_p} \left[\left(1 + \frac{6 G_N M}{R_\gamma} \right)^{1/3} - 1 \right], \tag{6.2.16}$$

where the linear approximation (5.2.40) was considered for the inner potential and the exact solution (5.2.5) for the outer region. After solving Eq. (6.2.7) for R_γ , one finds

$$R_\gamma \simeq \frac{6 G_N M}{\left[\frac{20}{3 \cdot 6^{2/3}} \left(\frac{\gamma}{\gamma+1} \right) \left(\frac{G_N M}{R} \right)^{1/3} + 1 \right]^3 - 1}. \tag{6.2.17}$$

It is easy to see that the threshold value of R_γ , corresponding to $\gamma = 1$, is still proportional to R in the regime $G_N M/R \gg 1$. On the other hand, Figs. 6.4 and 6.5 show that R_γ raises very quickly for $\gamma < 1$ and reaches values of order $G_N M$ or large for better precisions. Hence, from Eqs. (6.2.13) and (6.2.17), we see that R_γ qualitatively behaves as the scale R^* of Eq. (6.2.2): it is proportional to R for sources with small compactness (consistently with the quasi-Newtonian behaviour) while it is also related to the scale $G_N M$ when the compactness becomes large. In other words, we get a good description of the system by considering gravitons inside a ball of radius $R_\gamma \sim R$

6.2 Scaling relations from bootstrapped potential

for $G_N M/R \ll 1$ and $R_\gamma \sim R(G_N M/R)^{2/3}/\gamma$ for $G_N M/R \gg 1$ and $0 < \gamma \ll 1$. In particular, for large compactness, we can tune the precision coefficient γ so that $R_\gamma \sim G_N M$. As we mentioned at the end of Section 6.2.1, this suggests that there is a scale $\Lambda \sim 1/R^*$ in momentum space below which the contribution of gravitons becomes essentially irrelevant.

Finally, we simply evaluate the mean graviton wavelength as the ratio between Eq. (6.2.9) and Eq. (6.2.14) and get

$$\frac{\lambda_G}{R} \simeq \left(\frac{G_N M}{R} \right)^{2/3} \gg 1, \quad (6.2.18)$$

so that we can conclude that

$$1 \lesssim \frac{\lambda_G}{R} \lesssim \frac{G_N M}{R}, \quad (6.2.19)$$

and the compactness of the source yields a (rough) upper bound for the mean wavelength. The above expression also does not reproduce the expected scaling relation (3.1.7) of the corpuscular model, to wit $\lambda_G \sim M$, unless the compactness is of order one, rather than very large. However, we will see below that it might be the quantum nature of the source that requires this rather strong bound for the compactness.

6.2.3 Quantum source and GUP for the horizon

It was shown in Ref. [115] that a quantum source whose size R is comparable with its gravitational radius (2.1.4) satisfies a GUP [52, 101–112] of the form

$$\Delta R \sim \frac{\ell_p m_p}{\Delta P} + \gamma \ell_p \frac{\Delta P}{m_p}, \quad (6.2.20)$$

where ΔR is the uncertainty in the size of the source and ΔP the uncertainty in the conjugate radial momentum. The first term in the right hand side follows from the usual Heisenberg uncertainty relation, whereas the second term corresponds to the horizon fluctuations, $\Delta R_H \sim \Delta M_0 \sim \Delta P$, obtained from the Horizon Wave-Function (HWF) determining the size R_H of the gravitational radius [116–118]. In Eq. (6.2.20) the two terms are just linearly combined with an arbitrary coefficient $\gamma > 0$ [115]. In particular, one finds that the quantum fluctuations of the horizon depend strongly on the precise quantum state of the source: the quantum fluctuations of a macroscopic BH of mass $M \sim M_0 \gg m_p$ are very large (with $\Delta R_H/R_H \sim 1$) if the source is given by a localised single particle with Compton width $\Delta R \sim R \sim \ell_p m_p/M_0$ [115], whereas they can be negligibly small if the source contains a large number of components of individual energy $\epsilon \ll M_0$ and size $R \sim R_H$ [56, 57], like is the case for corpuscular BHs [12–14, 85–88].

6. Bootstrapped Newtonian gravity: quantum picture

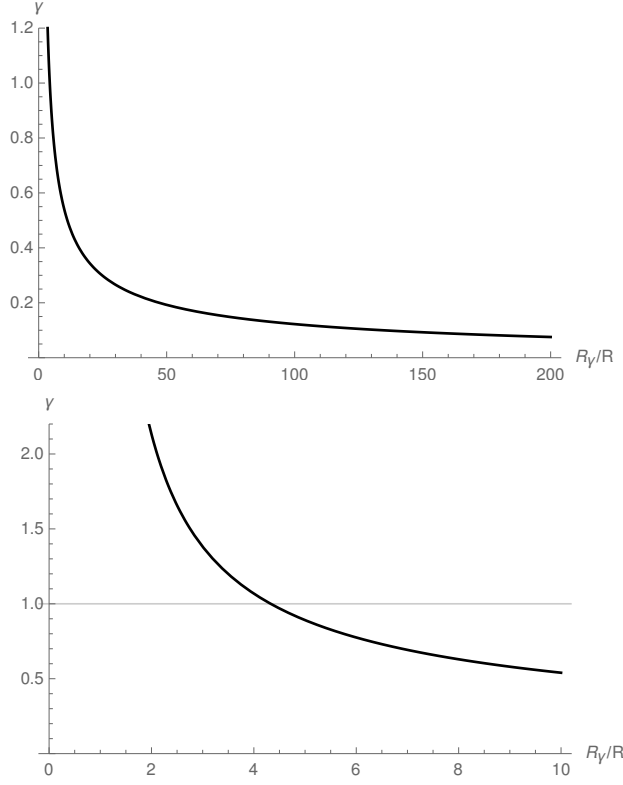


Figure 6.4: Ratio $k_\infty/k_{\text{eff}} = \gamma$ for the bootstrapped potential (left panel) and close-up view for small R_γ (right panel).

It is now interesting to note that the relation (5.2.42) for very compact sources directly implies a similar GUP for the gravitational radius, namely

$$\begin{aligned} \frac{\Delta R_{\text{H}}}{R_{\text{H}}} &\simeq \frac{\Delta M}{M} = \frac{\Delta M_0}{M_0} + \frac{\Delta R}{R} \\ &\sim \frac{\ell_{\text{p}}^2}{R^2} \left(\frac{R}{G_{\text{N}} M} \right)^{2/3} \frac{R}{\Delta R} + \frac{\Delta R}{R}, \end{aligned} \quad (6.2.21)$$

where we again assumed the Heisenberg uncertainty relation for the source,

$$\Delta M_0 \sim \frac{\ell_{\text{p}} m_{\text{p}}}{\Delta R}, \quad (6.2.22)$$

and used Eq. (5.2.42) to express the compactness in terms of the ADM mass M . In particular, the second term in Eq. (6.2.21) is analogous to the second term in Eq. (6.2.20) and would not be found in the case of Newtonian gravity (where $M = M_0$ exactly), or it would be negligibly small for small compact sources (for which $M \simeq M_0$). The fluctuations of the horizon are now dominated by the fluctuations of the source, $\Delta M \sim \Delta R$, for very large compactness $G_{\text{N}} M/R \gg 1$, if the size of the source $R \gtrsim \ell_{\text{p}}$ (otherwise the usual Heisenberg term cannot be neglected). This is analogous to the above mentioned results obtained from the HWF (except for the auxiliary condition $R \gtrsim \ell_{\text{p}}$).

6.2 Scaling relations from bootstrapped potential

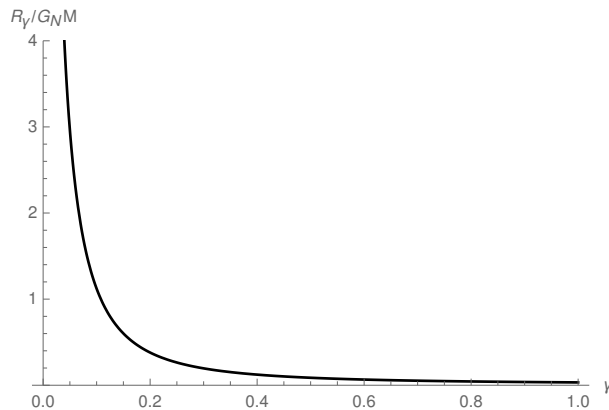


Figure 6.5: R_γ in units of $G_N M$ for the bootstrapped potential.

Let us continue to consider the case of large compactness and note that one needs $\Delta M/M \ll 1$ for the gravitational radius to show a classical behaviour. This can be obtained for a quasi-classical source with $\Delta R/R \ll 1$ provided the compactness is sufficiently large. Indeed, we can minimise the above expression (6.2.21), thus obtaining

$$\frac{\Delta R}{R} \simeq \frac{\ell_p}{R} \left(\frac{R}{G_N M} \right)^{1/3}. \quad (6.2.23)$$

The corresponding minimum value of the horizon fluctuations is then given by

$$\frac{\Delta M}{M} \simeq 2 \frac{\ell_p}{R} \left(\frac{R}{G_N M} \right)^{1/3} \sim \frac{\Delta R}{R}, \quad (6.2.24)$$

so that the condition of classicality of the source, $\Delta R/R \ll 1$, or

$$\frac{G_N M}{R} \gg \frac{\ell_p^3}{R^3}, \quad (6.2.25)$$

seems to ensure that the gravitational radius is also classical and satisfies $\Delta R_H/R_H \sim \Delta M/M \ll 1$.

However, the above argument does not yet take into consideration the quantum description of the gravitational potential in terms of a coherent state. Indeed, we should note that Eq. (6.2.18) implies that the above minimum uncertainty (6.2.24) for the horizon would correspond to a mean graviton wavelength

$$\frac{\lambda_G}{R} \sim \left(\frac{G_N M}{R} \right)^{2/3} \sim \frac{\ell_p^2}{\Delta R^2}. \quad (6.2.26)$$

Assuming the matter uncertainty cannot realistically be smaller than the Planck length, this appears to constrain the compactness to be of order one or less, in clear contradiction with the starting assumption $G_N M/R \gg 1$. On the other hand, for a compactness

6. Bootstrapped Newtonian gravity: quantum picture

of order one, both Eq. (5.2.42) and the analysis of the Newtonian case in Section 6.1.3 would imply that

$$\lambda_G \sim R \simeq \ell_p \frac{M}{m_p}, \quad (6.2.27)$$

which is precisely the prediction of the corpuscular model [12–14, 85–88]. Furthermore, we remark that the second approximation in the small compactness expression (5.2.24) clearly fails for $G_N M/R \simeq 1$ and Eq. (5.2.42) cannot yet be trusted in this intermediate regime⁸. If we evaluate the first line of Eq. (5.2.24) for $G_N M/R \simeq 1$, we obtain

$$M \simeq \frac{3}{2} M_0 \quad (6.2.28)$$

and

$$\frac{\Delta M}{M} \simeq \frac{\Delta M_0}{M_0} \sim \frac{m_p \ell_p}{M \Delta R} \lesssim \frac{1}{\sqrt{N_G}}, \quad (6.2.29)$$

where we used the scaling relation (3.1.6) and $\Delta R/\ell_p \gtrsim 1$. This result is consistent with the horizon of a macroscopic BH (with $N_G \gg 1$) being classical. Finally, we note that the scaling for the fluctuations derived for thermal BHs in Refs. [56, 57],

$$\frac{\Delta M}{M} \sim \frac{1}{N_G}, \quad (6.2.30)$$

is recovered from $\Delta R \sim \lambda_G \sim R_H$. Such a large uncertainty would apply to matter in a truly quantum state, like a condensate or the core of a neutron star.

⁸We showed numerically in Ref. [18] that this is in fact the most difficult regime to describe analytically.

Chapter 7

Conclusions and outlook

7.1 Conclusions

Under rather general assumptions in GR, systems that develop trapping surfaces will collapse into singularities [1]. This is what one expects would happen to a body that shrinks below the Buchdahl limit (2.1.1). On the other hand, a singularity is hardly acceptable in the quantum theory, just because of the Heisenberg uncertainty principle, and one could generically expect that the actual collapse of an astrophysical body will necessarily deviate from the general relativistic description at some point. The crucial question is whether such deviations occur after the horizon has appeared, and they therefore remain hidden forever, or the quantum effects induce departures from GR outside the gravitational radius which can therefore be observed by the next generation of Gravitational Waves (GWs) detectors such as LISA [119, 120]. Many works have shown the existence of regular BH solutions of modified gravitational equations which entail no significant departures from the corresponding general relativistic space-times outside the (outer) horizon (for some reviews, see Refs. [23, 121]). The corpuscular picture instead assumes that BHs are fully quantum objects in order to give a consistent description of the Hawking evaporation. The original proposal [12] however totally neglects the role of matter, whose effects are argued to be unimportant. On the other hand, it is hard to completely forget about the fate of the shrinking source causing the emergence of the BH geometry. Clearly, if GR remains a good theory of gravity up to extremely high energy densities, the collapsing matter should form a tiny ball with essentially no modifications of physics below the Planck energy scale. However, in the corpuscular picture one could actually conceive the possibility that the collapsing matter occupies a large volume inside the BH and gives rise to an effective gravitational potential that differs significantly from the general relativistic description.

For these reasons, in this thesis we addressed the possibility of an effective quantum deviation from GR at horizon scales, whose observable consequences should not be

excluded a priori. We therefore developed the *bootstrapped Newtonian gravity* approach and applied it to the case of a homogeneous source. Of course we do not expect it to produce phenomenological evidences for compact objects like neutron stars, but we understand it as a toy model of gravity tailored to further investigating the quantum picture of BHs. Let us then summarize the main content of the thesis.

In Chapter 2 we reviewed the singularity problem and gave its definition in terms of the Buchdahl theorem. This proves to be more convenient than the singularity theorems when studying compact objects by showing that the problem can be solved by giving away any of the assumptions of the theorem itself. We then proceeded to analyse the Hawking radiation as a consequence of the semiclassical approach unifying a quantum field description and the classical GR picture. We highlighted how the singularity issue naturally persists and shortly addressed the problems related to the evaporation effects, such as the information paradox.

In Chapter 3 we described the corpuscular model as an inspirational proposal to tackle the above issues and introduce useful relations to compare with. Here we showed how the BHs picture in terms of marginal bound states of soft off-shell gravitons offers the possibility of having a regular structure, with energy homogeneously distributed, as well as a natural way to reproduce Hawking thermal radiation as a depletion effect.

In Chapter 4 we introduced a scalar field theory description of the post-Newtonian potential by deriving the corresponding Lagrangian at second order in Newton's constant starting from the massless Fierz-Pauli Lagrangian. The solutions for a homogeneous and gaussian matter distributions were then considered, thus verifying the correct post-Newtonian behaviour of the theory.

The results of Chapter 4 laid the ground for the development of the bootstrapped approach for homogeneous and isotropic sources in Chapter 5. Inspired by Refs. [15, 16], we derived again the scalar field Lagrangian by coupling the gravitational potential to its own energy density and also adding the necessary pressure contribution. The bootstrap procedure is shown to essentially consist in studying Eq. (5.1.7) at face value, without requiring the non-linear effects it introduces to be small. The solutions can therefore be regarded as solitons which remarkably violate the Buchdahl limit. Indeed, they show a regular behaviour all the way down to the central singularity, irrespectively of the compactness of the source. Even if we are aware the homogeneous source is quite unrealistic, it still carries some physical interest as it is the only matter configuration which saturates the Buchdahl limit (as shown in Chapter 2). Therefore it is hard to expect that other more phenomenologically relevant sources would lead to a singular behaviour in this approach, leaving aside the obvious technical difficulties they would carry.

Finally, in Chapter 6 we provided the quantum picture of the above regular solutions. We first refined the coherent state formalism as it represents a convenient framework

7.2 Remarks

to catch the features of soft quanta in classical field configurations [91, 99] and also to study solitonic solutions in quantum field theory [100]. This approach suggested a quite direct connection with the scaling relations (3.1.6) and (3.1.7) of the corpuscular model. We could also envisage that this derivation tells us something more. First, it clearly shows that the scaling (3.1.6) for the ADM mass, responsible of reproducing the Bekenstein's area law, is a mere consequence of the boundary conditions at infinity. It is thus completely independent from the details of the gravitational interaction near the source. Secondly, our result on the typical wavelength of the gravitons clarifies that the advocated dependence on the mass of the source appears as a consequence of strong gravitational effects. On the other hand, the scaling in Eq. (3.1.7) can only be recovered in this context if one assumes some quantum effects (here the GUP is proposed but further work could be required) intervene to stop the source from shrinking at horizon scales. Hence the result in Eq. (3.1.7) actually turns out to be dependent on the matter content of the system.

7.2 Remarks

Few comments on the interpretation and possible issues of the bootstrapped approach are now required. First of all, from a quantum field theory perspective, the potential we employ to describe the gravitational pull on test particles should emerge from a suitable limit of the interacting propagator for test particles with the constituents of the matter source. Considering that we are interested in understanding gravity also in the interior of the self-gravitating object, and given the complexity of a macroscopic matter source, this approach seems hardly attainable (analytically). We have therefore assumed that a heuristic description in terms of a scalar potential represents a sensible mean field approximation, like the Coulomb potential yields a viable quantum description of the hydrogen atom or other bound states in quantum electrodynamics.

Another important remark is that, if one views the equation governing the bootstrapped potential as the truncated version of GR, including just the first nonlinearities sounds completely arbitrary and one might argue that there are no reasons to believe the results would remain unchanged by adding more terms. Actually, one could easily argue that, at the classical level, the inclusion of all terms stemming from GR would reintroduce the Buchdahl limit and the well-known singularities. However, if the singularities have to be removed, a modification of GR becomes necessary and the bootstrapped Newtonian potential is just one of the simplest toy models we can employ to study quantum features of the nonlinear dynamics for macroscopic sources. On the other hand, if it is indeed possible to recover the (quantum) gravitational dynamics at all orders in perturbation theory from the leading nonlinearities and diffeomorphism in-

variance (see the approach in Refs. [17, 122]), the results in the present work might help to understand the gravitational physics of macroscopic matter sources which cannot be treated as small perturbations about the vacuum.

7.3 Outlook

We finally conclude with some hints for future developments. As already mentioned, it is tempting to view this picture, in which the compactness of a self-gravitating object never exceeds values of order one, as pointing to the classicalization [42–45] in matter-gravity systems. However, more work is required to make the link stronger and the possibility that beyond standard model physics is necessary to describe matter in the interior should not be excluded.

Likewise, the reconstruction of an effective metric (as in Ref. [98]) will be essential for understanding the causal structure and possible phenomenological implications of the quantum model. In particular, the stage is set for a dynamical study of the system which could lead to a number of interesting results, like the investigation of radiation properties of the bootstrapped source. In this framework, deviations from GR can be easily parametrized in the quasi normal modes (QNMs) and could be constrained by the LISA mission with a precision that cannot be reached by any ground based GW interferometer [119, 120].

The next interesting development of the bootstrap picture concerns the quantum description. As we already stressed before, one of the main problems here is the understanding of the non-perturbative effects allowing for the existence of a non-trivial, highly populated vacuum state. Further insight on this issue could actually be obtained by deriving the Gross-Pitaevskii equation [53] associated to the Hamiltonian (5.1.4) and studying its properties. Also the emitting features could be considered from this perspective and some new light could be shed on the relation with the quantum depletion process. While all this could prove to be helpful, it probably involves numerical methods.

At last, we recall that the corpuscular picture of gravity can be applied to cosmology [85, 93], where the Universe is depicted as a cosmological condensate of gravitons and can give rise to dark energy and dark matter phenomenology [123–125], and reproduce the Starobinsky model of inflation [126]. It will therefore be very interesting to embed the description of compact sources in bootstrapped Newtonian gravity within such a cosmological perspective as local impurities affecting the cosmological condensate of gravitons. The cosmological perspective could also lead to novel hints on the stabilization of the two condensates as it is shown to happen in specific circumstances for two interacting BECs [127].

Appendix A

Post-Newtonian potential

In order to derive the post-Newtonian correction to the usual Newtonian potential from General Relativity, we consider a test particle of mass m freely falling along a radial direction in the Schwarzschild space-time around a source of mass M .

The Schwarzschild metric in standard form is given by ¹

$$ds^2 = - \left(1 - \frac{2M}{\tilde{r}}\right) d\tilde{t}^2 + \left(1 - \frac{2M}{\tilde{r}}\right)^{-1} d\tilde{r}^2 + \tilde{r}^2 d\Omega^2, \quad (\text{A.1})$$

and the radial geodesic equation for a massive particle turns out to be

$$\frac{d^2\tilde{r}}{d\tau^2} = -\frac{M}{\tilde{r}^2}, \quad (\text{A.2})$$

which looks formally equal to the Newtonian expression, but where \tilde{r} is the areal radial coordinate related to the Newtonian radial distance r by

$$dr = \frac{d\tilde{r}}{\sqrt{1 - \frac{2M}{\tilde{r}}}}. \quad (\text{A.3})$$

Moreover, the proper time τ of the freely falling particle is related to the Schwarzschild time \tilde{t} by

$$d\tau = \left(1 - \frac{2M}{\tilde{r}}\right) \frac{m}{E} d\tilde{t}, \quad (\text{A.4})$$

where E is the conserved energy of the particle. We thus have

$$\frac{d^2\tilde{r}}{d\tilde{t}^2} = -\frac{M}{\tilde{r}^2} \left(1 - \frac{2M}{\tilde{r}}\right)^2 \left[\frac{m^2}{E^2} - 2 \left(1 - \frac{2M}{\tilde{r}}\right)^{-3} \left(\frac{d\tilde{r}}{d\tilde{t}}\right)^2 \right]. \quad (\text{A.5})$$

Next, we expand the above expressions for $M/r \simeq M/\tilde{r} \ll 1$ (weak field) and $|d\tilde{r}/d\tilde{t}| \ll 1$ (non-relativistic regime). In order to keep track of small quantities, it is useful to introduce a parameter $\epsilon > 0$ and replace

$$\frac{M}{\tilde{r}} \rightarrow \epsilon \frac{M}{\tilde{r}}, \quad \frac{d\tilde{r}}{d\tilde{t}} \rightarrow \epsilon \frac{d\tilde{r}}{d\tilde{t}}. \quad (\text{A.6})$$

¹In this Appendix, we will use units with $G_N = 1$ for simplicity.

From the non-relativistic limit, it also follows that $E = m + \mathcal{O}(\epsilon^2)$ and any four-velocity

$$u^\mu = \left(1 + \mathcal{O}(\epsilon^2), \epsilon \frac{d\vec{x}}{d\tilde{t}} + \mathcal{O}(\epsilon^2) \right), \quad (\text{A.7})$$

so that the acceleration is also of order ϵ ,

$$\frac{d^2 x^\mu}{d\tau^2} = \epsilon \left(0, \frac{d^2 \vec{x}}{d\tilde{t}^2} \right) + \mathcal{O}(\epsilon^2). \quad (\text{A.8})$$

We then have

$$\epsilon \frac{d^2 \tilde{r}}{d\tilde{t}^2} = -\epsilon \frac{M}{\tilde{r}^2} \left(1 - \epsilon \frac{2M}{\tilde{r}} \right)^2 \left[1 + \mathcal{O}(\epsilon^2) - 2 \left(1 - \epsilon \frac{2M}{\tilde{r}} \right)^{-3} \epsilon^2 \left(\frac{d\tilde{r}}{d\tilde{t}} \right)^2 \right], \quad (\text{A.9})$$

and

$$r \simeq \int \left(1 + \epsilon \frac{M}{\tilde{r}} + \epsilon^2 \frac{3M}{2\tilde{r}^2} \right) d\tilde{r} \simeq \tilde{r} \left[1 - \epsilon \frac{M}{\tilde{r}} \log \left(\epsilon \frac{M}{\tilde{r}} \right) - \epsilon^2 \frac{3M^2}{2\tilde{r}^2} + \mathcal{O}(\epsilon^3) \right]. \quad (\text{A.10})$$

Since

$$r = \tilde{r} + \mathcal{O}(\epsilon \log \epsilon), \quad (\text{A.11})$$

it is clear that Eq. (A.9) to first order in ϵ reproduces the Newtonian dynamics,

$$\frac{d^2 r}{dt^2} \simeq \frac{d^2 \tilde{r}}{d\tilde{t}^2} \simeq -\frac{M}{r^2}. \quad (\text{A.12})$$

The interesting correction comes from including the next order. In fact, we have

$$\epsilon \frac{d^2 \tilde{r}}{d\tilde{t}^2} = -\epsilon \frac{M}{r^2} + \epsilon^2 \frac{4M^2}{r^3} + \mathcal{O}(\epsilon^2 \log \epsilon), \quad (\text{A.13})$$

or, neglecting terms of order $\epsilon^2 \log \epsilon$ and higher, and then setting $\epsilon = 1$,

$$\frac{d^2 r}{dt^2} = -\frac{M}{r^2} + \frac{4M^2}{r^3} = -\frac{d}{dr} \left(-\frac{M}{r} + \frac{2M^2}{r^2} \right). \quad (\text{A.14})$$

The correction to the Newtonian potential would therefore appear to be

$$V = \frac{2M^2}{r^2}, \quad (\text{A.15})$$

but one step is still missing.

Instead of the Schwarzschild time \tilde{t} , let us employ the proper time t of static observers placed along the trajectory of the falling particle, that is

$$dt = \left(1 - \frac{2M}{r} \right)^{1/2} d\tilde{t}. \quad (\text{A.16})$$

From Eq. (A.4) we obtain

$$\frac{d}{d\tau} = \left(1 - \frac{2M}{r}\right)^{-1/2} \frac{E}{m} \frac{d}{dt}, \quad (\text{A.17})$$

and Eq. (A.2) then becomes

$$\frac{d^2 \tilde{r}}{dt^2} = -\frac{M}{r^2} \left(1 - \frac{2M}{\tilde{r}}\right) \left[\frac{m^2}{E^2} - \left(1 - \frac{2M}{\tilde{r}}\right)^{-2} \left(\frac{d\tilde{r}}{dt}\right)^2 \right]. \quad (\text{A.18})$$

Introducing like before the small parameter ϵ yields

$$\epsilon \frac{d^2 \tilde{r}}{dt^2} = -\epsilon \frac{M}{\tilde{r}^2} \left(1 - \epsilon \frac{2M}{\tilde{r}}\right) \left[1 + \mathcal{O}(\epsilon^2) - \left(1 - \epsilon \frac{2M}{\tilde{r}}\right)^{-2} \epsilon^2 \left(\frac{d\tilde{r}}{dt}\right)^2 \right], \quad (\text{A.19})$$

The first order in ϵ is of course the same. However, up to second order, one obtains

$$\epsilon \frac{d^2 r}{dt^2} = -\epsilon \frac{M}{r^2} + \epsilon^2 \frac{2M^2}{r^3} + \mathcal{O}(\epsilon^2 \log \epsilon), \quad (\text{A.20})$$

which yields the correction to the Newtonian potential

$$V = \frac{M^2}{r^2}. \quad (\text{A.21})$$

This is precisely the expression following from the isotropic form of the Schwarzschild metric [74], and the one we will consider as our reference term throughout this thesis.

Appendix B

Linearised Einstein-Hilbert action at NLO

We shall here consider the Einstein-Hilbert and the matter actions in the non-relativistic limit, up to NLO in the weak field expansion

$$g_{\mu\nu} = \eta_{\mu\nu} + \epsilon h_{\mu\nu} . \quad (\text{B.1})$$

Unlike the main text, the parameter ϵ is here shown explicitly in order to keep track of the different orders in the expansions

$$X = \sum_n \epsilon^n X_{(n)} . \quad (\text{B.2})$$

First of all, one has

$$g^{\mu\nu} = \eta^{\mu\nu} - \epsilon h^{\mu\nu} + \epsilon^2 h^{\mu\lambda} h_{\lambda}^{\nu} + \mathcal{O}(\epsilon^3) , \quad (\text{B.3})$$

the integration measure reads

$$\sqrt{-g} = 1 + \frac{\epsilon}{2} h + \frac{\epsilon^2}{8} (h^2 - 2 h_{\mu}^{\nu} h_{\nu}^{\mu}) + \mathcal{O}(\epsilon^3) , \quad (\text{B.4})$$

and the scalar $\mathcal{R} = g^{\mu\nu} R_{\mu\nu}$ is obtained from the Ricci tensor

$$R_{\mu\nu} = \partial_{\lambda} \Gamma_{\mu\nu}^{\lambda} - \partial_{\nu} \Gamma_{\mu\lambda}^{\lambda} + \Gamma_{\lambda\rho}^{\lambda} \Gamma_{\mu\nu}^{\rho} - \Gamma_{\nu\rho}^{\lambda} \Gamma_{\mu\lambda}^{\rho} , \quad (\text{B.5})$$

provided one has computed the Christoffel symbols

$$\Gamma_{\mu\nu}^{\lambda} \simeq \frac{\epsilon}{2} (\eta^{\lambda\rho} - \epsilon h^{\lambda\rho} + \epsilon^2 h^{\lambda\sigma} h_{\sigma}^{\rho}) (\partial_{\mu} h_{\rho\nu} + \partial_{\nu} h_{\rho\mu} - \partial_{\rho} h_{\mu\nu}) . \quad (\text{B.6})$$

In the de Donder gauge (4.1.4), the effective Lagrangian (4.1.14) for the classical Newtonian field appears as the sum of two terms,

$$L[V_{\text{N}}] = \epsilon^2 L_{\text{FP}} + \epsilon L_{\text{M}} , \quad (\text{B.7})$$

with the gravitational part given by the massless Fierz-Pauli action [15, 16]

$$\begin{aligned}
L_{\text{FP}} &= \frac{m_{\text{p}}}{16 \pi \ell_{\text{p}}} \int d^3x \left(\frac{1}{2} \partial_{\mu} h \partial^{\mu} h - \frac{1}{2} \partial_{\mu} h_{\nu\sigma} \partial^{\mu} h^{\nu\sigma} + \partial_{\mu} h_{\nu\sigma} \partial^{\nu} h^{\mu\sigma} - \partial_{\mu} h \partial_{\sigma} h^{\mu\sigma} \right) \\
&= \frac{m_{\text{p}}}{16 \pi \ell_{\text{p}}} \int d^3x \left(\partial_{\mu} h_{\nu\sigma} \partial^{\nu} h^{\mu\sigma} - \frac{1}{2} \partial_{\mu} h_{\nu\sigma} \partial^{\mu} h^{\nu\sigma} \right) \\
&\simeq -\frac{m_{\text{p}}}{32 \pi \ell_{\text{p}}} \int d^3x \partial_{\mu} h_{00} \partial^{\mu} h_{00} \\
&= -4 \pi \int_0^{\infty} r^2 dr \frac{m_{\text{p}}}{8 \pi \ell_{\text{p}}} (V')^2, \tag{B.8}
\end{aligned}$$

where we used the de Donder gauge (4.1.4) and $h_{00} = -2V$. The matter Lagrangian is obtained from the matter Lagrangian density (4.1.9), that is

$$\begin{aligned}
L_{\text{M}} &= \int d^3x (\sqrt{-g} \mathcal{L}_{\text{M}})_{(1)} \\
&\simeq 4 \pi \int_0^{\infty} r^2 dr \frac{h_{00}}{2} \rho \\
&= -4 \pi \int_0^{\infty} r^2 dr V \rho. \tag{B.9}
\end{aligned}$$

Putting the two pieces together yields Eq. (4.1.14).

The above expressions at the Newtonian level show that the factor $m_{\text{p}}/(8 \pi \ell_{\text{p}})$ must be viewed as of order ϵ^{-1} , since the Einstein tensor at order ϵ^{n+1} couples to the stress-energy tensor at order ϵ^n . In order to go to the next order, we must then compute third-order terms for the gravitational part and second order terms for the matter part. After some tedious algebra, one finds

$$\begin{aligned}
-(\sqrt{-g} \mathcal{R})_{(3)} &\simeq h_{\nu}^{\mu} (\partial_{\mu} h_{\rho}^{\lambda} \partial^{\nu} h_{\lambda}^{\rho} - \partial^{\lambda} h_{\mu}^{\nu} \partial_{\lambda} h) + 2 h_{\nu}^{\mu} \partial_{\lambda} h_{\mu}^{\rho} (\partial^{\lambda} h_{\rho}^{\nu} - \partial^{\nu} h_{\rho}^{\lambda}) \\
&\quad - \frac{1}{2} h \partial^{\mu} h_{\nu}^{\lambda} \partial_{\mu} h_{\lambda}^{\nu} + \frac{1}{4} h \partial_{\mu} h \partial^{\mu} h \\
&\simeq -h_{00} (\partial_r h_{00})^2 \\
&\simeq V (V')^2, \tag{B.10}
\end{aligned}$$

which we notice is proportional to $-J_V$ in Eq. (4.1.18), and

$$(\sqrt{-g} \mathcal{L}_{\text{M}})_{(2)} = \frac{1}{8} h_{00}^2 T_{00} = \frac{1}{2} V^2 \rho. \tag{B.11}$$

Adding all the contributions, and explicitly rescaling $m_{\text{p}}/(8 \pi \ell_{\text{p}})$ by a factor of ϵ^{-1} , one obtains the action

$$S[V] = 4 \pi \int \epsilon dt \int_0^{\infty} r^2 dr \left\{ \frac{m_{\text{p}}}{8 \pi \ell_{\text{p}}} V \Delta V - \rho V + \frac{\epsilon}{2} \left[\frac{m_{\text{p}}}{4 \pi \ell_{\text{p}}} (V')^2 + V \rho \right] V \right\}. \tag{B.12}$$

A few remarks are now in order. First of all, we have derived Eq. (B.12) in the de Donder gauge (4.1.4), which explicitly reads

$$\partial_t h_{00} = 0 \tag{B.13}$$

for static configurations $h_{00} = h_{00}(r)$, and is therefore automatically satisfied in our case. This means that the above action can be used for describing the gravitational potential $V = V(r)$ measured by any static observer placed at constant radial coordinate r (provided test particles move at non-relativistic speed). In fact, there remains the ambiguity in the definition of the observer time t , which in turn determines the value of ϵ in Eq. (B.12), as can be seen by the simple fact that the time measure is ϵdt . On the other hand, changing ϵ , and therefore the time (albeit in such a way that motions remain non-relativistic) does not affect the dynamics of the Newtonian part of the potential, whereas the post-Newtonian part inside the curly brackets acquires a different weight. This is completely consistent with the expansion of the Schwarzschild metric described in Appendix A, in which we showed that the Newtonian potential is uniquely defined by choosing a static observer, whereas the form of the first post-Newtonian correction varies with the specific choice of time.

At this point, it is convenient to introduce the (dimensionless) “self-coupling” q_Φ , which will designate terms of higher order in ϵ . In particular, we set $\epsilon = 4 q_\Phi$ so that the post-Newtonian potential (A.21) is recovered for $q_\Phi = 1$ ¹. With these definitions, the above action yields the Lagrangian (5.1.3).

¹The post-Newtonian correction (A.15) can instead be obtained for $q_\Phi = 2$.

Appendix C

Gravitational current

We present here an alternative derivation of the gravitational current leading to the same Lagrangian (5.1.3) of Section 5.1. The starting point will now be the Newtonian energy evaluated on-shell inside a sphere of radius r , that is

$$\begin{aligned} U_{\text{N}}(r) &= 2\pi \int_0^r \bar{r}^2 d\bar{r} \rho(\bar{r}) V(\bar{r}) \\ &= \frac{1}{2G_{\text{N}}} \int_0^r \bar{r}^2 d\bar{r} V(\bar{r}) \Delta V(\bar{r}) , \end{aligned} \quad (\text{C.1})$$

in which we do not perform any integration by parts. We can then define a current \tilde{J}_V proportional to the energy density by deriving $U_{\text{N}}(r)$ with respect to the volume \mathcal{V} , which yields

$$\tilde{J}_V \simeq 2 \frac{dU_{\text{N}}}{d\mathcal{V}} = \frac{V(r) \Delta V(r)}{4\pi G_{\text{N}}} . \quad (\text{C.2})$$

One can immediately notice that we chose to have a different numerical factor in front of \tilde{J}_V from the one in J_V of Eq. (4.1.18) in order to keep the same coupling parameter $\tilde{q}_V = q_V$. It is now easy to see that by adding all other sources described in Section 5.1 together with (C.2), we end up with the same Lagrangian (5.1.3),

$$\tilde{L}[V] = L_{\text{N}}[V] - 4\pi \int_0^\infty r^2 dr \left[q_V \tilde{J}_V V + 3q_{\text{B}} J_{\text{B}} V + q_\rho J_\rho (\rho + 3q_{\text{B}} p) \right] = L[V] , \quad (\text{C.3})$$

where we discarded vanishing boundary terms. In fact, we have

$$\int_0^\infty r^2 dr J_V V = 2 \int_0^\infty r^2 dr \tilde{J}_V V + [r^2 V^2 V']_{r=0}^{r \rightarrow \infty} , \quad (\text{C.4})$$

and the second term in the right hand side vanishes because of the boundary conditions at $r \rightarrow \infty$ and Eq. (5.2.1) at $r = 0$.

Appendix D

Comparison method

We have shown in Section 5.2.3 that a solution to Eq. (5.2.13) satisfying Eq. (5.2.15) exists by employing comparison functions [94–97] and we recall the fundamentals of this method here for the sake of convenience.

Let us consider an equation of the form

$$u''(r) = F(r, u(r), u'(r)) , \quad (\text{D.1})$$

where F is a real function of its arguments, r varies in the finite interval $[r_1, r_2]$ and a prime denotes the derivative with respect to r . We want to find a solution which further satisfies the general boundary conditions

$$a_1 u(r_1) - a_2 u'(r_1) = A_0 , \quad (\text{D.2})$$

$$b_1 u(r_2) + b_2 u'(r_2) = B_0 , \quad (\text{D.3})$$

with A_0, B_0, a_1, b_1 real numbers and a_2, b_2 non negative real numbers satisfying $a_1^2 + a_2^2 > 0$ and $b_1^2 + b_2^2 > 0$. The theorems in Refs. [94–96] guarantee that such a solution $u \in C^2([r_1, r_2])$ exists under the following three conditions:

1. we can find a lower bounding function

$$u''_-(r) \geq F(r, u_-(r), u'_-(r)) \quad (\text{D.4})$$

$$a_1 u_-(r_1) - a_2 u'_-(r_1) \leq A_0 \quad (\text{D.5})$$

$$b_1 u_-(r_2) + b_2 u'_-(r_2) \leq B_0 , \quad (\text{D.6})$$

and an upper bounding function

$$u''_+(r) \leq F(r, u_+(r), u'_+(r)) \quad (\text{D.7})$$

$$a_1 u_+(r_1) - a_2 u'_+(r_1) \geq A_0 \quad (\text{D.8})$$

$$b_1 u_+(r_2) + b_2 u'_+(r_2) \geq B_0 ; \quad (\text{D.9})$$

2. the function F is continuous on the domain $D = \{(r, u, u') \in [r_1, r_2] \times \mathbb{R}^2 \mid u_- \leq u \leq u_+\}$;
3. the function F satisfies a *Nagumo condition*: there exists a continuous and positive function ϕ such that

$$\int_0^\infty \frac{s \, ds}{\phi(s)} = \infty \quad (\text{D.10})$$

and, $\forall (t, u, u') \in D$,

$$|F(r, u(r), u'(r))| \leq \phi(|u'|) . \quad (\text{D.11})$$

Moreover, the solution u will satisfy

$$u_-(t) \leq u(t) \leq u_+(t) . \quad (\text{D.12})$$

We can now apply the above general theorem to our problem inside the source, for which $r_1 = 0$ and $r_2 = R$. We first rewrite Eq. (5.2.13) as

$$\begin{aligned} V'' &= \frac{3 G_N M_0}{R^3} e^{V_R - V} + \frac{2 (V')^2}{1 - 4V} - \frac{2 V'}{r} \\ &\equiv F(r, V, V') , \end{aligned} \quad (\text{D.13})$$

and recall the boundary conditions (5.2.1) and (5.2.2), that is

$$V'(0) = 0 \quad (\text{D.14})$$

$$V(R) = V_R . \quad (\text{D.15})$$

We can now verify all the requirements of the theorem, and will do so for the case of large compactness analysed in Section 5.2.3. The upper and lower bounding functions are therefore V_\pm given in Eq. (5.2.37) and the domain

$$D = \{(r, V, V') \in [0, R] \times \mathbb{R}^2 \mid V_- \leq V \leq V_+\} . \quad (\text{D.16})$$

Continuity of F on D is easily verified. In fact, the first term on the right hand side of Eq. (D.13) is an exponential of V which is always regular in D . The same is true for the second term considering that $V_\pm < 0$, thus $V < 0$ as well. The last term could be tricky but the boundary condition (D.14) require that V' vanishes at $r = 0$ at least as fast as r [see the expansion around $r = 0$ in Eq. (5.2.16)] so that this is also regular in D . Finally, we can choose

$$\phi = \max_D(F) , \quad (\text{D.17})$$

which must be finite given that F is continuous in D .

All of the hypotheses of the theorem hold and a solution to Eq. (5.2.13) therefore exists and satisfies Eq. (5.2.15). By imposing the remaining boundary condition (5.2.3), one can then obtain a relation between M_0 , which appears in the equation (5.2.13), and M , which appears in the boundary conditions (5.2.2) and (5.2.3), for any given value of R .

Appendix E

Energy balance

In Section 5.3, we only computed the gravitational energy from the Hamiltonian (5.1.4). The purely baryonic contribution will be given by the proper mass M_0 and the pressure energy contribution found again from the newtonian argument (5.1.1), whereby

$$U_B(R) = D(M, R) - 4\pi \int_0^R r^2 dr p(r) . \quad (\text{E.1})$$

In the newtonian regime, the integration constant $D(M, R)$ can be fixed so as to guarantee that the work done by gravity is equal and opposite to the work done by the forces responsible for the pressure p . In other words, in that case we find $D(M, R)$ by requiring that the gravitational force is conservative. This will also ensure that the total energy related to the Hamiltonian constraint equals the ADM-like mass M of the system, that is

$$E = M_0 + U_G + U_B = M . \quad (\text{E.2})$$

Of course, in the Newtonian case Eq. (E.2) simply reads $E = M_0 \equiv M$, as shown in Ref. [19].

In the bootstrapped picture, gravity is not a linear interaction any more and it is not at all obvious that it will still be conservative. A precise energy estimate would therefore require a complete knowledge of the dynamical process which led to the formation of the equilibrium configuration of given ADM-like mass M and radius R . Without that knowledge, we can only assume that the total energy of the equilibrium configuration equals M and fix $D(M, R)$ so that the Hamiltonian constraint (E.2) is satisfied.

With that prescription, we can now evaluate the baryonic contributions. In the low compactness case, we expand all the terms in Eq. (E.2) to order M^3 , namely

$$M_0 \simeq M - \frac{5 G_N M^2}{2 R} + \frac{81 G_N^2 M^3}{8 R^2} , \quad (\text{E.3})$$

and the pressure energy

$$U_B \simeq D_s(M, R) - \frac{G_N M^2}{5 R} + \frac{61 G_N^2 M^3}{70 R^2} . \quad (\text{E.4})$$

Eq. (E.2) is then satisfied for

$$D_s(M, R) \simeq -\frac{33 G_N M^2}{10 R} + \frac{3439 G_N^2 M^3}{280 R^2} \quad (\text{E.5})$$

so that

$$U_B \simeq \frac{31 G_N M^2}{10 R} \left(1 - \frac{6390 G_N M}{1736 R} \right), \quad (\text{E.6})$$

which is positive only for small compactness, as its approximation requires.

The high compactness regime of course yields quite different results. To make things easier, we again look at the limiting case of very high compactness, where the linear approximation (5.2.40) holds, and consider the Hamiltonian constraint (E.2) only at leading order in M . The proper mass in Eq. (5.2.41) can be simplified further to give

$$M_0 \simeq \frac{5 M}{9 (6 G_N M/R)^{1/3}}, \quad (\text{E.7})$$

while the pressure energy can be written as

$$U_B \simeq D_b(M, R) - \frac{20 R^3}{G_N^3 M^2} \left(\frac{G_N M}{\sqrt{6} R} \right)^{2/3} e^{\left(\frac{G_N M}{\sqrt{6} R} \right)^{2/3}}. \quad (\text{E.8})$$

Again, we just impose Eq. (E.2) and find

$$D_b(M, R) \simeq M + \frac{20 R^3}{G_N^3 M^2} \left(\frac{G_N M}{\sqrt{6} R} \right)^{2/3} e^{\left(\frac{G_N M}{\sqrt{6} R} \right)^{2/3}} + \frac{125 R}{3 G_N} e^{\left(\frac{G_N M}{\sqrt{6} R} \right)^{2/3}} \quad (\text{E.9})$$

$$-\frac{7 G_N M^2}{36 R} - \frac{5 M}{9 (6 G_N M/R)^{1/3}}, \quad (\text{E.10})$$

so that

$$U_B \simeq \frac{125 R}{3 G_N} e^{\left(\frac{G_N M}{\sqrt{6} R} \right)^{2/3}}, \quad (\text{E.11})$$

which is positive as it should, and precisely counterbalances Eq. (5.3.12).

Appendix F

Effective wavenumber and graviton number for the Newtonian potential

We show here the explicit calculation of k_{eff} and $N_{\text{G}}^{\text{eff}}$ for $\Lambda_\alpha = 1/\alpha R$ and the corresponding functions $f(\alpha)$ and $g(\alpha)$ of Section. 6.1.3.

Eq. (6.1.24) with the g_k given by Eq. (6.1.19) yields

$$\begin{aligned}
 k_{\text{eff}} &= \int_{\Lambda_\alpha}^{\infty} \frac{dk}{2\pi^2} k^3 g_k^2 \\
 &= \frac{6M^2}{5m_{\text{p}}^2 R} \left[2\pi + \alpha^3 (3\alpha^2 + 5) - \alpha (3\alpha^4 - \alpha^2 + 2) \cos\left(\frac{2}{\alpha}\right) - \alpha^3 (6\alpha + 1) \sin\left(\frac{2}{\alpha}\right) \right. \\
 &\quad \left. - 4 \text{Si}\left(\frac{2}{\alpha}\right) \right] \\
 &\equiv \frac{M^2}{m_{\text{p}}^2 R} f(\alpha) , \tag{F.1}
 \end{aligned}$$

where

$$\text{Si}(x) = \int_0^x dt \frac{\sin t}{t} \tag{F.2}$$

is the sine integral. Since $\text{Si}(x \rightarrow \infty) = \pi/2$, we correctly obtain that $k_{\text{eff}} \rightarrow 0$ for $\alpha \rightarrow 0$ (that is, for $\Lambda_\alpha \rightarrow \infty$).

Likewise, Eq. (6.1.26) with the same g_k of Eq. (6.1.19) reads

$$\begin{aligned}
 N_{\text{G}}^{\text{eff}} &= \int_{\Lambda_\alpha}^{\infty} \frac{dk}{2\pi^2} k^2 g_k^2 \\
 &= \frac{\alpha M^2}{2m_{\text{p}}^2} \left[3\alpha^3 (2\alpha^2 + 3) - \alpha (6\alpha^4 - 3\alpha^2 + 2) \cos\left(\frac{2}{\alpha}\right) - \alpha^2 (6\alpha^2 + 1) \sin\left(\frac{2}{\alpha}\right) \right. \\
 &\quad \left. - 4 \text{Si}\left(\frac{2}{\alpha}\right) \right] \tag{F.3}
 \end{aligned}$$

$$\equiv \frac{M^2}{m_{\text{p}}^2} g(\alpha) , \tag{F.4}$$

and we again remark that $N_{\text{G}}^{\text{eff}} \rightarrow 0$ for $\Lambda_\alpha \rightarrow \infty$.

F. Effective wavenumber and graviton number for the Newtonian potential

Appendix G

Graviton number and mean wavelength for compact sources

As already pointed out in the main text, the exact analytical calculation of the Fourier transform is not possible for arbitrary potentials $V = V(\mathbf{x})$ generated by a compact source. We will therefore describe here an approximation obtained by rewriting the Fourier transform $\tilde{V} = \tilde{V}(\mathbf{k})$ in terms of a spatial integral of the Laplacian of the scalar field. In fact, if we apply the Laplacian operator on both sides of Eq. (6.1.2), we obtain

$$\tilde{V}(\mathbf{k}) = -\frac{1}{k^2} \int d\mathbf{x} \Delta V(\mathbf{x}) v_{\mathbf{k}}(\mathbf{x}) . \quad (\text{G.1})$$

Upon substituting the above expression together with Eq. (2.2.3) into Eq. (6.1.7) we get

$$\begin{aligned} N_{\text{G}} &= \frac{1}{2(2\pi)^3 \ell_{\text{p}}^2} \int d\mathbf{x} \int d\mathbf{y} \Delta V(\mathbf{x}) \Delta V(\mathbf{y}) \int d\mathbf{k} \frac{e^{i\mathbf{k}\cdot(\mathbf{x}-\mathbf{y})}}{k^3} \\ &= \frac{1}{(2\pi)^2 \ell_{\text{p}}^2} \int_{\mathcal{B}_0^\infty} d\mathbf{x} \int_{\mathcal{B}_0^\infty} d\mathbf{y} \Delta V(\mathbf{x}) \Delta V(\mathbf{y}) \int_{k_0}^\infty dk \frac{\sin(k\sigma)}{k^2 \sigma} , \end{aligned} \quad (\text{G.2})$$

where $\sigma = |\mathbf{x} - \mathbf{y}|$ and $k_0 = 1/R_\infty$ is the IR cut-off introduced in Section 6.1.3 for the purpose of regularising the diverging number of gravitons associated with the infinite spatial support of the potential. We have correspondingly restricted the spatial domain of integration to a ball of radius R_∞ centred in the origin, $\mathcal{B}_0^\infty = \{|\mathbf{x}| < R_\infty\}$.

Similarly for the mean wavenumber in Eq. (6.1.8) we have

$$\begin{aligned} \langle k \rangle &= \frac{1}{2(2\pi)^3 \ell_{\text{p}}^2} \int d\mathbf{x} \int d\mathbf{y} \Delta V(\mathbf{x}) \Delta V(\mathbf{y}) \int d\mathbf{k} \frac{e^{i\mathbf{k}\cdot(\mathbf{x}-\mathbf{y})}}{k^2} \\ &= \frac{1}{(2\pi)^2 \ell_{\text{p}}^2} \int d\mathbf{x} \int d\mathbf{y} \Delta V(\mathbf{x}) \Delta V(\mathbf{y}) \int_0^\infty dk \frac{\sin(k\sigma)}{k\sigma} \\ &= \frac{1}{8\pi \ell_{\text{p}}^2} \int d\mathbf{x} \int d\mathbf{y} \frac{\Delta V(\mathbf{x}) \Delta V(\mathbf{y})}{\sigma} , \end{aligned} \quad (\text{G.3})$$

where we used the property of the sine integral (F.2) that $\text{Si}(x \rightarrow \infty) = \pi/2$. This mean wavenumber is regular since only a finite part of the (infinite number of) gravitons effectively contribute to it, and does not require any cut-off.

Eqs. (G.2) and (G.3) show that the divergence of N_G and the finiteness of $\langle k \rangle$ do not depend on the actual shape of the potential V , as long as it falls off fast enough at large distance. We also anticipate that another relevant scale will be given by R^* defined in Eq. (6.2.2).

G.1 Mean graviton wavenumber

We will first show how to obtain Eq. (6.2.4) from Eq. (G.3). This is most easily done if we directly consider a spherically symmetric case such that

$$\langle k \rangle = \frac{1}{8\pi\ell_p^2} \int_0^\infty dr_1 \int_0^\infty dr_2 r_1^2 r_2^2 \Delta V(r_1) \Delta V(r_2) \int d\Omega_1 \int d\Omega_2 \frac{1}{|\mathbf{x} - \mathbf{y}|}, \quad (\text{G.4})$$

where $d\Omega_a = \sin\theta_a d\theta_a d\varphi_a$, with $a = 1, 2$. The freedom to rotate the system allows us to choose θ_2 as the angle between \mathbf{x} and \mathbf{y} , which introduces a factor of $8\pi^2$ from the integration in $d\Omega_1$ and $d\varphi_2$. The only angular integration left is in $ds \equiv \sin\theta_2 d\theta_2 = -d\cos\theta_2$, which yields

$$\begin{aligned} \langle k \rangle &= \frac{\pi}{\ell_p^2} \int_0^\infty dr_1 \int_0^\infty dr_2 r_1^2 r_2^2 \Delta V(r_1) \Delta V(r_2) \int_{-1}^1 \frac{ds}{\sqrt{r_1^2 + r_2^2 + 2r_1 r_2 s}} \\ &= \frac{\pi}{\ell_p^2} \int_0^\infty dr_1 \int_0^\infty dr_2 r_1 r_2 \Delta V(r_1) \Delta V(r_2) (r_1 + r_2 - |r_1 - r_2|). \end{aligned} \quad (\text{G.5})$$

Thanks to the symmetric role of r_1 and r_2 , the above integrals can be written as

$$\langle k \rangle = \frac{2\pi}{\ell_p^2} \int_0^\infty dr_1 r_1 \Delta V(r_1) \left[\int_0^{r_1} dr_2 r_2^2 \Delta V(r_2) + r_1 \int_{r_1}^\infty dr_2 r_2 \Delta V(r_2) \right]. \quad (\text{G.6})$$

From the definition (4.1.15) of the Laplacian, it is then easy to see that

$$\begin{aligned} \langle k \rangle &= \frac{2\pi}{\ell_p^2} \int_0^\infty dr_1 r_1 \Delta V(r_1) \left\{ \int_0^{r_1} dr_2 \frac{\partial}{\partial r_2} \left[r_2^2 \frac{\partial V(r_2)}{\partial r_2} \right] + r_1 \int_{r_1}^\infty \frac{dr_2}{r_2} \frac{\partial}{\partial r_2} \left[r_2^2 \frac{\partial V(r_2)}{\partial r_2} \right] \right\} \\ &= \frac{2\pi}{\ell_p^2} \int_0^\infty dr_1 r_1 \Delta V(r_1) \left\{ r_1^2 \frac{\partial V(r_1)}{\partial r_1} - r_1 \left[r_1 \frac{\partial V(r_1)}{\partial r_1} + V(r_1) \right] \right\} \\ &= -\frac{2\pi}{\ell_p^2} \int_0^\infty dr r^2 V(r) \Delta V(r), \end{aligned} \quad (\text{G.7})$$

where we integrated by parts taking into account the boundary conditions (5.2.1) and (6.2.1). After integrating by parts again, one finally obtains

$$\langle k \rangle = \frac{2\pi}{\ell_p^2} \int_0^\infty dr r^2 [V'(r)]^2, \quad (\text{G.8})$$

from which we see that we can indeed estimate $\langle k \rangle$ directly from the potential $V = V(r)$.

G.2 Graviton number

Next, we will show how to estimate N_G in Eq. (G.2). Our method relies on the introduction of the characteristic length scale R^* defined in Eq. (6.2.2) and in identifying the leading terms in the expansion for large R_∞/R^* . In fact, for the potential generated by a compact source, it is reasonable to consider $R^* \ll R_\infty$, provided the source itself has existed for long enough [20].

We first compute explicitly the integral in k in Eq. (G.2), that is

$$\begin{aligned} f(\sigma) &\equiv \int_{k_0}^{\infty} dk \frac{\sin(k\sigma)}{k^2 \sigma} \\ &= \int_{\sigma k_0}^{\infty} dz \frac{\sin(z)}{z^2} \\ &= \frac{\sin(\sigma k_0)}{\sigma k_0} - \text{Ci}(\sigma k_0) , \end{aligned} \tag{G.9}$$

where

$$\text{Ci}(x) = \int_0^x dt \frac{1 - \cos(t)}{t} - \gamma_E - \ln(x) , \tag{G.10}$$

is the cosine integral and γ_E the Euler-Mascheroni constant. It is then easy to show that the function $f(\sigma)$ is larger and contributes significantly to Eq. (G.2) only when its argument $\sigma \ll R_\infty$ (see Fig. G.1). In fact, for $\sigma \simeq R_\infty$, we have

$$|f(\sigma)| \leq \int_{\sigma k_0}^{\infty} \frac{dz}{z^2} = \frac{1}{\sigma k_0} = \frac{R_\infty}{\sigma} \simeq 1 . \tag{G.11}$$

On the other hand, when $\sigma \ll R_\infty$, we can expand Eq. (G.9) for $\sigma k_0 \ll 1$, and note that the leading term is given by $-\text{Ci}(\sigma k_0) \simeq \ln(\sigma k_0)$. To conclude, we can approximate

$$f(\sigma) \simeq \ln\left(\frac{R_\infty}{\sigma}\right) = \ln\left(\frac{R_\infty}{R^*}\right) + \ln\left(\frac{R^*}{\sigma}\right) , \tag{G.12}$$

where we explicitly introduced the scale R^* . The second term in Eq. (G.12) diverges for $\sigma = |\mathbf{x} - \mathbf{y}| \rightarrow 0$, but the spatial integrations in Eq. (G.2) will regularise it. In fact, we have explicitly shown in Section G.1 that the singular function $1/\sigma$ leads to the finite result (G.4) once integrated over the spatial domain. Since $0 < -\ln(\sigma/R^*) < R^*/\sigma$ for $\sigma \ll R^*$, we can safely neglect the second term in Eq. (G.12) and just keep the leading contribution coming from the first term which dominates (and actually diverges) for $R_\infty \gg R^*$.

We must now estimate the spatial integrals in Eq. (G.2), whose domains are effectively restricted by the condition $\sigma = |\mathbf{x} - \mathbf{y}| \ll R_\infty$ for which the function $f(\sigma)$ is the largest. Given the symmetry in \mathbf{x} and \mathbf{y} , we can achieve this by integrating \mathbf{y} inside

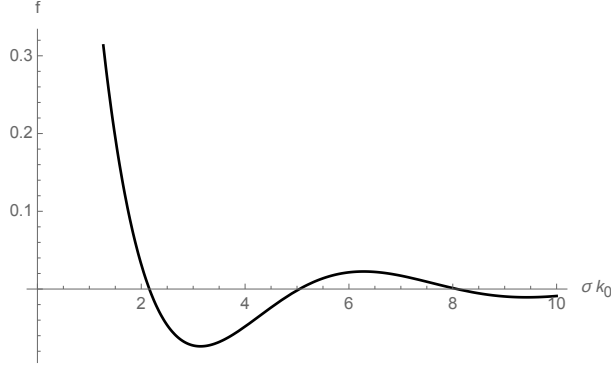


Figure G.1: Function $f(\sigma)$.

a ball $\mathcal{B}_{\mathbf{x}}^*$ of radius $R^* \ll R_\infty$ centred around \mathbf{x} and then summing over \mathbf{x} inside \mathcal{B}_0^∞ , that is

$$N_G \simeq \frac{1}{(2\pi)^2 \ell_p^2} \int_{\mathcal{B}_0^\infty} d\mathbf{x} \Delta V(\mathbf{x}) \int_{\mathcal{B}_{\mathbf{x}}^*} d\mathbf{y} \Delta V(\mathbf{y}) \log\left(\frac{R_\infty}{R^*}\right). \quad (\text{G.13})$$

The explicit evaluation of this integral is not any simpler than the starting Eq. (G.2). However, we can now more easily find upper and lower bounds by observing that the Laplacians are everywhere positive, as can be seen from the fact that the right hand side of Eq. (5.1.7) is positive. An upper bound is obtained by extending the domain of \mathbf{y} to all of \mathcal{B}_0^∞ ,

$$\begin{aligned} N_G &\leq \frac{1}{(2\pi)^2 \ell_p^2} \int_{\mathcal{B}_0^\infty} d\mathbf{x} \Delta V(\mathbf{x}) \int_{\mathcal{B}_0^\infty} d\mathbf{y} \Delta V(\mathbf{y}) \log\left(\frac{R_\infty}{R^*}\right) \\ &\simeq 4 \frac{M^2}{m_p^2} \log\left(\frac{R_\infty}{R^*}\right), \end{aligned} \quad (\text{G.14})$$

where we used the Gauss theorem in the form

$$\begin{aligned} \int_{\mathcal{B}_0^\infty} d\mathbf{x} \Delta V(\mathbf{x}) &= \int_{\partial\mathcal{B}_0^\infty} d\mathbf{s} \cdot \nabla V \\ &\simeq R_\infty^2 \int d\Omega \frac{G_N M}{R_\infty^2} \\ &\simeq 4\pi G_N M, \end{aligned} \quad (\text{G.15})$$

with $d\mathbf{s} = R_\infty^2 d\Omega \mathbf{n}$ the measure on the sphere $\partial\mathcal{B}_0^\infty$ of radius R_∞ whose unit normal vector is \mathbf{n} . Note also that the second line follows from the Newtonian behaviour at large distance from the source, namely for $r \gtrsim R^*$. A lower bound can be obtained by first restricting the domain of \mathbf{x} to a ball \mathcal{B}_0^* of radius R^* and then, instead of integrating \mathbf{y} over all the balls centred around \mathbf{x} , only taking the one centred in the origin as well.

G.2 Graviton number

The result is

$$\begin{aligned} N_G &\geq \frac{1}{(2\pi)^2 \ell_p^2} \int_{\mathcal{B}_0^*} d\mathbf{x} \Delta V(\mathbf{x}) \int_{\mathcal{B}_x^*} d\mathbf{y} \Delta V(\mathbf{y}) \log\left(\frac{R_\infty}{R^*}\right) \\ &\geq \frac{1}{(2\pi)^2 \ell_p^2} \int_{\mathcal{B}_0^*} d\mathbf{x} \Delta V(\mathbf{x}) \int_{\mathcal{B}_0^*} d\mathbf{y} \Delta V(\mathbf{y}) \log\left(\frac{R_\infty}{R^*}\right) \end{aligned} \quad (\text{G.16})$$

$$\simeq 4 \frac{M^2}{m_p^2} \log\left(\frac{R_\infty}{R^*}\right), \quad (\text{G.17})$$

where we used the defining assumption of R^* that

$$V'(R^*) \simeq \frac{G_N M}{(R^*)^2}. \quad (\text{G.18})$$

Therefore, we can safely approximate N_G as

$$N_G \simeq 4 \frac{M^2}{m_p^2} \log\left(\frac{R_\infty}{R^*}\right). \quad (\text{G.19})$$

We point out that this result only depends on the boundary conditions on the potential at large distance from the source and bears no dependence on the details of the source or of the gravitational interaction at shorter distances.

We conclude by estimating the number of effective gravitons. Like in Section 6.1.3, we introduce the splitting scale Λ in Eq. (G.9) and write

$$\begin{aligned} f(\sigma) &= \int_{\sigma k_0}^{\sigma \Lambda} dz \frac{\sin(z)}{z^2} + \int_{\sigma \Lambda}^{\infty} dz \frac{\sin(z)}{z^2} \\ &= f^{\text{IR}} + f^{\text{eff}}, \end{aligned} \quad (\text{G.20})$$

where f^{IR} is dominated by the logarithmic IR divergence in Eq. (G.12) for $k_0 = 1/R_\infty \rightarrow 0$. For the finite part, we obtain

$$f^{\text{eff}} = \frac{\sin(\sigma \Lambda)}{\sigma \Lambda} + \int_0^{\sigma \Lambda} dt \frac{1 - \cos(t)}{t} - \gamma_E - \ln(\sigma \Lambda), \quad (\text{G.21})$$

in which the dominant term is again given by $\ln(\sigma \Lambda)$ for $\sigma \Lambda$ small (but still larger than σk_0). Since again $0 < -\ln(\sigma \Lambda) < 1/\sigma \Lambda$, we obtain

$$N_G \lesssim \frac{1}{(2\pi)^2 \ell_p^2 \Lambda} \int d\mathbf{x} \int d\mathbf{y} \frac{\Delta V(\mathbf{x}) \Delta V(\mathbf{y})}{\sigma} \quad (\text{G.22})$$

$$\simeq \frac{\langle k \rangle}{\Lambda}. \quad (\text{G.23})$$

In Section 6.2, we show that we can consider $\Lambda \sim 1/R^*$, from which we obtain for the mean wavelength

$$\lambda_G \simeq \frac{N_G^{\text{eff}}}{\langle k \rangle} \lesssim R^*, \quad (\text{G.24})$$

so that again this representative scale belongs to the effective part of the spectrum, that is $1/\lambda_G \gtrsim \Lambda$.

Bibliography

- [1] S. Hawking and G. Ellis, *The Large Scale Structure of Space-Time*, Cambridge Monographs on Mathematical Physics (Cambridge University Press, Feb. 2011).
- [2] R. Penrose, [Phys. Rev. Lett. **14**, 57–59 \(1965\)](#).
- [3] S. Hawking and R. Penrose, [Proc. Roy. Soc. Lond. A **314**, 529–548 \(1970\)](#).
- [4] S. Chandrasekhar, [Mon. Not. Roy. Astron. Soc. **95**, 207–225 \(1935\)](#).
- [5] J. Oppenheimer and G. Volkoff, [Phys. Rev. **55**, 374–381 \(1939\)](#).
- [6] J. Oppenheimer and H. Snyder, [Phys. Rev. **56**, 455–459 \(1939\)](#).
- [7] H. A. Buchdahl, [Phys. Rev. **116**, 1027 \(1959\)](#).
- [8] R. Brustein and A. M. Medved, [Fortsch. Phys. **67**, 1900058 \(2019\)](#).
- [9] R. Brustein and A. Medved, [Phys. Rev. D **99**, 064019 \(2019\)](#).
- [10] S. Hawking, [Commun. Math. Phys. **43**, 199–220 \(1975\)](#).
- [11] K. S. Thorne, *John Archibald Wheeler: A Biographical Memoir*, [arXiv: 1901.06623 \[physics.hist-ph\]](#), Jan. 2019.
- [12] G. Dvali and C. Gomez, [Fortsch. Phys. **61**, 742–767 \(2013\)](#).
- [13] G. Dvali and C. Gomez, [Eur. Phys. J. C **74**, 2752 \(2014\)](#).
- [14] G. Dvali and C. Gomez, [Phys. Lett. B **716**, 240–242 \(2012\)](#).
- [15] S. Deser, [Gen. Rel. Grav. **1**, 9–18 \(1970\)](#).
- [16] S. Deser, [Gen. Rel. Grav. **42**, 641–646 \(2010\)](#).
- [17] R. Carballo-Rubio, F. Di Filippo, and N. Moynihan, [JCAP **10**, 030 \(2019\)](#).
- [18] R. Casadio, M. Lenzi, and O. Micu, [Eur. Phys. J. C **79**, 894 \(2019\)](#).
- [19] R. Casadio, M. Lenzi, and O. Micu, [Phys. Rev. D **98**, 104016 \(2018\)](#).
- [20] R. Casadio, A. Giugno, A. Giusti, and M. Lenzi, [Phys. Rev. D **96**, 044010 \(2017\)](#).
- [21] R. Casadio, M. Lenzi, and A. Ciarfella, [Phys. Rev. D **101**, 124032 \(2020\)](#).
- [22] S. Hawking, [Proc. Roy. Soc. Lond. A **294**, 511–521 \(1966\)](#).

-
- [23] V. Cardoso and P. Pani, [Living Rev. Rel.](#) **22**, 4 (2019).
- [24] K. Schwarzschild, *Sitzungsber. Preuss. Akad. Wiss. Berlin (Math. Phys.)* **1916**, 424–434 (1916).
- [25] R. C. Tolman, [Phys. Rev.](#) **55**, 364–373 (1939).
- [26] P. Pani and V. Ferrari, [Class. Quant. Grav.](#) **35**, 15LT01 (2018).
- [27] A. Urbano and H. Veermäe, [JCAP](#) **04**, 011 (2019).
- [28] N. Birrell and P. Davies, *Quantum Fields in Curved Space*, Cambridge Monographs on Mathematical Physics (Cambridge Univ. Press, Cambridge, UK, Feb. 1984).
- [29] S. Hollands and R. M. Wald, [Phys. Rept.](#) **574**, 1–35 (2015).
- [30] A. Fabbri and J. Navarro-Salas, *Modeling black hole evaporation* (Imperial College Press, London, UK, Aug. 2005).
- [31] D. N. Page, [Phys. Rev. D](#) **13**, 198–206 (1976).
- [32] S. Hawking, [Phys. Rev. D](#) **14**, 2460–2473 (1976).
- [33] S. Hawking, [Phys. Rev. D](#) **72**, 084013 (2005).
- [34] G. 't Hooft, [Nucl. Phys. B Proc. Suppl.](#) **43**, 1–11 (1995).
- [35] J. Bekenstein, [Lett. Nuovo Cim.](#) **4**, 737–740 (1972).
- [36] J. D. Bekenstein, [Phys. Rev. D](#) **7**, 2333–2346 (1973).
- [37] J. M. Bardeen, B. Carter, and S. Hawking, [Commun. Math. Phys.](#) **31**, 161–170 (1973).
- [38] S. Hawking, [Commun. Math. Phys.](#) **25**, 152–166 (1972).
- [39] R. M. Wald, [Living Rev. Rel.](#) **4**, 6 (2001).
- [40] D. N. Page, [New J. Phys.](#) **7**, 203 (2005).
- [41] R. Casadio, P. Nicolini, and R. da Rocha, [Class. Quant. Grav.](#) **35**, 185001 (2018).
- [42] G. Dvali, G. F. Giudice, C. Gomez, and A. Kehagias, [JHEP](#) **08**, 108 (2011).
- [43] G. Dvali and D. Pirtskhalava, [Phys. Lett. B](#) **699**, 78–86 (2011).
- [44] G. Dvali, C. Gomez, and A. Kehagias, [JHEP](#) **11**, 070 (2011).
- [45] G. Dvali, [Subnucl. Ser.](#) **53**, 189–200 (2017).
- [46] J. F. Donoghue, [Phys. Rev. D](#) **50**, 3874–3888 (1994).
- [47] J. F. Donoghue, M. M. Ivanov, and A. Shkerin, *EPFL Lectures on General Relativity as a Quantum Field Theory*, [arXiv: 1702.00319 \[hep-th\]](#).
- [48] K. G. Wilson, [Phys. Rev. D](#) **3**, 1818 (1971).

BIBLIOGRAPHY

- [49] K. Wilson and J. B. Kogut, *Phys. Rept.* **12**, 75–199 (1974).
- [50] G. Dvali, C. Gomez, R. Isermann, D. Lüst, and S. Stieberger, *Nucl. Phys. B* **893**, 187–235 (2015).
- [51] G. 't Hooft, *Phys. Lett. B* **198**, 61–63 (1987).
- [52] D. Amati, M. Ciafaloni, and G. Veneziano, *Phys. Lett. B* **197**, 81 (1987).
- [53] F. Dalfovo, S. Giorgini, L. P. Pitaevskii, and S. Stringari, *Rev. Mod. Phys.* **71**, 463–512 (1999).
- [54] D. Flassig, A. Pritzel, and N. Wintergerst, *Phys. Rev. D* **87**, 084007 (2013).
- [55] R. Casadio, A. Giugno, O. Micu, and A. Orlandi, *Phys. Rev. D* **90**, 084040 (2014).
- [56] R. Casadio, A. Giugno, and A. Orlandi, *Phys. Rev. D* **91**, 124069 (2015).
- [57] R. Casadio, A. Giugno, O. Micu, and A. Orlandi, *Entropy* **17**, 6893–6924 (2015).
- [58] F. Kühnel, *Phys. Rev. D* **90**, 084024 (2014).
- [59] F. Kühnel and B. Sundborg, *JHEP* **12**, 016 (2014).
- [60] F. Kühnel and B. Sundborg, *Phys. Rev. D* **90**, 064025 (2014).
- [61] R. Casadio and A. Orlandi, *JHEP* **08**, 025 (2013).
- [62] W. Mück and G. Pozzo, *JHEP* **05**, 128 (2014).
- [63] R. Casadio, A. Giugno, A. Giusti, and O. Micu, *Eur. Phys. J. C* **77**, 322 (2017).
- [64] R. Ruffini and S. Bonazzola, *Phys. Rev.* **187**, 1767–1783 (1969).
- [65] M. Colpi, S. Shapiro, and I. Wasserman, *Phys. Rev. Lett.* **57**, 2485–2488 (1986).
- [66] M. Membrado, J. Abad, A. Pacheco, and J. Sanudo, *Phys. Rev. D* **40**, 2736–2738 (1989).
- [67] T. M. Nieuwenhuizen, *EPL* **83**, 10008 (2008).
- [68] P.-H. Chavanis and T. Harko, *Phys. Rev. D* **86**, 064011 (2012).
- [69] G. Dvali and A. Gußmann, *Nucl. Phys. B* **913**, 1001–1036 (2016).
- [70] G. Dvali and A. Gußmann, *Phys. Lett. B* **768**, 274–279 (2017).
- [71] F. Kühnel and M. Sandstad, *Phys. Rev. D* **92**, 124028 (2015).
- [72] R. Casadio, A. Giugno, and A. Giusti, *Phys. Lett. B* **763**, 337–340 (2016).
- [73] R. L. Arnowitt, S. Deser, and C. W. Misner, *Phys. Rev.* **116**, 1322–1330 (1959).
- [74] S. Weinberg, *Gravitation and cosmology: principles and applications of the general theory of relativity* (Wiley and Sons, New York, 1972).

- [75] V. Faraoni, *Symmetry* **7**, 2038–2046 (2015).
- [76] M. Duff, *Phys. Rev. D* **7**, 2317–2326 (1973).
- [77] M. Madsen, *Class. Quant. Grav.* **5**, 627–639 (1988).
- [78] J. Brown, *Class. Quant. Grav.* **10**, 1579–1606 (1993).
- [79] T. Harko, *Phys. Rev. D* **81**, 044021 (2010).
- [80] N. Dadhich, *Current Science* **109**, 260–264 (2015).
- [81] R. M. Wald, *Phys. Rev. D* **33**, 3613 (1986).
- [82] K. Heiderich and W. Unruh, *Phys. Rev. D* **38**, 490–497 (1988).
- [83] M. P. Hertzberg and M. Sandora, *JHEP* **09**, 119 (2017).
- [84] D. Bai and Y.-H. Xing, *Nucl. Phys. B* **932**, 15–28 (2018).
- [85] G. Dvali and C. Gomez, *JCAP* **01**, 023 (2014).
- [86] G. Dvali and C. Gomez, *Phys. Lett. B* **719**, 419–423 (2013).
- [87] G. Dvali and C. Gomez, *Black Hole’s Information Group*, [arXiv: 1307.7630](https://arxiv.org/abs/1307.7630) [hep-th].
- [88] G. Dvali, C. Gomez, and S. Mukhanov, *Black Hole Masses are Quantized*, [arXiv: 1106.5894](https://arxiv.org/abs/1106.5894) [hep-th].
- [89] G. Schäfer and P. Jaranowski, *Living Rev. Rel.* **21**, 7 (2018).
- [90] R. Casadio and O. Micu, *Polytropic stars in bootstrapped Newtonian gravity*, [arXiv:2005.09378](https://arxiv.org/abs/2005.09378) [gr-qc].
- [91] W. Mück, *Eur. Phys. J. C* **73**, 2679 (2013).
- [92] V. F. Foit and N. Wintergerst, *Phys. Rev. D* **92**, 064043 (2015).
- [93] A. Giusti, *Int. J. Geom. Meth. Mod. Phys.* **16**, 1930001 (2019).
- [94] C. D. Coster and P. Habet, *Two-point boundary value problems: lower and upper solutions* (Elsevier, Oxford, 2006).
- [95] R. Gaines, *J. Differential Equations* **12**, 291–312 (1972).
- [96] K. Schmitt, *J. Differential Equations* **7**, 527–537 (1970).
- [97] A. C. King, J. Billingham, and S. R. Otto, *Differential equations: linear, nonlinear, ordinary, partial* (Cambridge University Press, Cambridge, 2003).
- [98] R. Casadio, A. Giusti, I. Kuntz, and G. Neri, *Phys. Rev. D* **103**, 064001 (2021).
- [99] W. Mück, *Can. J. Phys.* **92**, 973–975 (2014).
- [100] G. Dvali, C. Gomez, L. Gruending, and T. Rug, *Nucl. Phys. B* **901**, 338–353 (2015).

BIBLIOGRAPHY

- [101] H. S. Snyder, *Phys. Rev.* **71**, 38–41 (1947).
- [102] C. Yang, *Phys. Rev.* **72**, edited by M. Li and Y.-S. Wu, 874 (1947).
- [103] C. Mead, *Phys. Rev.* **135**, B849–B862 (1964).
- [104] F. Karolyhazy, *Nuovo Cim. A* **42**, 390–402 (1966).
- [105] D. J. Gross and P. F. Mende, *Phys. Lett. B* **197**, 129–134 (1987).
- [106] D. Amati, M. Ciafaloni, and G. Veneziano, *Phys. Lett. B* **216**, 41–47 (1989).
- [107] K. Konishi, G. Paffuti, and P. Provero, *Phys. Lett. B* **234**, 276–284 (1990).
- [108] M. Maggiore, *Phys. Lett. B* **304**, 65–69 (1993).
- [109] A. Kempf, G. Mangano, and R. B. Mann, *Phys. Rev. D* **52**, 1108–1118 (1995).
- [110] M. Bojowald and A. Kempf, *Phys. Rev. D* **86**, 085017 (2012).
- [111] F. Scardigli, *Phys. Lett. B* **452**, 39–44 (1999).
- [112] R. J. Adler and D. I. Santiago, *Mod. Phys. Lett. A* **14**, 1371 (1999).
- [113] R. Percacci and L. Rachwal, *Phys. Lett. B* **711**, 184–189 (2012).
- [114] R. Casadio and I. Kuntz, *Eur. Phys. J. C* **80**, 581 (2020).
- [115] R. Casadio and F. Scardigli, *Eur. Phys. J. C* **74**, 2685 (2014).
- [116] R. Casadio, *Localised particles and fuzzy horizons: A tool for probing Quantum Black Holes*, [arXiv:1305.3195](https://arxiv.org/abs/1305.3195) [gr-qc].
- [117] R. Casadio, A. Giugno, and A. Giusti, *Gen. Rel. Grav.* **49**, 32 (2017).
- [118] R. Casadio, A. Giugno, and O. Micu, *Int. J. Mod. Phys. D* **25**, 1630006 (2016).
- [119] P. Amaro-Seoane et al., *Laser Interferometer Space Antenna*, [arXiv: 1702.00786](https://arxiv.org/abs/1702.00786) [astro-ph.IM].
- [120] E. Barausse et al., *Gen. Rel. Grav.* **52**, 81 (2020).
- [121] P. Nicolini, *Int. J. Mod. Phys. A* **24**, 1229–1308 (2009).
- [122] D. Hansen, J. Hartong, and N. A. Obers, *Phys. Rev. Lett.* **122**, 061106 (2019).
- [123] M. Cadoni, R. Casadio, A. Giusti, W. Mück, and M. Taveri, *Phys. Lett. B* **776**, 242–248 (2018).
- [124] M. Cadoni, R. Casadio, A. Giusti, and M. Taveri, *Phys. Rev. D* **97**, 044047 (2018).
- [125] M. Taveri and M. Cadoni, *Phys. Rev. D* **100**, 024029 (2019).
- [126] R. Casadio, A. Giugno, and A. Giusti, *Phys. Rev. D* **97**, 024041 (2018).
- [127] D. S. Petrov, *Phys. Rev. Lett.* **115**, 155302 (2015).